CAPITAL UNIVERSITY OF SCIENCE AND TECHNOLOGY, ISLAMABAD

Determination of Efficacy of *Nigella sativa* Bioactive Compounds Against ALK and EML4 For The Treatment of Lungs Cancer.

by

Rubab Sikandar

A thesis submitted in partial fulfillment for the degree of Master of Science

in the

Faculty of Health and Life Sciences
Department of Bioinformatics and Biosciences

2022

I dedicate this project to Allah Almighty, my creator, my strong pillar, and my source of inspiration, wisdom, knowledge, and understanding. He has been the source of my strength throughout this program.Every challenging work needs self-efforts as well as the guidance of elders especially those who are very close to our hearts. My humble efforts I dedicated to my loving and caring Father and Mother whose affection, love, encouragement and prays of day and night make me able to get such success and honor.

CERTIFICATE OF APPROVAL

Determination of Efficacy of *Nigella sativa* Bioactive Compounds Against ALK and EML4 For The Treatment of Lungs Cancer.

by

Rubab Sikandar

(MBS203039)

THESIS EXAMINING COMMITTEE

S. No.	Examiner	Name	Organization
(a)	External Examiner	Dr. Faiza Munir	ASAB, NUST Islamabad
(b)	Internal Examiner	Dr. Arshia Amin Butt	CUST, Islamabad
(c)	Supervisor	Dr. Erum Dilshad	CUST, Islamabad

Dr. Erum Dilshad
Thesis Supervisor
November, 2022

Dr. Syeda Marriam Bakhtiar
Head
Dept. of Bioinformatics & Biosciences
November, 2022

Dr. Sahar Fazal
Dean
Faculty of Health & Life Sciences
November, 2022

Author's Declaration

I, **Rubab Sikandar** hereby state that my MS thesis titled "**Determination of Efficacy of *Nigella sativa* Bioactive Compounds Against ALK and EML4 For The Treatment of Lungs Cancer.**" is my own work and has not been submitted previously by me for taking any degree from Capital University of Science and Technology, Islamabad or anywhere else in the country/abroad.

At any time if my statement is found to be incorrect even after my graduation, the University has the right to withdraw my MS Degree.

(Rubab Sikandar)

Registration No: MBS203039

Plagiarism Undertaking

I solemnly declare that research work presented in this thesis titled "**Determination of Efficacy of *Nigella sativa* Bioactive Compounds Against ALK and EML4 For The Treatment of Lungs Cancer.**" is solely my research work with no significant contribution from any other person. Small contribution/help wherever taken has been dully acknowledged and that complete thesis has been written by me.

I understand the zero tolerance policy of the HEC and Capital University of Science and Technology towards plagiarism. Therefore, I as an author of the above titled thesis declare that no portion of my thesis has been plagiarized and any material used as reference is properly referred/cited.

I undertake that if I am found guilty of any formal plagiarism in the above titled thesis even after award of MS Degree, the University reserves the right to withdraw/revoke my MS degree and that HEC and the University have the right to publish my name on the HEC/University website on which names of students are placed who submitted plagiarized work.

(Rubab Sikandar)

Registration No: MBS203039

Acknowledgement

"Trust in the LORD with all your heart and lean not on your understanding; in all your ways acknowledge him and he shall direct your paths". (Proverbs 3:5, 6)

First and foremost, I would like to thank God Almighty for giving me the strength, knowledge, ability, and opportunity to undertake this research study and to persevere and complete it satisfactorily. I could never have done this and my achievement would not possible without the faith I have in you, the Almighty.

After an intensive study period, today is the day: writing this note of thanks is the finishing touch on my dissertation. It has been a period of intense learning for me, not only in the scientific arena but also on a personal level. This thesis would not possible without the inspiration and support of some wonderful individuals my thanks and appreciation to all of them for being part of this journey and making this thesis possible.

I offer my sincerest gratitude to my supervisor, Dr. Erum Dilshad, Assistant Professor, who has supported me throughout my thesis with her patience and knowledge whilst allowing me the room to work in my way.

It is pleasure to thank my friends and seniors for supporting and helping me in the compilation of the dissertation. Further, I would like to thank the other faculty members in the Department of Bioinformatics and Biosciences at Capital University of Science and Technology, Islamabad. Finally, my deep and sincere gratitude to my family for their continuous and unparalleled love, help, and support. I am grateful to my brother for always being there for me. I am forever indebted to my parents for giving me the opportunities and experiences that have made me who I am. They selflessly encouraged me to explore new directions in life and seek my destiny. This journey would not have been possible if not for them, and I dedicate this milestone to them.

(Rubab Sikandar)

Abstract

Lungs cancer is the most common cancer type in the world. Due to the developments in diagnostic techniques, therapeutic approaches and traditional remedies, the survival rate has increased but the adverse effects of treatment strategies are also considerable. People around the world are becoming more concerned to use natural products than synthetic drugs. That is the reason for doing this research to explore the potential anticancer agents from *Nigella sativa*. Fifteen bioactive compounds namely Isoquinoline, β-pinene, Apigenin, Salfredin B11, Pyrazole, Pyragallol, Salicylic acid, Syringic acid, Gallic acid, Camphene, 3,4-dihydroxybenzoic acid, 4-dihydroxycinnamic acid, Caffeic acid, Myristic acid and Stearic acid were selected as ligands. All these ligands were screened out on the basis of Lipinski's rule of five and by studying their ADME properties. Virtual screening of the above mentioned ligands were carried out against Anaplastic Lymphoma kinase and Echinoderm Microtubule associated Protein Like-4 by online tool CB-Dock. Crizotinib and Paclitaxel were selected as standard drugs for comparison. Lead compounds were selected from the above mentioned ligands, which were less toxic than the selected drugs. Visualization analysis studies related to the interaction of selected compound and the drugs were performed by using PyMol and LIGPLOT+ tools. After the complete analysis, Apigenin and Salfredin B11 were selected as potential anticancer compounds which can be considered in future as drug candidate for the treatment of lungs cancer. However further research is required to elucidate their potential medical use.

Contents

List of Figures

List of Tables

Abbreviations

ADMET: Adsorption Distribution Metabolism Excretion

ALK: Anaplastic Lymphoma Kinase

BBB: Blood Brain Barrier

BCL2: B-cell lymphoma 2

CB-Dock: Cavity-Detection guided Blind Docking

CNS: Central Nervous System

CT: Computed Tomography

CYP2D6: Cytochrome P450 2D6

EFGR: Epidermal growth factor receptor

EML4: Echinoderm Microtubule Associated Protein Like 4

EMN: Electromagnetic navigation

FDA: Food Drug Authority

GPCRs: G-protein coupled receptors

GRAVY: Grand average of hydropathicity

HBA: Hydrogen bond acceptor

HBD: Hydrogen bond donor

hERG: Human Ether-a-go-go-Related Gene

HIV: Human immunodeficiency virus

II: Instability Index

KRAS: Kristin rat sarcoma

MAPK: Mitogen-activated protein kinase

MRI: Magnetic resonance imaging

MRTD: Maximum rate tolerated dose

MW: Molecular weight

NR: Total number of negative charged residues

***N. sativa*:** *Nigella sativa*

NSCLC: Non-small cell lung cancer

OCT: Organic cation transporter

PDB: Protein Data Bank

PR: Total number of positive charged residues

pI: Theoretical pI

R-EBUS: Radial endobronchial ultrasound

SCLC: Small cell lung cancer

TTNA: Transthoracic needle aspiration

VDss: Volume distribution at steady state

Chapter 1

Introduction

1.1 Background

Cancer is the most leading and prominent cause of death at these days. The mortality ratio increases more than 10 million deaths per year [1]. This dramatically increase in cancer incidence rate may be due to many factors like eating habits, age, lifestyle , changing reproductive trends, obesity or overweightness, tobacco use [2]. Many countries of world including developed and developing countries, different types of cancer effect males and females like breast cancer is common in females, lung cancer is common in males. More types of cancer like colorectal cancer, liver, stomach, cervical cancer and prostate cancer are also the cause of death in many developed and under-developed countries [3].

In developed countries Tobacco is the main leading factor that is responsible for 85% cases of lung cancer. Recent statistics shows that over 1.80 million deaths may occur due to lung cancer by 2020 [4].

Lung cancer is the chief cause of death, approximately making 25% death rate due to cancer. Lung cancer is distinguished by uncontrolled growth of cells. This proliferation of cells produces abnormal cellular mass. This mass or tumor grows to different other regions and, with time, attains metastatic capacity and spreads to other parts, at the end cause death. The cancer cell arises due to mutation in

genetic complement or may be due to environmental factors [5]. Lung cancer is the common malignant type of cancer around the globe. Oncogenic fusion genes EML4 and ALK are present in Non-Small Lung Cancer cells (NSCLC), which represent almost 7% of such kind of cancers. In cancer disease, ALK proteins have an essential role to withstand the process of apoptosis.

Lungs cancer is the severe form of Cancer that ratio of spread increase day after day. Oncogenic fusion genes are basically the EML4 and ALK kinases that are found in non-small cell lung cancers, making 7% of such tumors. ALK kinases play an important role to halt the apoptotic phenomenon in cancer disease. The fusion of anaplastic lymphoma kinase (ALK) and echinoderm microtubule associated protein-like 4 (EML4) has lately been identified in non-small cell lung cancers (NSCLC) [6].

Many anticancer drugs are used to treat the lung cancer disease. Avastin is the drug approved by FDA because of its improved survival significance when added to several standard first line chemotherapy regimes in non-small cell lung cancer [7]. Erlotinib is also used for treating patients with EGFR mutant non-small lung cancer (NSCLC) [8]. Gefitinib is viable treatment for non-small cell lung cancer (NSCLC) patients whose growths harbor physical transformations in EGFR [9]. Gefitinib and Erlotinib are best in never-smokers with NSCLC having antitumor activity [10]. Interleukin-8 has been widely implicated in processes like angiogenesis and metastasis in lung cancer. In lung cancer, the adenocarcinoma cells produce significant amount of Interleukin-8 [11]. IL-8 increased the growth of non-small cell lung cancer cells, involving activation of epidermal growth factor receptors (EGFR). This receptor plays a key role in proliferation of cells in lung cancer. EFGR receptor and ligand leads to signaling events like mitogen activated protein kinase (MAPK) activation. Transactivation of receptor and EGFR ligand occur due to many G-protein coupled receptors (GPCRs) and involves metalloproteinase-mediated membrane bound EGFR ligands [12]. The activity of IL-8 to take part in cell proliferation is blocked by EGFR tyrosine kinase. This is done by specific antibody called anti-EGFR antibody and a metalloproteinase inhibitor. Resistance of MAPK also blocks the effect of IL-8 [13]. With the advancement in

science and technology, new techniques are invented that help reduce the rate to cancer and increase the survival of cancer patients. Although with the availability of suitable drug for the disease to prevent it but there are some side effects also that the patients develop resistance against the pharmaceutical drugs. So for better treatment process, there is a need to use medicinal drugs obtained from medicinal plants.

Nigella genus has been an important component of traditional medicine like Unani and Tibb. Because of its marvelous healing power, it has been ranked at the top among medicinal plants [14]. *Nigella* species are broadly used as a medicinal plant for their therapeutic properties. Seeds and the oils extracted from seeds have old history of use in different frameworks of medications and also utilized as eatables [15]. Extracts from *Nigella* species have mitigating action, principally due to the presence of numerous bioactive molecules. Natural oil obtained from seeds act as secondary metabolites and these metabolites are some sort of monoterpenes [16]. Important therapeutic effects of *Nigella* species include anti-cancer, antioxidant, hypotensive, hepatoprotective, spasmolytic, anti-inflammatory, and bronchodilator, hypoglycemic, hypolipidemic, anti-allergic and immunomodulating properties [17]. Alkaloids, steroids, carbohydrates, flavonoids, fatty acids, etc. are the secondary metabolites found in Nigella genus [18]. Molecular Docking is use for designing computer assisted drug. Docking is an In-silico method to determine the correct structure of ligand with the target binding site. A basic property of molecular docking is to estimate the predominant attachment site of a ligand with the three dimensional structure of protein using a special scoring feature. The setting up of input for docking is the 3D structure of target proteins and ligands. Docking can be done for virtual screening on large variety of compounds, ranking the result and propose structural hypothesis of ligands inhibiting the target [19]. This new class of small molecular compounds has been shown to have high interaction between target protein and target binding as well as proper absorption, distribution, metabolism and excretion (ADME) to help in target lead selection [20]. Molecular docking also focuses on achieving the system's minimal independent energy, which includes properly aligned proteins and ligands [21].

Small ligands, protein proteins, protein peptides, protein nucleotides can be used in molecular docking. Some of the docking mechanisms are algorithm, ligand flexibility and receptors flexibility. Auto Dock Vina, Auto Dock, CB Dock and some others are mainly the used docking applications [22].

1.2 Problem Statement

Cancer is the second most prevalent cause of death and morbidity in the world. The increase in cancer rate influence the scientist to look for novel drugs obtained from plants sources that have fewer or no side effects as compared to the synthetic drugs. Extracts obtain from plants have been widely used in ethanomedical treatments that have fewer side effects.

1.3 Aims and Objectives

The aim is to identify the novel inhibitors, natural anti-cancer compounds and harmless elements from *Nigella sativa*. Therefore, we focus on protein ligand interactions, which play an important role in structural drug design. To achieve the goal, we have following objectives:

1. Identification of various bioactive compounds from *Nigella sativa*, as potential inhibitors of Anaplastic Lymphoma Kinase (ALK) and Echinoderm Microtubule-Associated Protein-like 4 (EML4).

2. To perform the molecular docking mechanism for analyzing the binding confirmation between targeted proteins and ligands.

3. To find out the most suitable interacting molecules those have the inhibitory effect against the targeted receptors by physiochemical properties.

1.4 Scope

Cancer is the group of illnesses, which is prevailed in this world and increases the rate of mortality also. It is also very challenging to develop drugs against lung cancer because of the certain reasons like unavailability of complete data, as a result drug formed is not as much effective. Drugs obtained from natural sources are of more worth as compared to the synthetic drugs because of their less toxicity and immunosuppressive activity. Many bioactive compounds are found in the medicinal plants that may prove to be effective for treating such type of cancer. For this purpose, there is a need to identify such compounds that shows inhibitory actions against ALK and EML 4 that could prove beneficial in treating lung cancer.

Chapter 2

Review of Literature

2.1 Cancer

Cancer is meant for a group of illnesses. Any body's cells that start to undergo divisions which are uncontrolled and these cells invade other tissues in the body. The apoptotic process is the programmed cell death mechanism in which cell dies when they become old and perform their assigned task and new cells replace them. This organized process get disrupted by genetic and environmental factors that causes cells to grow and divide indefinitely leading to tumor formation as shown in Figure 2.1. The tumor cells invasion to other nearby tissues is the main cause of mortality and morbidity in cancer patients.

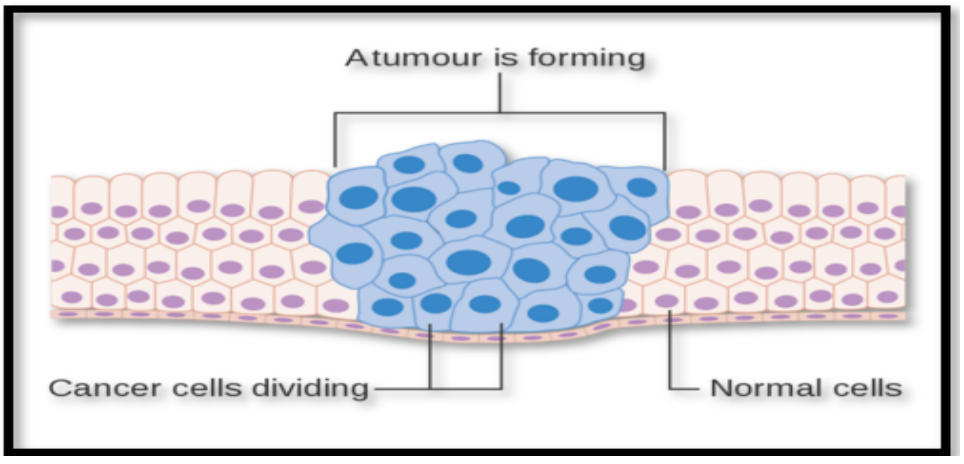

FIGURE 2.1: Tissue showing healthy and cancer cells [24].

2.2 Lung Cancer

Lungs cancer is a form of cancer in which cells in the lungs show uncontrolled division. Lung cancer arises due to uncontrolled division of cells, cause tumor to develop. Lung cancer grows and blocks the airways in the lungs. Fluid accumulates around the lungs pleural space. The tumor may also invade the other parts of body. Lung cancer develops due to change in gene like mutations and environmental factors also contribute in developing lung cancer. Lung cancer mainly diagnosed in older people around the age of 65 and less common in people younger than 45.

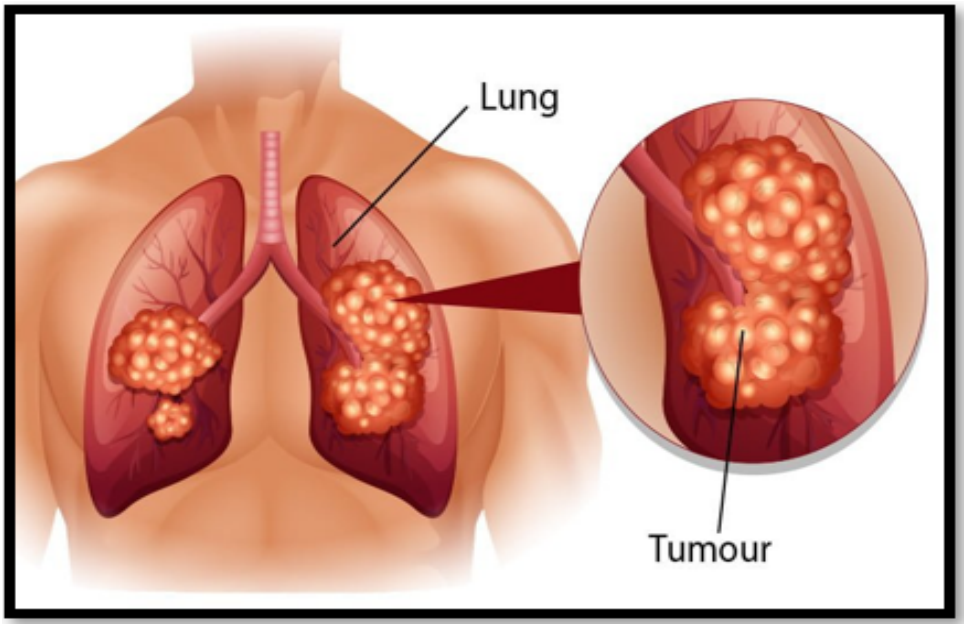

FIGURE 2.2: Tumor shown in Lungs [25].

2.2.1 Lungs Cancer Incidence

Lung cancer is the most common cancer form in US. The incidence varies on the basis of histology. In both males and females, lung cancer is diagnosed. Lung cancer causes more death in males. It reports for 11.6% of the total cases and the mortality rate accounts for 18.4% of the total cancer deaths in 2012. Death rate due to lung cancer caused by passive intake of smoke is 21,400 deaths annually. The leading cause of lung cancer that is smoking attributes to death sentence, ranging more than 80% in United States.

2.2.2 Lungs Cancer Symptoms

Symptoms of Lungs cancer includes:

- Shortness of breath
- Bloody sputum (mucus coughed up from the lungs)
- Fluid in Chest cavity
- Chest pain or discomfort
- Fatigue
- Hoarseness
- Weight loss for not known reason
- Fatigue
- Trouble swelling
- Swelling in the face and/or veins in the neck
- Lack of appetite
- Insomnia [26].

2.2.3 Risk factors for Lungs Cancer

Significant risk factor for Lungs Cancer is increasing age. Other risk factors of Lungs Cancer includes over use of tobacco like use of cigarettes, cigars and pipes.

- Contact to cancer causing substance in passive smoke.
- Experience to different metals like Chromium, Arsenic, Asbestos, Nickle, Beryllium etc.
- Radiation exposure by any of the mean:

  - Radiation therapy to the chest.
  - Radon exposure at home or at workplace.
  - MRI test like computed Tomography (CT) scans [27].
    1. Living in area with high air pollution level.
    2. Lung Cancer in family history.
    3. Human Immunodeficiency Virus (HIV) infection
    4. Beta carotene supplements [28].

- Genetics:

  Various gene loci are involved in causing the Lungs Cancer. The defects found in growth promoting oncogenes and growth suppressing tumor genes.

  - Oncogene KRAS muted in 30% of cases in lung adenocarcinomas [29]
  - MYC, Cyclin D1 and EGFR15 are over expressed in 2.5-10%, 5% and 6% of NSCLC, respectively.
  - BCL2 over-articulation is associated with 25% of cases [30].
  - BRAF, present in around 2% of adenocarcinoma patients and confined to cancers that didn't show KRAS changes [31].

2.2.4 Lungs Cancer Types

Each type of cancer cells develop and spread in different ways. The most common types of lungs cancer includes following:

- **Non-Small Cell Lung Cancer (NSCLC)** Non-Small Cell Lung Cancer contribute 80-85% of all lung cancer cases. It further comprises 2 types [32].
- **Non squamous carcinoma** (includes large-cell carcinoma, adenocarcinoma and other cells types). Adenocarcinoma is the most common type of cancer in non-smokers in United States.
- **Squamous carcinoma** (include epidermoid carcinoma) [33].

- **Small Cell Lung Cancer (SCLC)** Small Cell Lung Cancer contributes almost 15 % of the Lung cancer cases. SCLC has more rapid multiplication duration, has high growth fraction and also has an ability to wide spread [34].

- **Bronchioloalveolar carcinoma (BAC)** It is less common and less prevalent type of cancer. This type of cancer comprises 3-4% of cases, 10-15% of adenocarcinomas having BAC properties [35].

2.2.5 Diagnosis of Lung Cancer

Following are procedures that aid in diagnosing the Lung cancer disease.

- **Sputum Cytology:** Sputum Cytology is the examination of sputum (mucus) that is the fluid secreted by the cells of bronchi and lower respiratory tract. The sputum is examined under microscope to look for cancerous cells.

- **Computed Tomography (CT) bronchoscopy:** it is the non-invasive technique that shows the internal view of trachea and bronchi in 3D reconstruction [36].

- **Flexible bronchoscopy:** It is an invasive technique that has been use for diagnostic and for therapeutic processes. It is a safe procedure to diagnose respiratory diseases. It helps in diagnosing patients with infection of chest, parenchymal lung disease, lung nodules, persistent lung infiltrates and lung transplant rejection [37].

- **Electromagnetic navigation (EMN) bronchoscopy:** It is a procedure that utilizes electromagnetic technique to view and localize endoscopic tools through the bronchial pathway. By using a 3D bronchial map, Physicians are able to locate the desired location in the lungs [38].

- **Radial Endobronchial Ultrasound (R-EBUS)-guided Lung Biopsy:** For diagnosing peripheral pulmonary malignancies R-EBUS-guided lung biopsy provides a fair diagnostic yield in detecting pulmonary malignancies.

- **Transthoracic Needle Aspiration (TTNA):** It is an accurate modality that is used for biopsy of lung pathology. It directs the biopsy tools toward the area of abnormality [39].
- **Pleural Biopsy:** Pleural biopsy is a minimal invasive procedure that is much sensitive and specific. It diagnoses pleural diseases. A small piece is taken by using the special biopsy needle to look for infection, cancer or any other disease condition [40].

2.2.6 Lung Cancer Treatments

Surgery: Surgery entails the physical removal of the tumor as well as any of the underlying tissue that cause spread of disease. Certain procedure involve in treating lungs cancer are:

Lobectomy: The affected lobe of lung is removed by applying this procedure. It is the most commonly performed surgical treatment against lung cancer.

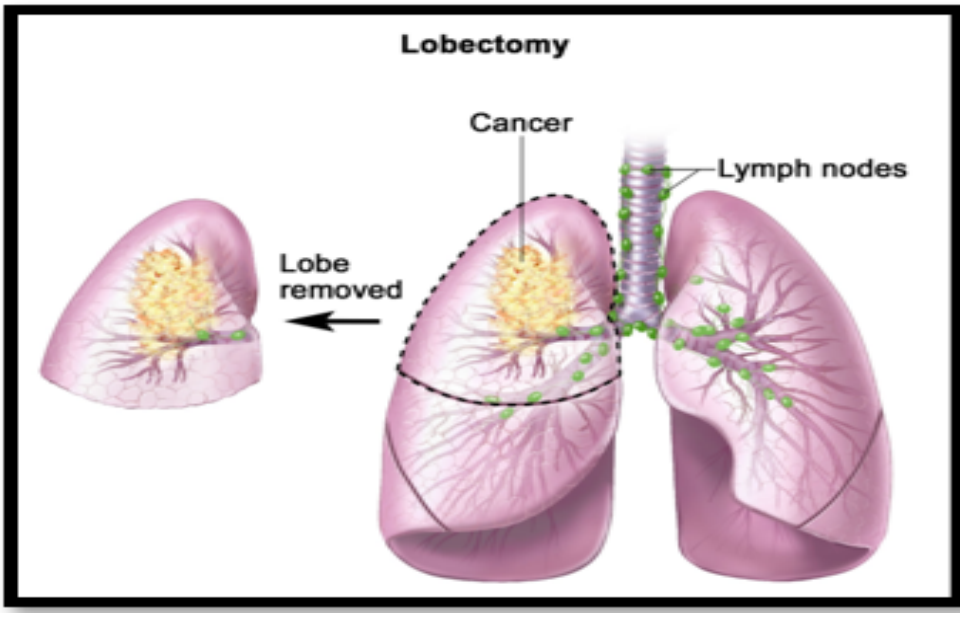

FIGURE 2.3: Removal of affected part by Lobectomy.

Segmentectomy: Each of the lungs comprises of two to five segments and surgeons removed that segments which are infected leaving the uninfected one.

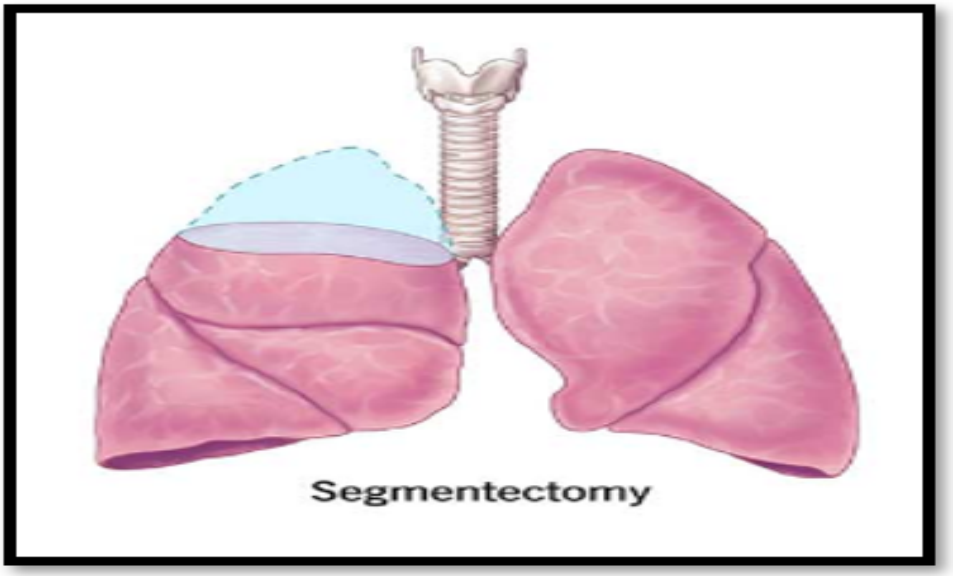

FIGURE 2.4: Removal of infected part by Segmentectomy.

Wedge Resection: The Removal of small wedge shape part of lung that surrounds the tumor.

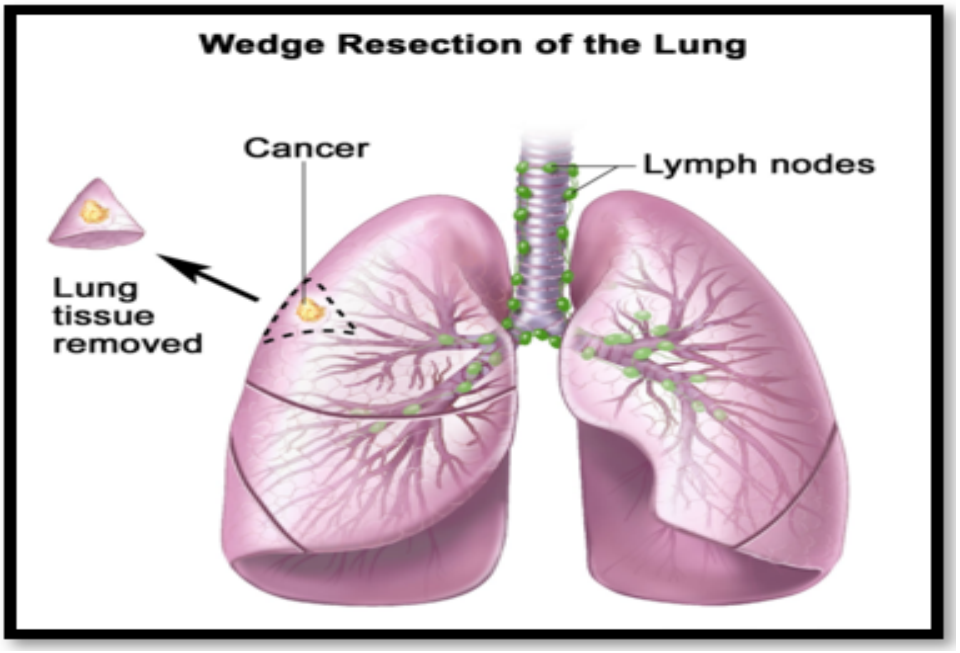

FIGURE 2.5: Removal of wedge shape part of lung by Wedge Resection.

Pneumonectomy: The removal of whole lung affected by the cancer. This procedure is mainly done when the cancer cannot be removed easily by lobectomy

[41].

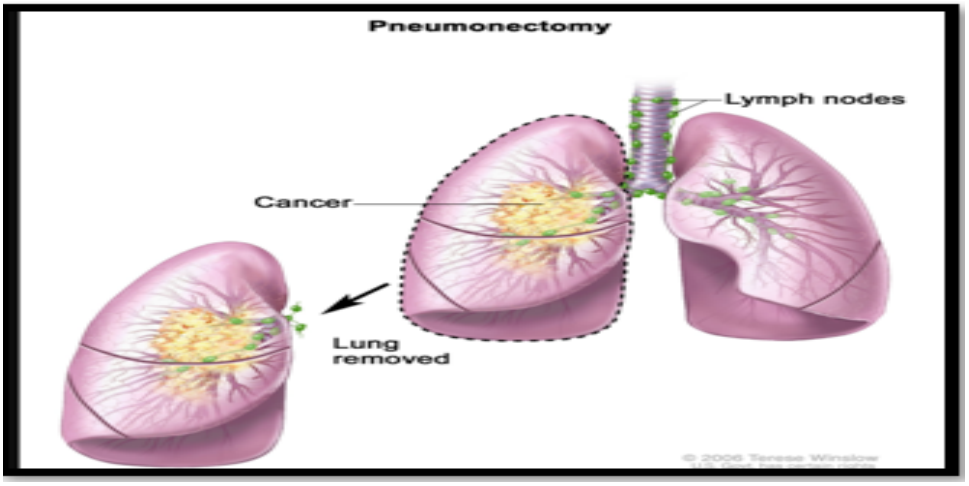

FIGURE 2.6: Removal of whole lung by Pnuemonectomy.

Radiation Therapy: It involves the use of high frequency rays including X-rays or Gamma rays to treat a cancer or post-surgery tumor site. The rays are strong enough to destroy the cancer cells that can recruit growth where they were removed. Treatments are usually issued five days a week for duration of five to seven months. Each treatment takes approximately 15 minutes [42].

Chemotherapy: It is a form of drug therapy that is used to destroy cancerous cells. This therapy can be used alone or sometimes it can be used in combination with other clinical treatments like surgery. Most of the commonly used medicines for non-small cell lung cancer are Crizotinib, Sunitinibmalate, and Tandutinib. Chemotherapy has many unfavorable ill effects, so there is a need to consult the doctor before the start of chemotherapy [43].

2.3 Medicinal Plants

Usage of medicinal plants for the treatment purpose is very old. In the ancient time, due to less knowledge, people firstly use the herb and afterward get knowledge about its efficacy. Awareness about the use of medicinal plants is the result of many years of man struggles for their discovery, their usage and their beneficial

effects. Contemporary science has recognized their dynamic activity that wide range of drugs that have plant origin has been known by the ancient civilization. The development in the ideas related to medicinal plants as well as increased awareness make physicians and scientists to respond to the emerging situations in health sector [44]. The word 'Medicinal Plants refers to a variety of plants used in herbal medicines. . It is the practice of using plants for medicinal purposes as well as for study purpose. . Medicinal plants contain the rich source of ingredients that can be used to make pharmacopoeia, non- pharmacopoeia and synthetic drugs. . Since ancient time, medicinal plants and aromatic plants have been used as therapeutic agents [45]. Natural source drugs accounts for about 40% of newly approved drugs in the last two decades. They play an important role in the discovery of drugs for cancer treatment and dealing with other infectious ailments [46]. In ancient medicinal systems, such as Ayurvedic, Unani and Chinese traditional medicines, hers has been used to treat different kinds of diseases and infections [47].

2.4 Natural Compounds Targeting Cells of Lungs Cancer

Natural products contain lead compounds that have been used for targeting cells of Lung Cancer. Some of these are mentioned in the Table 2.1 given below

TABLE 2.1: Natural products targeting lung cancer cells [48].

Compounds	**Structure**	**Source**	**Protein/signal**
Curcumin	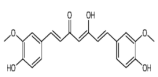	*Cucurma longa*	DNA damage or repair, JAK-STAT, Sonic Hedgehog, CD133, CD44, ALDHA1, Nanog, Oct4

TABLE 2.1: Natural products targeting lung cancer cells [48].

Compounds	**Structure**	**Source**	**Protein/signal**
Gigantol	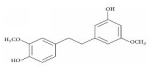	*Dendribium draconis*	AKT, CD133, ALDH1A1
Salinomycin	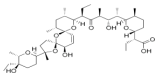	*Streptomyces albus*	OCT-4, Nanog, Sox2
Silibinin	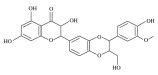	*Silybum mariamum*	ALDH activity
Vanilin	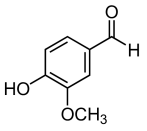	*Vanilla planifolia*	AKT-proteasomal degradation, CD133, ALDH1A1, Oct4, Nanog
Renieranycin	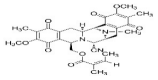	*Xestospongia sp*	CD133, CD44, ALDH1A1
Parthenolide	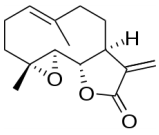	*Tanacetum parthenium*	ER stress, Apoptosis, ATF4, DDIT3, PMAIP

2.5 *Nigella sativa*

Nigella belongs to family Ranunculaceae is a small genus comprising around 20 species. The plants belong to this genus are annuals and get through unfavorable

condition as seeds. The seeds are bifurcate or discoid shape and have characteristics black color that's why they are commonly called "Black cumin" [49]. This genus produces secondary metabolites and essential oils that are used to treat various diseases. *Nigella spp.* has a strong healing powers and food importance. As well as *Nigella* seeds are rich in Linoleic acid and Omerga-6 fatty acid and provide dietary phytochemicals including thymoquinone, saponins, flavonoids and alkaloids [50]. The evolutionary origin of Nigella species are the Western-Irano-Turanian region. This Species is found in Pakistan, India, Bangladesh, Russia, Southern Europe, North Africa, Turkey and Middle-East [51].

Nigella sativa is widely used in ancient times for treating lung cancer, diabetes, high BP, respiratory pathologies, allergy and hyper-sensibility. It also acts as anti-rheumatic and analgesic (pain reliever). *N. sativa* is also use as food preservative and as spice [52]. The seeds of *N. sativa* contain very low degree of toxicity. The extract of seed has a property against nephrotoxicity and hepatotoxicity. The other functions performed by the N. sativa are as antimicrobial, antipyretic, anti-inflammatory and antineoplastic [53].

FIGURE 2.7: The figure represents *Nigella sativa* flower [54].

2.5.1 Taxonomic Hierarchy

Nigella sativa is the binomial name of the plant belonging to family Ranunculaceae. They are easily grown in loamy soil. The plants grow best in full sunlight however it also show tolerance in shady places. It is widely distributed in different regions of the world. The taxonomic hierarchy is shown in Table 2.2.

TABLE 2.2: Taxonomic hierarchy of *Nigella sativa* [55].

Sr no.	**Domain**	**Eukarya**
1-	Kingdom	Plantae
2-	Subkindgom	Tracheobionta (Vascular plants)
3-	Division	Spermatophyta (Seeded plants)
4-	Class	Magnoliphyta (Flowering plants)
5-	Subclass	Magnoliidae
6-	Order	Ranunculales
7-	Family	Ranunculaceae
8-	Genus	*Nigella*
9-	Species	*Nigella sativa*

2.6 Anti-Cancer Mechanism of Action of Bioactive Constituents of *Nigella species*

N. sativa contains bioactive like Isoquinoline, Beta-pinene, Apigenin, Salfredin B11, Pyrazole, Pyragallol, Salicylic acid. *N. sativa* exhibit anticancer effect due

to the presence of TQ, which is extracted from the seeds of *N.sativa*. Concentration of 100µm is significant enough to inhibit cancer cells growth by about 90% [56]. Essential oils are also the part of bioactive compounds like linoleic acid.

2.7 Targeted Proteins

There are 2 different types of proteins which are used as the targeted protein for molecular docking process such as Anaplastic Lymphoma kinase and Echinoderm Microtubule-associated Protein-Like 4.

2.7.1 EML 4 and ALK Fusion Oncogenes

Lung cancer development is linked to the EML4 and AKL fusion oncogenes that arise from the inversion on chromosome 2. In adult tissues, ALK fuse with the EML4 results in the formation of tumor in the lungs. ALK is a receptor of tyrosine kinase. The fusion of ALK to EML4 does not always occur in the same location rather it gets change, as a result give rise to multiple variants [57]. EML4-ALK fusion proteins go through the process of dimerization which is ligand independent. This type of fusion including other types has been seen in NSCLC. The chromosomal inversion does not usually arise within the identical precise location, however, giving upward push to more than one ALK-EML4 forms, five all of which incorporate the equal intracellular tyrosine kinase domain of ALK but exclusive truncations of EML4. Fusion of ALK with other genes like TFG and KIF5B has also been diagnosed in NSCLC, although those fusions seem like lots less commonplace than ALK-EML4. ALK fusion proteins, which include ALK-EML4, undergo ligand-impartial dimerization mediated by way of the coiled-coil domain of the fusion accomplice, resulting in constitutive activation of the ALK tyrosine kinase. The ALK-EML4 fusion protein uncovers marked remodeling hobby both in vitro and in vivo. In a transgenic mouse model, lung-precise expression of ALK-EML4 outcomes accordingly within the development of lung adenoma.

Chapter 3

Research Methodology

3.1 Context Diagram

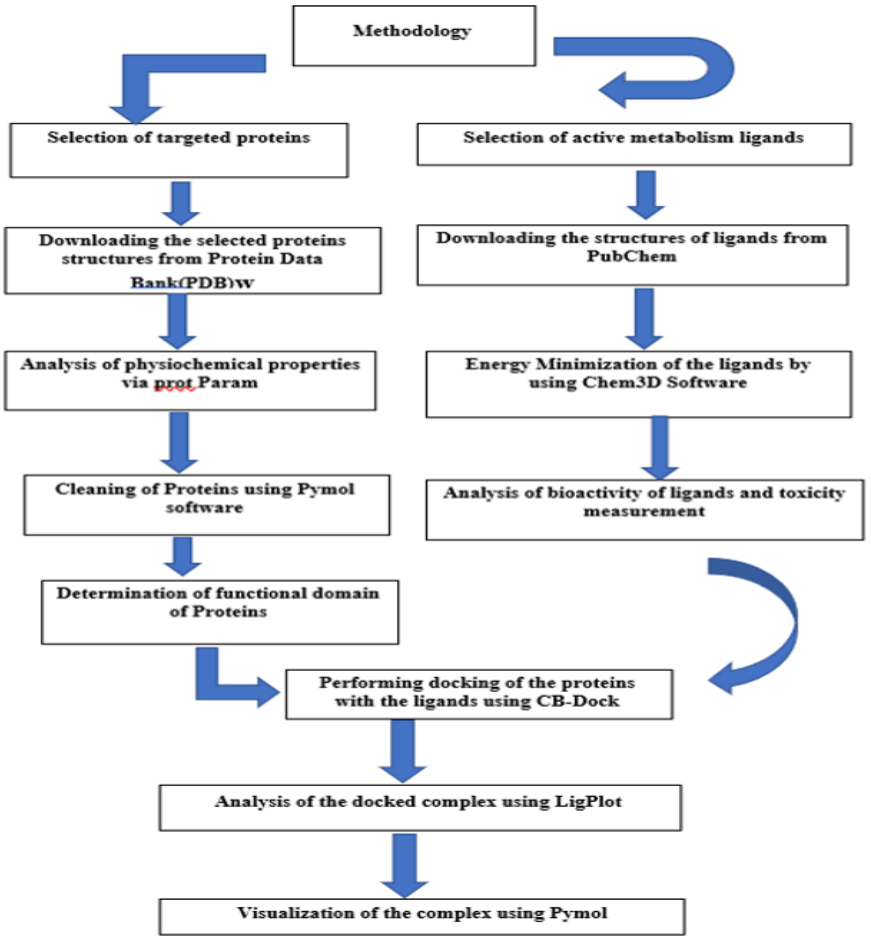

FIGURE 3.1: The methodology flow chart.

3.2 Selection of Disease

Cancer can be described as the out of control boom of extraordinary cells. Most lungs cancer is non-small cell lung cancer (NSCLC). Oncogenic fusion genes together with ALK and EML4 are found in non–small–cell lung cancers, act for 2 to 7% of such tumors. ALK proteins play a critical function in deactivating the apoptosis system in cancer. Non–small cell lung cancer cells need ALK to mobile increase and proliferation of the cells in lungs cancer [59].

3.3 Selection of Proteins

Structure of ALK and EML4 were taken from protein databank. The PDB archive is the only site where you can learn about the three dimensional structure of large biological molecules like proteins and nucleic acid [60].

3.4 Primary Sequence Retrieval

The primary sequence of target proteins (ALK and EML4) were obtained in FASTA format from UniProt Database (`https://www.uniprot.org`) [61].

3.5 Analysis of Physiochemical Properties

The function of proteins is primarily determined by their physiochemical properties. These properties were predicted by using ProtParam.

Physiochemical parameters were investigated using the ProtParam tool of Expasy including molecular weight number of amino acids, iso electric point, instability index, grand average of hydropathicity (GRAVY), number of negatively charge residues, number of positively charge residues, aliphatic index and amino acids and atomic composition [62].

3.6 Cleaning of the Downloaded Proteins

The extra constituents attached to the proteins must be extracted after downloading the proteins structures, which was achieved using the open source system PyMol [63].

3.7 Determination of Functional Domains of Target Proteins

InterPro, a database that can analyze a protein and provide information about the families, functional sites and domains of the proteins under study, is used to determine the domains of the target proteins. The polypeptide binding sites and homo dimer interfaces were obtained by inserting the receptor proteins FASTA sequence.

3.8 Selection of Active Metabolic Ligands

The ligands that have already shown antiviral, antioxidants and antimalarial properties were chosen. Sterols, Phenolic compounds, Terpenes, monoterpenes, flavonoids, sesquiterpenes, and ad monoterpenes are among them [64].

3.9 Ligands Preparation

PubChem database was used to download the three dimensional structures of all the above ligands. PubChem is a database that contains information about the chemical molecules and is run by the National Center for Biotechnology Information (NCBI). The data is correlated with chemical names and molecular formulas, 3D or basic structures, their isomers and canonic structures. The structures of the ligands which were obtained from PubChem was downloaded and then the ligands

MM2 energy was minimized by using Chem3D ultra. At the end, SDF format was select to save the energy minimized structures of the ligands [65].

3.10 Molecular Docking

For the purpose of interpreting docking effects the interaction of the ligands active pockets with the protein were measure. Ionic bonding, Hydrogen Bonding and hydrophobic bonding are the three types of interactions investigated. CB-Dock were used to performed the molecular docking between the protein and the ligand. CD-Dock automatically locates docking positions. CB Dock is a docking method for proteins and ligands that measures the bonding sites, their duration, and their center. The size of the box is changed to match the ligand and then docking is completed. Since the docking is based on cavity binding, the accuracy ratio is higher. 3D structures of the protein in PDB format and the 3D structure of the ligand in SDF format were uploaded to perform the docking [66].

3.11 Visualization of Docking Results via PyMol

Over the past few years, the PyMol has emerged as an efficient molecular tool of visualization. The graphics and its ability to view 3D structures have been extra ordinary [67]. PyMol provides a plug in which can access the results and make their visualization clearer so that the docking results can be studied easily. The pictures of the docking results were captured also. The docking results were saved in PDB format throughout the process.

3.12 Analysis of Dock Complexes via LigPlot

Once the dock complexes were obtained with lowest Vina score, the analysis of docking complex were the next step. The complexes were stored as a PDB files

the program LigPlot were used to perform the research. The schematic diagram of the proteins and ligand interactions were created automatically for the given PDB file format. The hydrophobic and the hydrogen bonding interactions were studied using LigPlot. LigPlot provides a 2D representation of the protein ligands complex using this tool [68].

3.13 Selection of Standard Drug against Lungs Cancer

Standard drugs against lung cancer were selected based on docking values, physiochemical properties and ADMET properties.

3.14 Ligands ADME Poperties

Is in general, a more effective drug discovery needs a lead is more like the drug. The compounds was then tested for the drug score, drug similarity and toxicity. The ADME or Absorption, Distribution, Metabolism and Excretion of the human body can be optimized using the pkCSM [69].

3.15 Lead Compounds Analysis and Toxicity Measurements

The most active inhibitors were discovered after a careful study of proteins and ligands interactions, docking ratings and toxicity studies. Our lead compounds are the one we've choose. After applying the rules of 5, the lead compound is defined.

1. The log value of the drug like compound must be limited to five
2. The molecular weight of the compound must be less than 500

3. Hydrogen bond acceptors number must be ten.

4. Hydrogen bond donors number must be 5

Once any compound fit these rules, it is selected as lead compound.

3.16 Comparison of Standard Drugs and Lead Compounds

The comparison between standard anticancer drugs and the proposed lead compounds were done through comparing docking values, physiochemical properties and ADMET properties [70].

Chapter 4

Results and Discussions

4.1 Structure Modeling

4.1.1 Primary Sequence Retrieval

Primary sequences of target proteins (ALK and EML4) were taken in FASTA format from Uniprot database (http://www.uniprot.org) under accession number of Q9UM73 for ALK and P68363-P07437 for EML4 chains.

>sp—Q9UM73—ALK-HUMAN ALK tyrosine kinase receptor
OS=Homo sapiens OX=9606 GN=ALK PE=1 SV=3

MGAIGLLWLLPLLLSTAAVGSGMGTGQRAGSPAAGPPLQPREPLSYSRLQR
VDFVVPSLFRVYARDLLLPPSSSELKAGRPEARGSLALDCAPLLRLLGPAP
TAGSPAPAEARTLSRVLKGGSVRKLRRAKQLVLELGEEAILEGCVGPPGEA
LQFNLSELFSWWIRQGEGRLRIRLMPEKKASEVGREGRLSAAIRASQPRLL
GTGHSSLESPTNMPSPSPDYFTWNLTWIMKDSFPFLSHRSRYGLECSFDFP
YSPPLHDLRNQSWSWRRIPSEEASQMDLLDGPGAERSKEMPRGSFLLLNTS
HTILSPWMRSSSEHCTLAVSVHRHLQPSGRYIAQLLPHNEAAREILLMPTP
WTVLQGRIGRPDNPFRVALEYISSGNRSLSAVDFFALKNCSEGTSPGSKMA
FTCWNGTVLQLGQACDFHQDCAQGEDESQMCRKLPVGFYCNFEDGF
GLPLEAATAPGAGHYEDTILKSKNSMNQPGP

>sp—P68363—TBA1B-HUMAN OS=Homo sapiens OX=9606 GN=TUBA1B PE = 1 SV=1

MRECISIHVGQAGVQIGNACWELYCLEHGIQPDGQMPSDKTIGGGDDSF
TGAGKHVPRAVFVDLEPTVIDEVRTGTYRQLFHPEQLITGKEDAANNYA
GKEIIDLVLDRIRKLADQCTGLQGFLVFHSFGGGTGSGFSLLMERLSVD
LEFSIYPAPQVSTAVVEPYNSILTTHTTLEHSDCAFMVDNEAIYDICRR
PTYTNLNRLISQIVSSITASLRFDGALNVDLTEFQTNLVPYPRIHFPLA
SAEKAYHEQLSVAEITNACFEPANQMVKCDPRHGKYMACCLLYRGDVVPK
NAA IATIKTKRSIQFVDWCPTGFKVGINYQPPTVVPGGDLAKVQRAVCML-
SNTTAIAEA WARLDHKFDLMYAKRAFVHWYVG EGMEEGEFSEARED
MAALEKDYEEVGVDSVEG EGEEEGEEY

>sp—P07437—TBB5-HUMAN OS=Homo sapiens OX=9606 GN=TUBB PE=1 SV=2

MREIVHIQAGQCGNQIGAKFWEVISDEHGIDPTGTYHGDSDLQLDRISVYYNEA
TGG KYVPRAILVDLEPGTMDSVRSGPFGQIFRPDNFVFGQSGAGNNWAKGH-
GAELVD SVLDVVRKEAESCDCLQGFQLTHSLGGGTGSGMGTLL
ISKIREEYPDRIMNTFSVVP SPKVSDTVVEPYNATLSVHQLVENTDETYCID-
NEALYDICFRTLKLTTPTYGDLNHL VSATMSGVTTCLRFPGQLNAMVPFPRL-
HFFMPGFAPLTSRGSQQYRALT VPELTQQVFDAKNMMAACDPRHAAVFR-
GRMSMKEVDEQMLNVQNKNSSYFV EWIPNNVKTAVCDIPPRGLKMAVTFI
GNTEAESNMNDLVSEYQQYQDATAEEEEDFGEEAEEEAMFRRKAFLHWYT
STAIQELFKRISEQFTAMFRRKAFLHWYT GEGMDEEFTEAESNMNDLVSEY
QQYQDATAEEEEDFGEEAEEEA

Anaplastic Lymphoma Kinase and Echinoderm Microtubule associated Protein like 4 were selected as the target proteins and Isoquinoline, β-pinene, apigenin, Salfredin B11 , pyrazole, pyragallol, salicylic acid, syringic acid, gallic acid, camphene, 3,4-dihydroxybenzoic acid, 4-dihydroxycinnamic acid, caffeic acid, myristic acid and stearic acid were selected as ligands in this research work.

4.1.2 Physiochemical Characterization of ALK and EML 4

ProtParam is a tool of Expasy which is used online for the calculation of various physical and chemical parameters for ALK and EML4 proteins stored in Swiss-prot or TrEMBL or for a user entered protein sequence. The estimated values of following parameters includes the molecular weight, amino acid composition, theoretical pI, atomic composition, extinction coefficient, estimated half-life, instability index, aliphatic index and grand average of hydropathicity (GRAVY). The calculated pI greater than 7 represents the basic nature of the protein while less than 7 show acidic nature of protein. Extinction coefficient represents light absorption. In stability index if less than 40 shows stability of the protein while greater than 40 indicates the instability of the protein [71].

The table 4.1 and 4.2 shows the physiochemical properties of ALK and EML4 respectively.

TABLE 4.1: Physiochemical Properties of ALK.

PROPERTIES	VALUES
Molecular Weight	174606.62 Da
Theoretical pI	6.68
Negative- charged Residues	161
Positive-charged Residues	154
Extinction Coefficient 1	233505 M-1 cm-1
Extinction Coefficient 2	231130 M-1 cm-1

Table 4.1: Physiochemical Properties of ALK.

PROPERTIES	VALUES
Instability index	51.29
Aliphatic index	77.08
GRAVY	-0.322

Table 4.2: Physiochemical Properties of EML4.

PROPERTIES	VALUES
Molecular Weight	108916.22 Da
Theoretical pI	5.96
Negative- charged Residues	129
Positive-charged Residues	109
Extinction Coefficient 1	135885 M-1 cm-1
Extinction Coefficient 2	134760 M-1 cm-1
Instability index	37.32
Aliphatic index	75.31
GRAVY	-0.538

The protein's aliphatic composition is indicated by the aliphatic index. The high value of the aliphatic index indicates the thermo stability of the protein. Molecular weight includes both positive and negative charged residues of the protein. At 280nm the ranging extinction coefficient of 73980, 67965, 20105 and 112270 indicates Tyr and Trp high concentration [72].

Low GRAVY shows better interaction with water molecules. All these parameters which are selected for this research work are taken according to previous research work. MW stands for Molecular Weight pI for theoretical isoelectric point (pH at which protein is neutral, without any charge), NR for total negatively charged residues (Asp+ Glu), PR for total positively charged residues (Arg + Lys), Ext.Co1for extinction coefficients when assuming all pairs of Cys residues from cysteine, Ext.Co2 for extinction coefficients when assuming all Cys residues are reduced, and GRAVY for grand average of hydropathicity.

4.1.3 3D Structure Predictions of Proteins

3D Structure of targeted proteins was downloaded from RCSB PDB in PDB format. Protein Data Bank is a three dimensional database of complex molecules of living organisms, like nucleic acids and proteins. The 3D Structures of ALK and EML4 were obtained from PDB named as 2XB7 and 6I2I under accession number `10.2210/pdb2XB7/pdb` and `10.2210/pdb4CGC/pdb` respectively 4.1, 4.2.

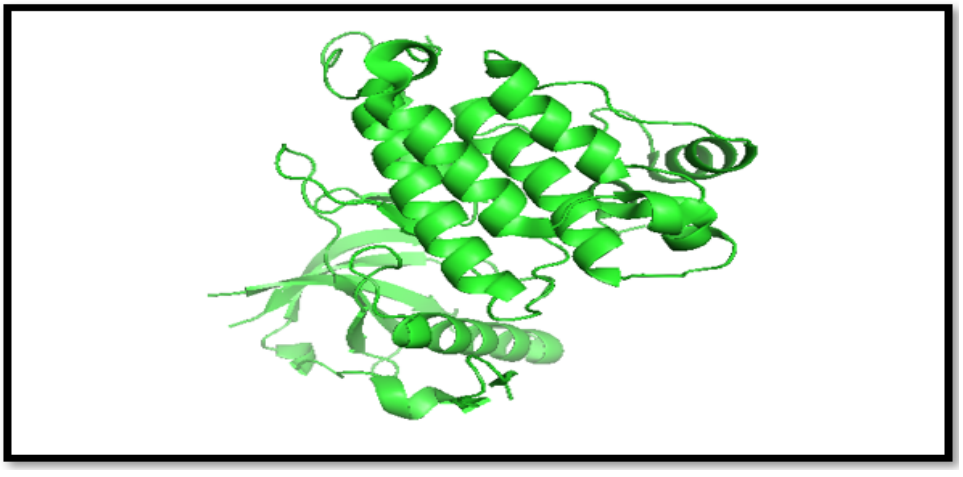

FIGURE 4.1: Human Anaplastic Lymphoma Kinase

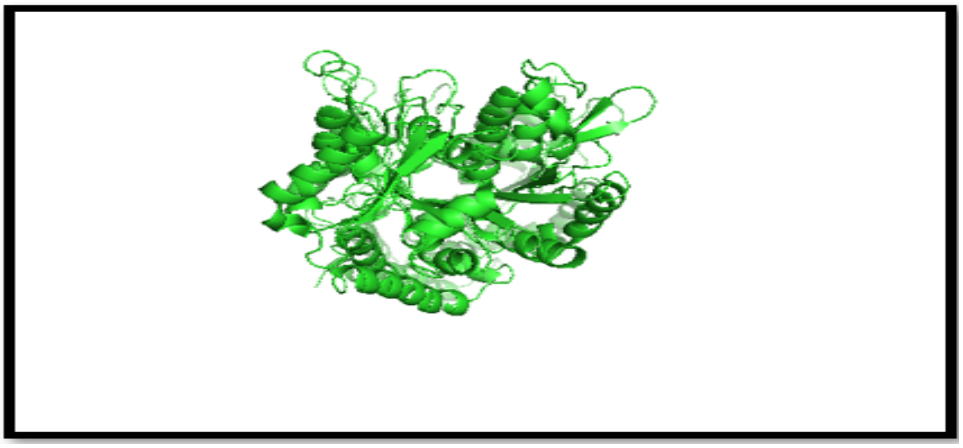

FIGURE 4.2: Human Echinoderm microtubule associated Protein Like-4

4.1.4 Functional Domain Identification of Proteins

Functional domain is the active part of protein that is involve in interactions of protein with other substances. Protein can have more than one functional domain that performs different functions [73].

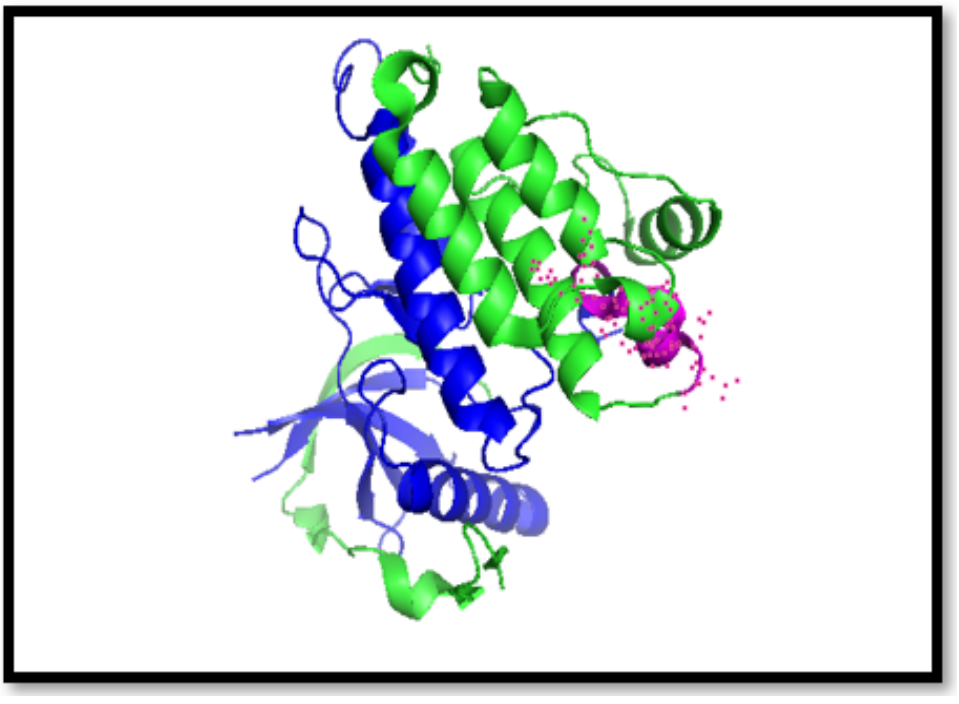

FIGURE 4.3: Functional domains of Human ALK

Figure 4.3 shows functional domains of human ALK protein. ALK has many like MAM domain (264-427), MAM domain 478-636, Ser-Thr/Tyr-kinase-cat-domain (1117-1383), Prot-kinase-domain (1116-1392).

Figure 4.4 shows functional domains of human EML4 protein. EML4 has Tubulin -layer-sand-domain (248-393), Tubulin-FtsZ-GTPase domain (3-246) domains.

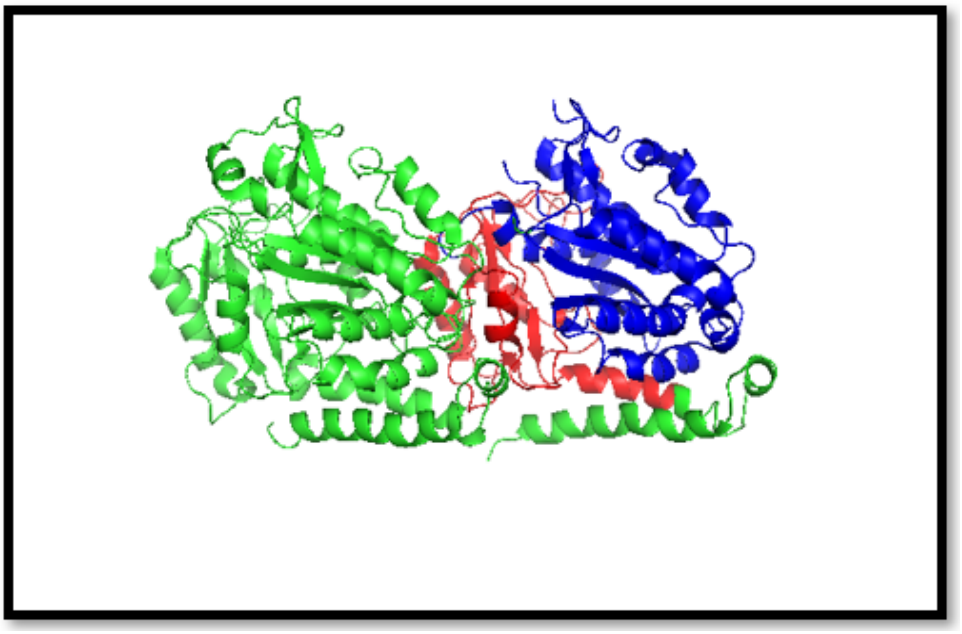

FIGURE 4.4: Functional domains of Human EML4

4.1.5 Templates Selection

The 3D structure of the selected templates were taken from the protein data bank (PDB) and listed in 4.3.

TABLE 4.3: Selected PDB Templates Structures.

Templates	**Resolution**	**PDB ID**	**Structures**
Human Anaplastic Lymphoma Kinase	2.50 Å	2XB7	
Human Echinoderm Microtubule Associated Protein Like-4	3.60 Å	6I2I	

4.2 Structures of Proteins Refined for Docking

The selected 3D structures were refined by PyMol for docking and are shown in Figures 4.5 and 4.6.

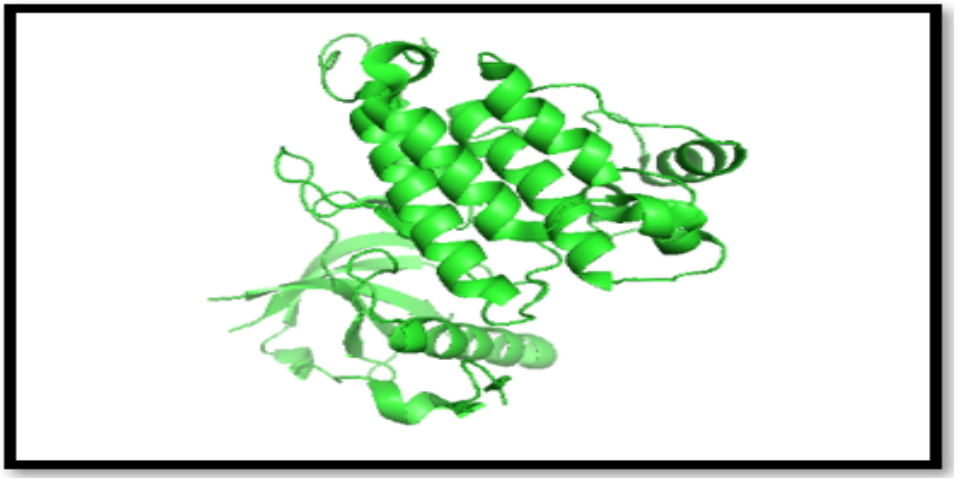

FIGURE 4.5: Refined 3D Structure of Human ALK

Figure 4.5 shows the refined structure of protein ALK. The tool PyMol removes any additional ligand and the water droplets. Now the protein is ready for docking purpose.

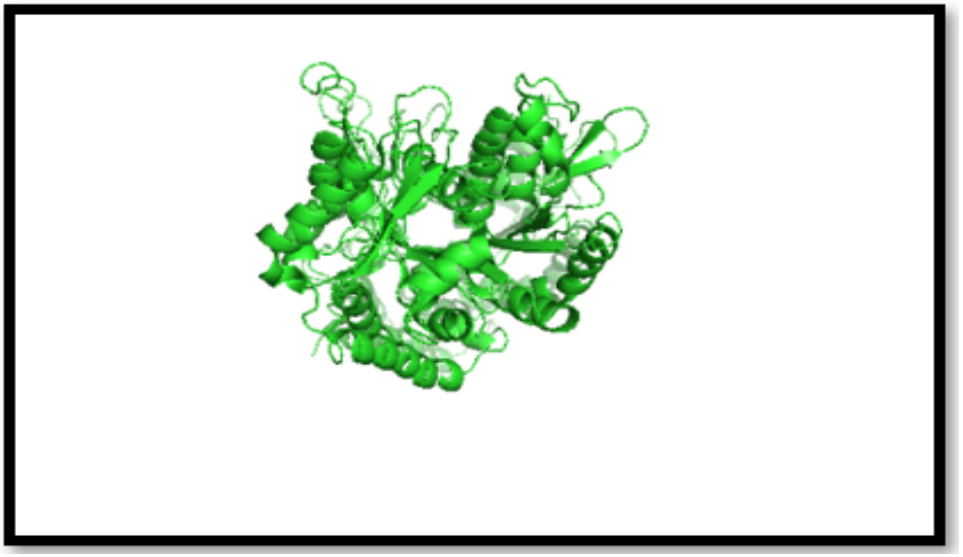

FIGURE 4.6: Refined 3D Structure of Human EML-4

Figure 4.6 shows the refined structure of protein EML4. The tool PyMol removes any additional ligand and the water droplets. Now the protein is ready for docking purpose.

4.3 Ligands Selection

Protein data bank contains a large amount of protein ligand complex, especially for the protein target. Therefore, the selection of ligands is based on the best resolution of the structure, the chemical class of the co-crystal ligand bound to the protein structure and the best binding affinity. Conformational selection is a process in which ligand selectively binds to one of these conformers, strengthening it and increasing its population with respect to the total population of the protein is ultimately resulting in the final observed complex. Ligands (compounds of the selected plant) were searched out from PubChem, which is the world's largest freely accessible chemical information database. Their 3-D structures were downloaded from PubChem in SDF format. Selected compounds were representing all the classes of compounds like Alkaloids, essential oils etc. After selection of ligands, energy minimization of ligands was done which was carried out by Chem pro software (Chem 3D v 12.0.2). This was a mandatory step in the preparation of ligands for docking because unstable ligands will show unreliable vina scores in docking results. Bioactive compounds of *Nigella sativa* were selected as ligands for the present study (Table 4.4). The 3D structures and information of selected ligands that were Isoquinoline, β-pinene, apigenin, salfredin B11, pyrazole, pyragallol, salicylic acid, syringic acid, gallic acid, camphene, 3,4-dihydroxybenzoic acid, 4-dihydroxycinnamic acid, caffeic acid, myristic acid and stearic acid were downloaded from PubChem. This database (`http://pubchem.ncbi.nih.gov`) is a public repository for information on chemical substances and their biological activities [74]. 4.4 shows the selected Ligands with their structural information.

Table 4.4: Selected Ligands with Structural Information

Name	**Molecular Formula**	**Molecular Weight**	**Structure**
Isoquinoline	C_9H_7N	129.16 g/mol	

β-pinene	$C_{10}H_{16}$	136.23 g/mol	
Apigenin	$C_{15}H_{10}O_5$	270.24 g/mol	
Salfredin B11	$C_{10}H_{12}O_4$	232.23 g/mol	
Pyrazole	$C_3H_4N_2$	68.03 g/mol	
Pyragallol	$C_6H_6O_3$	126.11 g/mol	
Salicylic Acid	$C_7H_6O_3$	138.12 g/mol	
Syringic Acid	$C_9H_{10}O_5$	198.17 g/mol	
Gallic Acid	$C_7H_6O_5$	170.12 g/mol	
Camphene	$C_{10}H_{16}$	136.23 g/mol	
3,4-dihydroxy-benzoic Acid	$C_7H_6O_4$	154.12 g/mol	
4-dihydroxy-cinnamic Acid	$C_9H_8O_3$	164.16 g/mol	
Caffeic Acid	$C_9H_8O_4$	180.16 g/mol	
Myristic Acid	$C_{14}H_{28}O_2$	228.37 g/mol	
Stearic Acid	$C_{18}H_{36}O_2$	284.5 g/mol	

4.4 Virtual Screening and Toxicity Prediction

Drug like compounds are separated from non-drug like compounds by following certain parameters like Lipinski's rule of five and ADMET properties test [75]. The original rule of five deals with four physiochemical parameters (Molecular weight $\leq$ 500, log P value $\leq$ 5, H-bond $\leq$ 5, and H-bond acceptors $\leq$ 10) that is associated with orally active compounds [76]. A compound considered as drug likeness if it is complying with three or more of the RO5. If a compound violates more than two of these rules, it is assumed to be poorly absorbed [76]. 4.5 showed the applicability of Lipinski's rule of five on selected ligands. All ligands follow these rules.

TABLE 4.5: Applicability of Lipinski's Rule on Ligands

Ligand	**Log P**	**Molecular Weight**	**H-Bond Acceptor**	**H-Bond Donor**
Isoquinoline	2.2348	129.16 g/mol	1	0
β-pinene	2.9987	136.23 g/mol	0	0
Apigenin	2.5768	270.24 g/mol	5	3
Salfredin B11	2.2468	232.23 g/mol	4	1
Pyrazole	0.4097	68.03 g/mol	1	1
Pyragallol	0.8034	126.11 g/mol	3	3
Salicylic acid	1.0904	138.12 g/mol	2	2
Syringic acid	1.1076	198.17 g/mol	4	2

Table 4.5: Applicability of Lipinski's Rule on Ligands

Ligand	**Log P**	**Molecular Weight**	**H-Bond Acceptor**	**H-Bond Donor**
Gallic acid	0.5016	170.12 g/mol	4	4
Camphene	2.997	136.23 g/mol	0	0
3,4-dihydroxy-benzoic acid	0.796	154.12 g/mol	3	3
4-dihydroxy-cinnamic acid	1.49	164.16 g/mol	2	2
Caffeic acid	1.1956	180.16 g/mol	3	3
Myristic acid	4.7721	228.37 g/mol	1	1
Stearic acid	6.335	284.5 g/mol	1	1

4.4.1 Toxicity Prediction

pkCSM is an online tool used to find the ADMET (Absorption, Distribution, Metabolism, Excretion and Toxicity) properties of bioactive compounds and drugs. By using this tool, we will determine the toxicity of selected ligands.

AMES toxicity test is used to test the mutagenic potential of the compound by using bacteria. If it shows a positive response, then ligand is mutagenic which act as a carcinogen. The maximum tolerated dose (MRTD) provides a measure of toxic

chemical limits on individuals. This will help in directing the first recommended dose of the treatment regimen in phase 1 clinical trials. MRTD is expressed in the form of logarithms (log mg/kg/day). For a specific compound, MRTD is higher if it is greater than 0.477log (mg/kg/day), and lower if it is less than 0.477log (mg/kg/day). The hERGI and II inhibitors model determine the potential of any compound to cause the inhibition of potassium channels induced by the hERG (human ether-a-go-go gene). An inhibitor of these channels could probably lead to the chronic QT syndrome and a long term basis the person could develop fatal ventricular arrhythmia. Many useful products from the pharmaceutical market have been removed as a result of hERG channel inhibitor.

LD50 is the quantity of a compound that causes the deaths of 50% of experimental animals (mice). The LD50 (mol/kg) predicts toxicity of a probable compounds whereas LOAEL aims to identify the lowest dosage of a compound with a significant adverse effect. Exposure to low to moderate chemical dose for a long time is very important in medicine and is expressed in a log (mg/kg-bw/day). Hepatotoxicity determines liver damage that is induced by drug and is a major safety issue for drug development. Skin sensitization is a potential negative effect of skin care products. *T. pyriformis* is protozoan bacteria which toxin is often used as toxic endpoint (IGC50) and inhibits 50% growth. *T.pyriformis* IGC50 (negative concentration logarithm required to prevent 50% growth) in log ug/L predicted value >-0.5 log ug/L is considered toxic.The lethal concentration (LC50) represents the concentration of molecules needed to cause the death of 50% of Flathead Minnows (small bait fishes). In Minnow toxicity LC50 values below 0.5mM (log LC50 <-0.3) are regarded as high acute toxicity.

4.4.2 Toxicity Predicted Values of Selected Ligands

4.4.2.1 Isoquinoline

Isoquinoline is non-carcinogenic and it shows high Max.tolerated dose. Maximum tolerated dose helps in deciding maximum starting dose in phase I of clinical trial.

It is supporter of potassium channels and is non-hepatotoxic. This ligand is skin sensitive. *T. pyriformis* and Minnow toxicity are within recommended range.

4.4.2.2 β-pinene

β-pinene is non-carcinogenic and it shows high Max.tolerated dose. It is supporter of potassium channels and is non-hepatotoxic. *T. pyriformis* showed high value of toxicity. Minnow toxicity is within recommended range.

4.4.2.3 Apigenin

Apigenin is non-carcinogenic and it shows low Max.tolerated dose. It is supporter of potassium channels and is non-hepatotoxic. *T. pyriformis* and Minnow toxicity are also within recommended range.

4.4.2.4 Salfredin B11

Salfredin B11 is non-carcinogenic and it shows low Max.tolerated dose. It is supporter of potassium channels and is non-hepatotoxic. *T. pyriformis* and Minnow toxicity are also within recommended range. This ligand shows all the predicted value within the safe range.

4.4.2.5 Pyrazole

Pyrazole is non-carcinogenic and it shows high Max.tolerated dose. All the toxicity value are within recommended range.

4.4.2.6 Pyragallol

Pyragallol is non-carcinogenic and it shows low Max.tolerated dose. It is supporter of potassium channels and is non-hepatotoxic. *T. pyriformis* and Minnow toxicity are also within recommended range.

4.4.2.7 Salicylic Acid

Salicylic acid is non-carcinogenic and it shows high Max.tolerated doses. It is supporter of potassium channels and is non-hepatotoxic. *T. pyriformis* and Minnow toxicity are also within recommended range.

4.4.2.8 Syringic Acid

Syringic acid is non-carcinogenic and it shows high Max.tolerated doses. It is supporter of potassium channels and is non-hepatotoxic. *T. pyriformis* and Minnow toxicity are also within recommended range. This ligand shows all the predicted value within the safe range.

4.4.2.9 Gallic Acid

Gallic acid is non-carcinogenic and it shows high Max.tolerated dose. It is supporter of potassium channels and is non-hepatotoxic. *T.pyriformis* and Minnow toxicity are also within recommended range. This ligand shows all the predicted value within the safe range.

4.4.2.10 Camphene

Camphene is non-carcinogenic and it shows low Max.tolerated doses. It is supporter of potassium channels and is non-hepatotoxic. *T. pyriformis* value show slightly high range. Minnow toxicity is also within recommended range. This ligand shows all the other predicted value within the safe range.

4.4.2.11 3,4-dihydrobenzoic Acid

3,4-dihydrobenzoic acid is non-carcinogenic and it shows high Max.tolerated doses. It is supporter of potassium channels and is non-hepatotoxic. *T. pyriformis* and Minnow toxicity are also within recommended range.

4.4.2.12 4-dihydroxycinnamic Acid

4-dihydroxycinnamic acid is non-carcinogenic and it shows high Max.tolerated dose. It is supporter of potassium channels and is non-hepatotoxic. *T. pyriformis* and Minnow toxicity are also within recommended range. This ligand shows all the other predicted value within the safe range.

4.4.2.13 Caffeic Acid

Caffeic acid is non-carcinogenic and it shows high Max.tolerated dose. It is supporter of potassium channels and is non-hepatotoxic. *T. pyriformis* and Minnow toxicity are also within recommended range. This ligand shows all the predicted value within the safe range.

4.4.2.14 Myristic Acid

Myristic acid is non-carcinogenic and it shows low Max.tolerated dose. It is supporter of potassium channels and is non-hepatotoxic. Myristic acid shows skin sensitization. *T. pyriformis* and Minnow toxicity values show high toxicity range.

4.4.2.15 Stearic Acid

Stearic acid is non-carcinogenic and it shows low Max.tolerated doses. It is supporter of potassium channels and is non-hepatotoxic. Stearic acid shows skin sensitization. *T. pyriformis* and Minnow toxicity values show high toxicity range.

Toxicity predicted values of selected ligands are listed in 4.6 and 4.7. This table include the

1. Ligands, AMES toxicity, max. tolerated dose, hERG I inhibitor, hERG II inhibitor, oral rat acute toxicity, oral chronic toxicity,

2. Hepatotoxicity, skin sensitization, *T. pyriformis* toxicity and minnow toxicity.

TABLE 4.6: 4.6a)Toxicity predicted values of Ligands

Ligands	**AMES Toxicity**	**Max. Tolerated Dose-Human (mg/kg)**	**hERG I Inhibitor**	**hERG II Inhibitor**	**Oral Rat Acute Toxicity (mol/kg)**
Isoquinoline	No	0.694	No	No	2.216
β-pinene	No	0.371	No	No	1.673
Apigenin	No	0.328	No	No	2.45
Salfredin B11	No	-0.051	No	No	1.701
Pyrazole	No	0.818	No	No	2.186
Pyragallol	No	-0.269	No	No	2.049
Salicylic Acid	No	0.61	No	No	2.282
Syringic Acid	No	1.374	No	No	2.157
Gallic Acid	No	0.7	No	No	2.218
Camphene	No	0.305	No	No	1.554
3,4-Dihydroxy-benzoic Acid	No	0.814	No	No	2.423
4-Dihydroxy-cinnamic Acid	No	1.111	No	No	2.155
Caffeic Acid	No	1.145	No	No	2.383

TABLE 4.6: 4.6a)Toxicity predicted values of Ligands

Ligands	**AMES Toxicity**	**Max. Tolerated Dose-Human (mg/kg)**	**hERG I Inhibitor**	**hERG II Inhibitor**	**Oral Rat Acute Toxicity (mol/kg)**
Myristic Acid	No	-0.559	No	No	1.477
Stearic Acid	No	-0.791	No	No	1.406

TABLE 4.7: b).Toxicity predicted values of Ligands

Ligands	**Oral Rat Chronic Toxicity (mg/kg)**	**Hepato-toxicity**	**Skin Sensit-ization**	***T. pyriformis Toxicity (log ug/L)***	**Minnow toxicity (log mM)**
Isoquinoline	2.189	No	Yes	0.148	0.972
β-pinene	2.28	No	No	0.628	1.012
Apigenin	2.298	No	No	0.38	2.432
Salfredin B11	2.419	No	No	0.494	1.492
Pyrazole	1.607	No	No	-1.123	3.048
Pyragallol	2.374	No	No	0.127	2.734
Salicylic Acid	2.483	No	No	0.263	1.812
Syringic Acid	2.157	No	No	0.281	2.554
Gallic Acid	3.06	No	No	0.285	3.188
Camphene	2.247	No	No	0.533	1.19

TABLE 4.7: b).Toxicity predicted values of Ligands

Ligands	**Oral Rat Chronic Toxicity (mg/kg)**	**Hepato-toxicity**	**Skin Sensit-ization**	***T. pyriformis Toxicity (log ug/L)***	**Minnow toxicity (log mM)**
3,4-Dihydroxy-benzoic Acid	2.021	No	No	0.273	2.451
4-Dihydroxy-cinnamic Acid	2.534	No	No	0.319	1.607
Caffeic Acid	2.092	No	No	0.293	2.246
Myristic Acid	3.034	No	Yes	0.978	-0.601
Stearic Acid	3.33	No	Yes	0.65	-1.565

4.5 Molecular Docking

Molecular docking is a technique that is used to estimate the strength of a bond between a ligand and a target protein through a special scoring function and also to find out the correct structure of the ligand within the target binding site. The 3D structure of the target proteins and the ligand is taken as input for docking. After preparing proteins and ligands ready for docking, docking is performed by CB-Dock which is well trusted online blind auto docking tool. The results and time required for docking is dependent upon structures of receptors, ligands, refinements and net speed. It may take several hours for a single result, so patience was shown while doing docking. CB dock gave us five possible possess and receptors models

and among these possess best one was selected by observing certain properties like vina score and size of cavity etc.

Molecular docking without having information of binding sites is performed by using a user friendly blind docking web server called as CB Dock, that predicts and estimate a bonding site for a given protein and calculate centers and sizes with a novel rotation cavity detection method and perform docking with proper docking program known as Auto dock Vina [79]. Molecular dockings are performed by using ALK-EML4 as receptors and 15 selected compounds as ligands [80]. After submitting input files (receptor files in PDB format and ligand file in SDF format), CB-Dock checks the input files and convert them to PDB formatted files using Open Babel and MAGL Tools.

The molecular docking technique has recently become a crucial tool in computer-assisted drug design to estimate the binding affinity and examine the interactive mode since it may significantly increase efficiency and lower research costs. Effective docking methods use a scoring system that correctly ranks candidate dockings and efficiently explore high-dimensional spaces. Lead optimization benefits greatly from the use of docking to do virtual screening on huge libraries of compounds, rate the outcomes, and offer structural ideas for how the ligands inhibit the target.

- After that CB-Dock predicts cavities of the receptor and calculated the centers and sizes of the top N (n=5 by default) cavities.
- Each center, size and PDB files are submitted by Auto Dock Vina for docking.
- Among 5 best confirmations, best one is selected on the basis of highest affinity score of ligand-receptor interaction.
- Ligands with best binding scores values with ALK and EML 4 receptors are shown in the table below 4.8.

Table 4.8: Ligands with best binding score values with ALK

Compounds	**Binding Score**	**Cavity size**	**HBD**	**HBA**	**Log P**	**Molecular Weight (g/mol)**	**Rotatable Bond**	**Grid Map**
Iso-quinoline	-5.8	1932	0	1	2.2348	129.16	0	27
β-pinene	-5.4	1932	0	0	2.9987	136.23	0	27
Apigenin	-7.9	1932	3	5	2.5768	270.24	1	27
Salfredin B11	-7.4	1932	1	4	2.2468	232.32	0	27
Pyrazole	-3.3	1932	1	1	0.4097	68.03	0	27
Pyragallol	-4.8	1932	3	3	0.8034	126.11	0	27
Salicylic Acid	-5.2	1932	2	2	1.0904	138.12	1	27

Table 4.8: Ligands with best binding score values with ALK

Compounds	**Binding Score**	**Cavity size**	**HBD**	**HBA**	**Log P**	**Molecular Weight (g/mol)**	**Rotatable Bond**	**Grid Map**
Syringic Acid	-5.5	1932	2	4	1.1076	198.17	3	27
Gallic Acid	-5.4	1932	4	4	0.5016	170.12	1	27
Camphene	-5.3	1932	0	0	2.997	136.23	0	27
3,4-Benzoic Acid	-5.2	1932	3	3	0.796	154.12	1	27
4-Dihydroxy Cinnamic Acid	-5.8	1932	2	2	1.49	164.16	2	27
Caffeic Acid	-6	1932	3	3	1.19	180.16	2	27
Myristic Acid	-5.2	1932	1	1	4.7721	228.37	12	27
Stearic Acid	-5.5	105	1	1	6.335	284.5	16	26

Table 4.9: Ligands with best binding score values with EML4

Compounds	**Binding Score**	**Cavity Size**	**HBD**	**HBA**	**Log P**	**Molecular Weight (g/mol)**	**Rotatable Bond**	**Grid Map**
Isoquinoline	-5.6	1415	0	1	2.2348	129.16	0	46
β-pinene	-5.5	11648	0	0	2.9987	136.23	0	66
Apigenin	-8.1	11648	3	5	2.5768	270.24	1	66
Salfredin B11	-7.2	11648	1	4	2.2468	232.32	0	66
Pyrazole	-4.2	11648	1	1	0.4097	68.03	0	66
Pyragallol	-5.7	11648	3	3	0.8034	126.11	0	66
Salicylic Acid	-5.7	11648	2	2	1.0904	138.12	1	66

Table 4.9: Ligands with best binding score values with EML4

Compounds	**Binding Score**	**Cavity Size**	**HBD**	**HBA**	**Log P**	**Molecular Weight (g/mol)**	**Rotatable Bond**	**Grid Map**
Syringic Acid	-6	11648	2	4	1.1076	198.17	3	66
Gallic Acid	-6.3	11648	4	4	0.5016	170.12	1	66
Camphene	-5.4	11648	0	0	2.997	136.23	0	66
3,4-Dihydroxybenzoic Acid	-6	11648	3	3	0.796	154.12	1	66
4-Dihydroxy Cinnamic Acid	-6.4	1415	2	2	1.49	164.16	2	46
Caffeic Acid	-6.5	11648	3	3	1.19	180.16	2	66
Myristic Acid	-5.6	11648	1	1	4.7721	228.37	12	66
Stearic Acid	-5.7	1415	1	1	6.335	284.5	16	46

4.6 Interaction of Ligands and Target Protein

The docking analysis is performed by using LigPlot+ (version v. 1.4.5) and PyMol Edu (v 1.7.4.5). Interactions of ligands and target proteins are predicted by using LigPlot plus (version v.1.4.5). The Graphical system of LigPlot+ automatically generates multiple 2D diagrams of interactions from 3D coordinates. These 2D diagrams portray the hydrogen-bond interaction pattern and hydrophobic contacts between the ligand and the main-chain or side-chain elements of the protein [81]. The 2D diagrams of the best binding score ligands with respective proteins are shown in Figures 4.7 to 4.12. while their hydrogen bonds and hydrophobic interactions are listed in Table 4.10 and 4.11.

4.6.1 Interaction of Ligands with Anaplastic Lymphoma Kinase

Figure Figures 4.7 shows the interaction of Isoquinoline, β-pinene, Apigenin, Salfredin B11 and Pyrazole with ALK. As observed from the 2D diagram ligand show only one hydrogen bond with Methionine. The ligand show many hydrophobic interactions with protein. The ligand contains 9 carbons and forms hydrophobic interaction with Glu1197, Leu1122, Val1130, Ala1148, Lys1150, Leu1196, Gly1269 residues. β-pinene show only hydrophobic interactions with protein. The ligand forms 9 hydrophobic interactions as shown in Figure 4.7. The ligand consist of 10 carbons and shows interaction with residues Glu1197, Leu1122, Val1130, Ala1148, Lys1150, Leu1196, Leu1256, Met1199 and Gly1269. Apigenin is a 15 carbons compound that forms 2 hydrogen bonds with the protein ALK. 7 residues form hydrophobic interactions with protein that includes Leu1196, Lys1150, Ala1148, Leu1198, Leu1122, Asp1203 and Leu1256. Figure 4.9 also shows the interaction of Salfredin B11 with protein ALK. One hydrogen bond is formed with Methionine. Salfredin B11 is a 13 carbons compound and forms 7 hydrophobic interactions with Ala1148, Leu1256, Leu1198, Lys1150, Val1130, Leu1122 and Gly1202. Pyrazole is a 3 carbons compound and forms 2 hydrogen bonds with Alanine and Glutamine.

It forms 5 hydrophobic interactions with protein. These interactions are formed by residues Glu1197, Leu1198, Ala1148, Val1180, Leu1256 and Leu 1196. Figure 4.8 shows the interaction of Pyragallol, Salicylic acid, Syringic acid, Gallic acid, Camphene with ALK. Pyragallol is a 6 carbons sugar that forms one hydrogen bond with protein by methionine. 6 hydrophobic interactions are found in this interaction. The residues forms hydrophobic interactions are Glu1197, Leu1198, Ala1148, Val1180, Leu1256 and Leu1196. Salicylic acid is a 7 carbons compound and forms a single hydrogen bond with protein by Methionine. Many hydrophobic interactions are formed by Leu1198, Val1130, Leu1122, Ala1148, Leu1256 and Glu1197. Syringic acid 9 carbons compound form 1 hydrogen bond by methionine.

5 hydrophobic interactions are formed by residues includes Val1130, Lys1150, Ala1148, Leu1189, Leu112. Gallic acid is a 7 carbons compound and forms 2 hydrogen bonds by methionine and Glutamine. 5 residues involved in hydrophobic interactions are Leu1198, Ala1148, Val1130, Leu1256 and Lys1150. Camphene is a 10 carbons sugar and forms no hydrogen bond with protein. 7 hydrophobic interactions formed by camphene involved residues Val1130, Gly1269, Lys1150, Leu1196, Ala1148, Leu1122 and Leu1256. Figure 4.9 shows the interaction of 3,4-Dihydroxybenzoic acid, 4-Dihydroxycinnamic acid, Caffeic acid, Myristic acid and Stearic acid with ALK. 3,4-Dihydroxybenzoic acid is a 7 carbons compound and forms 1 hydrogen bond by methionine. 6 residues form hydrophobic interaction that includes Leu1198, Glu1197, Leu1256, Ala1148, Val1130 and Lys1150.

4-Dihydroxycinnamic acid is a 9 carbons compound that forms 1 hydrogen bond and 8 hydrophobic interactions. Hydrogen bond is formed by methionine and hydrophobic interactions are formed by residues Gly1123, Val1130, Leu1122, Leu1124, Ala1148, Leu1256, Leu1198 and Glu1197 as shown in Figure 4.9. Caffeic acid is a 9 carbons compound and forms 2 hydrogen bond and 8 hydrophobic interactions. Hydrogen bonds are formed by methionine and glutamine. Hydrophobic interactions are formed by residues Val1180, Leu1256, Ala1148, Val1130, Leu1122, Gly1123, Leu1198 and His1124. Myristic acid is a 14 carbons compound that forms a single hydrogen bond with protein and 11 hydrophobic interactions. Asn forms a hydrogen bond and residues involved in hydrophobic interactions are Arg1253,

Leu1256, Gly1269, Asp1270, Ala1148, Glu1197, Leu1196, Met1199, Gly1269, Val1130 and Leu 1122.

Stearic acid is 18 carbons sugar and forms no hydrogen bond with protein but it is the ligands that form maximum hydrophobic interactions. 13 residues namely Lys1333, Pro1331, Tyr1330, Met1348, Asp1349, pro1350, Lys1352, Tyr1327, Trp1320, Ser1324, Pro1398, Ile1399 and Glu1400 forms hydrophobic interactions with protein ALK.

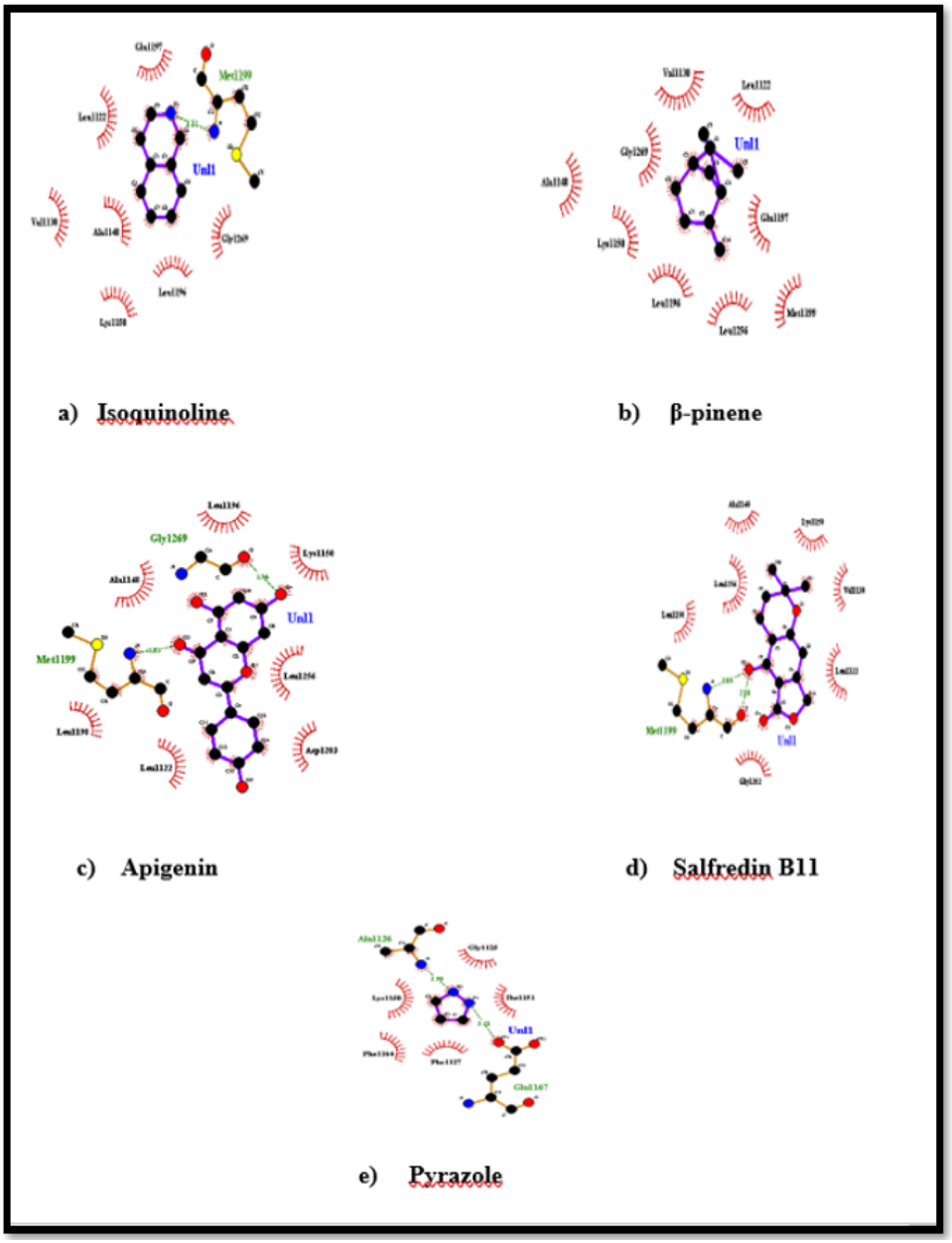

FIGURE 4.7: Interactions of ligands with the receptor protein ALK, a) Isoquinoline b) β-pinene, c) Apigenin, d) Salfredin B11, e) Pyrazole

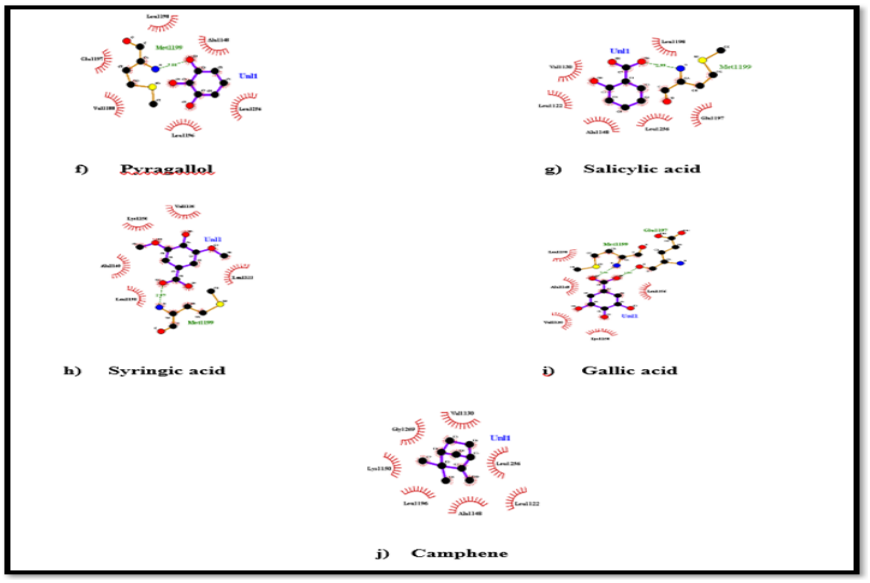

FIGURE 4.8: Interactions of ligands with the receptor protein ALK, f) Pyragallol, g) Salicylic acid, h) Syringic acid, i) Gallic acid, j) Camphene

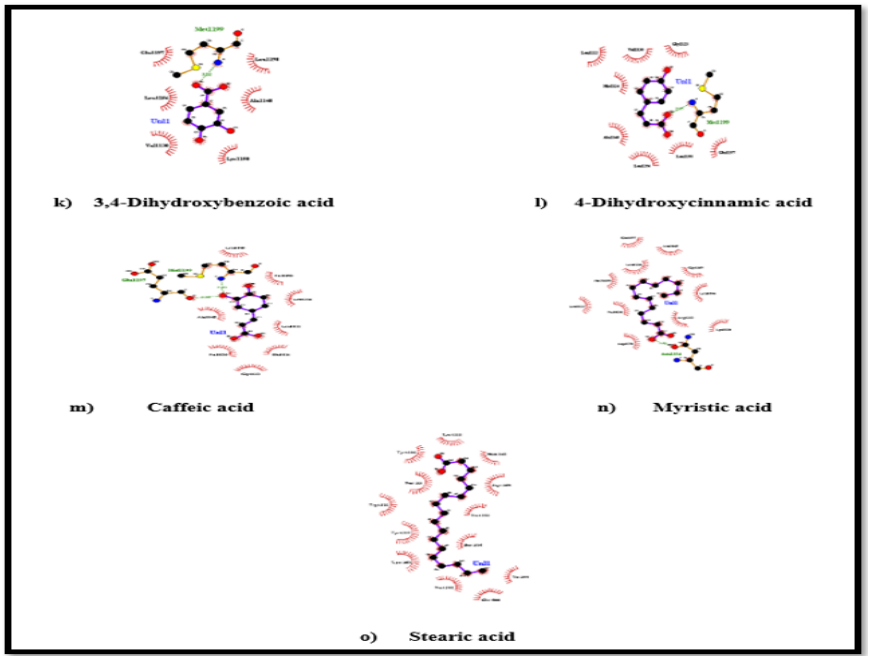

FIGURE 4.9: Interactions of ligands with the receptor protein ALK, k) 3,4-Dihydroxybenzoic acid, l) 4-Dihydroxycinnamic acid, m) Caffeic acid, n) Myristic acid

These 2D diagrams portray the hydrogen-bond interaction pattern and hydrophobic contacts between the ligand and the main-chain or side-chain elements of the protein [81]. The 2D diagrams of the best binding score ligands with respective proteins while their hydrogen bonds and hydrophobic interactions are listed in Table 4.10 and 4.11.

TABLE 4.10: Active Ligand Showing Hydrogen and Hydrophobic Interactions with ALK.

Ligands	**Binding Energy**	**No of H.B**	**Amino Acids**	**Distance**	**Hydrophobic interaction**
Isoquinoline	-5.8	1	Met1199	3.12	Glu1197 Leu1122 Val1130 Ala1148 Lys1150 Leu1196 Gly1269
β-pinene	-5.4	0			Glu1197 Leu1122 Val1130 Ala1148 Lys1150 Leu1196 Leu1256 Met1199 Gly1269
Apigenin	-7.9	2	Met1199 Gly1296	2.96 2.26	Leu1196 Lys1150 Leu1122 Ala1148 Leu1256
Salfredin B11	-7.4	1	Met1199	2.88	Leu1198 Lys1150 Val1130 Leu1122 Gly1202

TABLE 4.10: Active Ligand Showing Hydrogen and Hydrophobic Interactions with ALK.

Ligands	**Binding Energy**	**No of H.B**	**Amino Acids**	**Distance**	**Hydrophobic interaction**
Pyrazole	-3.3	2	Ala1126 Glu1167	2.90 3.21	Gly1125 Thr1151 Lys1150 Phe1164 Phe1127
Pyragallol	-4.8	1	Met1199	2.88	Glu1197 Leu1198 Ala1148 Val1180 Leu1256
Salicylic Acid	-5.2	1	Met1199	2.99	Leu1196 Leu1198 Val1130 Leu1122 Ala1148 Leu1256
Syringic Acid	-5.5	1	Met1199	2.97	Glu1197 Val1130 Lys1150 Ala1148 Leu1198
Gallic Acid	-5.4	02	Met1199 Glu1197	3.14 2.51	Ala1148 Val1130 Leu1256 Lys1150

TABLE 4.10: Active Ligand Showing Hydrogen and Hydrophobic Interactions with ALK.

Ligands	**Binding Energy**	**No of H.B**	**Amino Acids**	**Distance**	**Hydrophobic interaction**
Camphene	-5.3	0			Val1130 Gly1269 Lys1150 Leu1196 Ala1148 Leu1198 Glu1197
3,4-dihydroxy benzoic acid	-5.2	1	Met1199	3.12	Leu1256 Ala1148 Val1130 Lys1150 Gly1123
4-dihydroxy cinnamic acid	-5.8	1	Met1199	2.87	Val1130 Leu1122 Leu1124 Ala1148 Leu1256 Leu1198 Glu1197
Caffeic acid	-6	2	Met1199 Glu1197	2.83 3.08	Val1180 Leu1256 Ala1148 Val1130 Leu1122 Gly1123

TABLE 4.10: Active Ligand Showing Hydrogen and Hydrophobic Interactions with ALK.

Ligands	**Binding Energy**	**No of H.B**	**Amino Acids**	**Distance**	**Hydrophobic interaction**
Myristic acid	-5.2	1	Asn1254	2.83	Arg1253 Leu1256 Gly1269 Asp1270 Ala1148 Glu1197 Leu1196 Met1199 Gly1269 Val1130 Leu1122 Lys1333 Pro1331 Tyr1330 Met1348 Asp1349 Pro1350 Lys1352
Stearic acid	-5.5	0			Tyr1327 Trp1320 Ser1324 Pro1398 Ile1399 Glu1400

TABLE 4.11: Active Ligand Showing Hydrogen and Hydrophobic Interactions with ALK.

Ligands	**Binding Energy**	**No of H.B**	**Amino Acids**	**Distance**	**Hydrophobic Interaction**
Isoquinoline	-5.8	1	Met1199	3.12	Glu1197 Leu1122 Val1130 Ala1148 Lys1150 Leu1196 Gly1269
β-pinene	-5.4	0	-	-	Glu1197 Leu1122 Val1130 Ala1148 Lys1150 Leu1196 Leu1256
Apigenin	-7.9	2	Met1199 Gly1296	2.96 2.26	Met1199 Gly1269 Leu1196 Lys1150 Ala1148 Leu1198 Leu1122 Asp1203 Leu1256

TABLE 4.11: Active Ligand Showing Hydrogen and Hydrophobic Interactions with ALK.

Ligands	**Binding Energy**	**No of H.B**	**Amino Acids**	**Distance**	**Hydrophobic Interaction**
Salfredin B11	-7.4	1	Met1199	2.88	Ala1148 Leu1256 Leu1198 Lys1150 Val1130 Leu1122 Gly1202 Gly1125
Pyrazole	-3.3	2	Ala1126 Glu1167	2.90 3.21	Thr1151 Lys1150 Phe1164 Phe1127 Glu1197
Pyragallol	-4.8	1	Met1199	2.88	Leu1198 Ala1148 Val1180 Leu1256 Leu1196
Salicylic Acid	-5.2	1	Met1199	2.99	Leu1198 Val1130 Leu1122 Ala1148 Leu1256 Glu1197 Ala1148

TABLE 4.11: Active Ligand Showing Hydrogen and Hydrophobic Interactions with ALK.

Ligands	**Binding Energy**	**No of H.B**	**Amino Acids**	**Distance**	**Hydrophobic Interaction**
Syringic Acid	-5.5	1	Met1199	2.97	Val1130 Lys1150 Ala1148 Leu1198 Leu1122
Gallic Acid	-5.4	2	Met1199 Glu1197	3.14 2.51	Leu1198 Ala1148 Val1130 Leu1256 Lys1150
Camphene	-5.3	0	-	-	Val1130 Gly1269 Lys1150 Leu1196 Ala1148 Leu1122 Leu1256 Leu1198
3, 4-dihydroxy benzoic Acid	-5.2	1	Met1199	3.12	Glu1197 Leu1256 Ala1148 Val1130 Lys1150 Leu1256

TABLE 4.11: Active Ligand Showing Hydrogen and Hydrophobic Interactions with ALK.

Ligands	**Binding Energy**	**No of H.B**	**Amino Acids**	**Distance**	**Hydrophobic Interaction**
4-dihydroxy cinnamic Acid	-5.8	1	Met1199	2.87	Gly1123 Val1130 Leu1122 Leu1124 Ala1148 Leu1256 Leu1198 Glu1197 Val1180
Caffeic Acid	-6	2	Met1199 Glu1197	2.83 3.08	Leu1256 Ala1148 Val1130 Leu1122 Gly1123 Leu1198 Arg1253
Myristic Acid	-5.2	1	Asn1254	2.83	Leu1256 Gly1269 Asp1270 Ala1148 Glu1197 Leu1196 Met1199 Gly1269 Val1130 Leu1122

TABLE 4.11: Active Ligand Showing Hydrogen and Hydrophobic Interactions with ALK.

Ligands	**Binding Energy**	**No of H.B**	**Amino Acids**	**Distance**	**Hydrophobic Interaction**
Stearic Acid	-5.5	0	-	-	Lys1333 Pro1331 Tyr1330 Met1348 Asp1349 Pro1350 Lys1352 Tyr1327 Trp1320 Ser1324 Pro1398 Ile1399 Glu1400

4.6.2 Interaction of Ligands with EML4

Figure 4.10 shows the interaction of Isoquinoline, β-pinene, Apigenin, Salfredin B11 and Pyrazole with EML4. As observed from the 2D diagrams the ligand show only hydrophobic interactions with protein. The ligand contains 9 carbons and forms hydrophobic interaction with Asn206, Tyr226, Asn228, Gln11, Gln15, Ala12, Ile16, Ile171 residues as evident from the table 4.12. β-pinene show only hydrophobic interactions with protein. The ligand forms 7 hydrophobic interactions. The ligand consist of 10 carbons and shows interaction with residues Ala330, Val177, Lys176, Phe214, Tys210, Lys326 and Asn329 as shown in Figure 4.10. Apigenin is a 15 carbons compound that forms 4 hydrogen bonds with the protein EML4 by glutamine, asparagine and glutamic acid. 4 residues form

hydrophobic interactions with protein that includes Tys224, Cys12, Leu248 and Glu11. Figure 4.10 also shows the interaction of Salfredin B11 with protein EML4. Two hydrogen bonds are formed with glutamic acid and asparagine. Salfredin B11 is a 13 carbons compound and forms 6 hydrophobic interactions with Gln11, Asp179, Leu248, Tyr224 Asn206 and Cys12. Pyrazole is a 3 carbon compound and forms 3 hydrogen bonds with leucine, asparagine and valine. It forms 5 hydrophobic interactions with protein. These interactions are formed by residues Gly354, Ala240, Ser241, Asn356 and Ile355. Figure 4.11 shows the interaction of Pyragallol, Salicylic acid, Syringic acid, Gallic acid, Camphene with EML4. Pyragallol is a 6 carbons sugar that forms 4 hydrogen bonds with protein by glycine, asparagine, alanine and glycine. 6 hydrophobic interactions are found in this interaction. The residues forms hydrophobic interactions are Gly143, Asp69, Thr145, Glu71 and Glu254. Salicylic acid is a 7 carbons compound and forms 3 hydrogen bonds with protein by glutamine, glycine and threonine. 8 hydrophobic interactions are formed by Gly10, Gly144, Gly143, Glu254, Asn101, Glu71, Ala99 and Asp69. Syringic acid 9 carbons compound forms 4 hydrogen bonds by glycine, glutamine, threonine and asparagine. 5 hydrophobic interactions are formed by residues includes Gly144, Ser140, Gln11, Glu254 and Ala99. Gallic acid is a 7 carbons compound and forms 3 hydrogen bonds by asparagine, glycine and Glutamine. 7 residues involved in hydrophobic interactions are Gly143, Thr145, Asp69, Gly10, Glu71, Gly144 and Glu254.

Camphene is a 10 carbons sugar and forms no hydrogen bond with protein. 8 hydrophobic interactions formed by camphene involved residues Lys176, Val177, Lys326, Tyr20, Glu207, Asp211, Phe214 and Asn329. Figure 4.12 shows the interaction of 3,4-Dihydroxybenzoic acid, 4-Dihydroxycinnamic acid, Caffeic acid, Myristic acid and Stearic acid with EML4. 3,4-Dihydroxybenzoic acid is a 7 carbons compound and forms 4 hydrogen bonds by glycine, glutamine, threonine and asparagine.

6 residues form hydrophobic interaction that includes Gly144, Gly143, Gly10, Glu71, Glu254 and Ala99. 4-Dihydroxycinnamic acid is a 9 carbons compound that forms 1 hydrogen bond and 7 hydrophobic interactions. Hydrogen bond is

formed by tyrosine and hydrophobic interactions are formed by residues Gln14, Ala12, Ile16, Asn228, Ile171, Asn206 and Thr179. Caffeic acid is a 9 carbons compound and forms 5 hydrogen bond and 6 hydrophobic interactions. Hydrogen bonds are formed by alanine, glutamine, asparagine, selenocysteine and cysteine. Hydrophobic interactions are formed by residues Glu154, Gly144, Gly10, Glu11, Asp69 and Thr145. Myristic acid is a 14 carbons compound that forms a single hydrogen bond with protein and 12 hydrophobic interactions. Selenocysteine forms a hydrogen bond and residues involved in hydrophobic interactions are Lys326, Tyr210, Lys326, Lys176, Thr349, Phe351, Ile332, Ala333, Pro175, Val1177, Phe214 and Asn329. Stearic acid is 18 carbons sugar and forms 3 hydrogen bonds with protein by glycine, threonine and glycine. 12 residues namely Gln15, Gly10, Asn206, Thr126, Ile171, Gly143, Glu133, Tyr224, Asn228, Ser140, Thr179 and Asn228 forms hydrophobic interactions with protein EML4.The ligand contains 9 carbons and forms hydrophobic interaction with Asn206, Tyr226, Asn228, Gln11, Gln15, Ala12, Ile16, Ile171 residues as evident from the table 4.12.

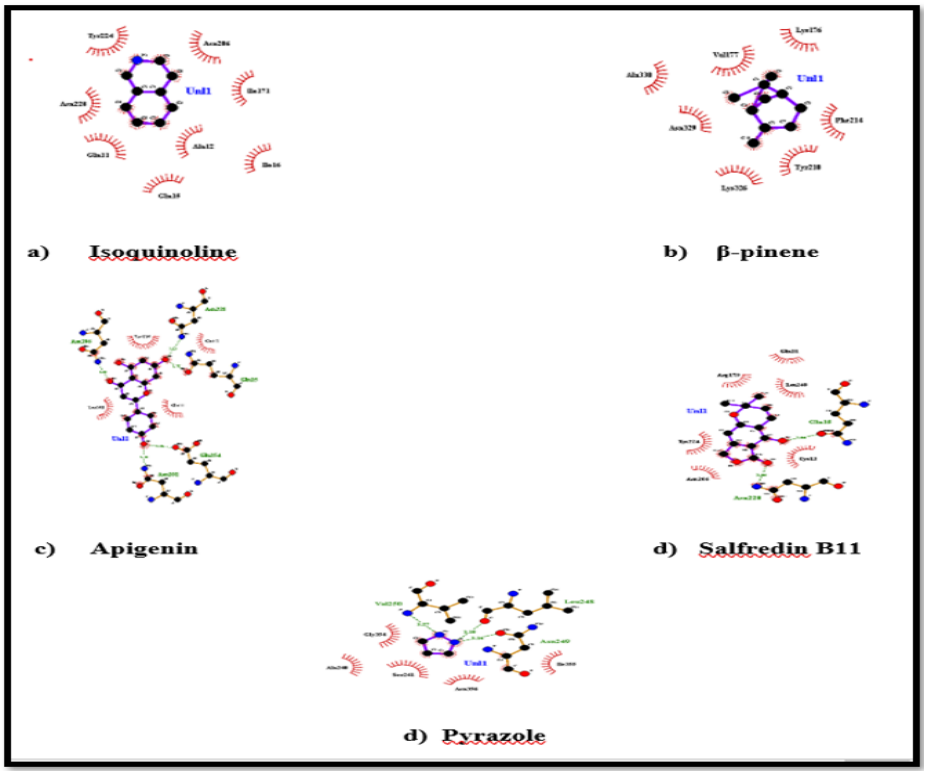

FIGURE 4.10: Interactions of ligands with the receptor protein EML4, a) Isoquinoline b) β-pinene, c) Apigenin, d) Salfredin B11, e) Pyrazole

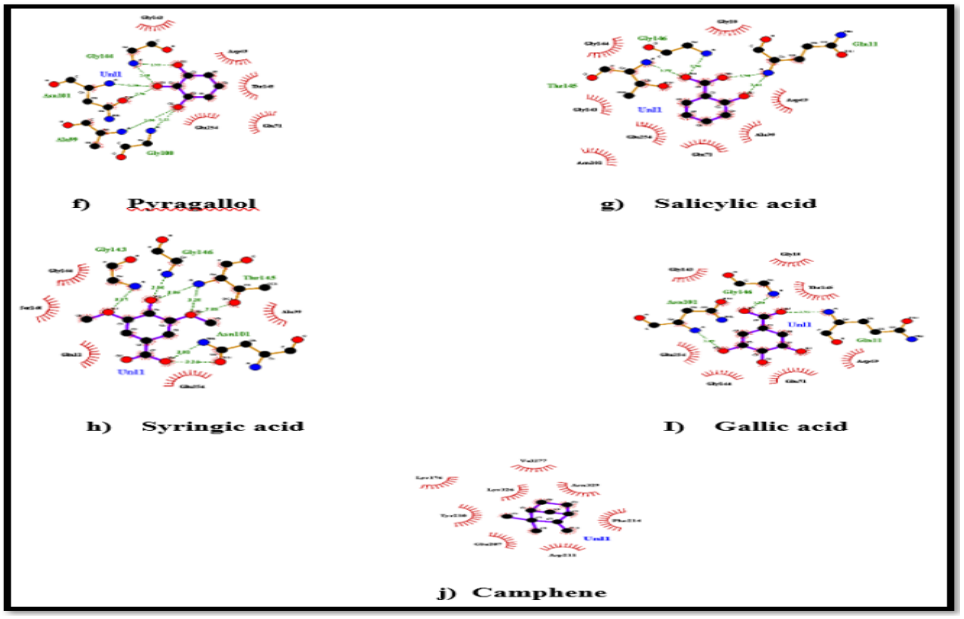

FIGURE 4.11: Interactions of ligands with the receptor protein EML4, f) Pyragallol, g) Salicylic acid, h) Syringic acid, i) Gallic acid, j) Camphene

Above interactions of ligands with the receptor protein EML4, f) Pyragallol, g) Salicylic acid, h) Syringic acid, i) Gallic acid, j) Camphene

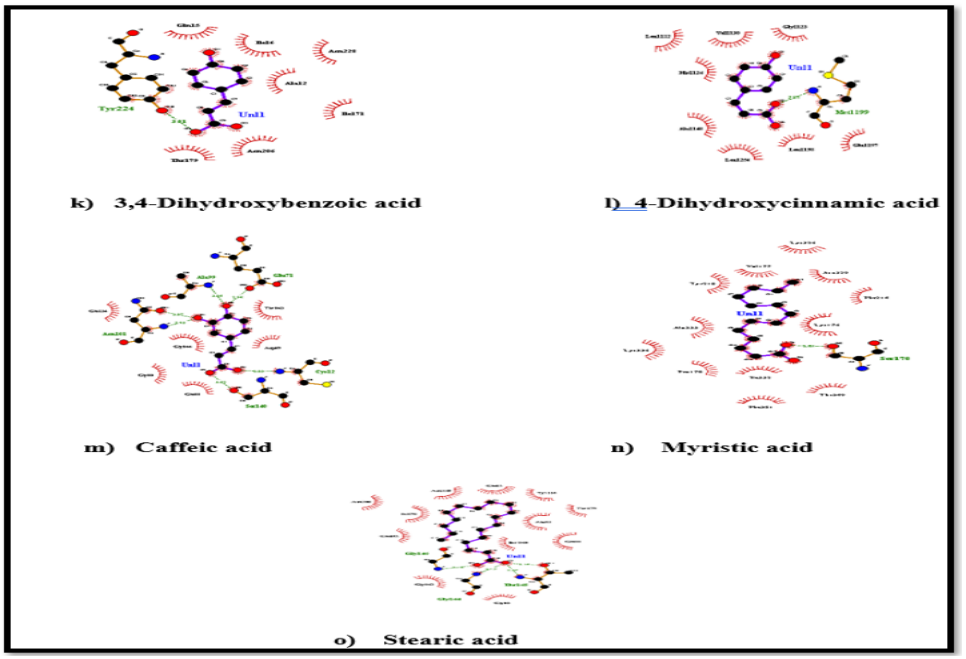

FIGURE 4.12: Interactions of ligands with the receptor protein ALK, k) 3,4-Dihydroxybenzoic acid, l) 4-Dihydroxycinnamic acid, m) Caffeic acid, n) Myristic acid

Above interactions of ligands with the receptor protein ALK, k) 3,4-Dihydroxybenzoic acid, l) 4-Dihydroxycinnamic acid, m) Caffeic acid, n) Myristic acid

TABLE 4.12: Active Ligands Showing Hydrogen and Hydrophobic Interactions with EML4

Ligands	**Binding Energy**	**No of H.B**	**Amino Acids**	**Distance**	**Hydrophobic Interaction**
					Asn206
					Tyr226
					Asn228
Iso-quinoline	-5.6	0	-	-	Gln11
					Gln15
					Ala12
					Ile16
					Ile171
					Ala330
					Val177
					Lys176
β-pinene	-5.5	0	-	-	Phe214
					Tys210
					Lys326
					Asn329
					Tys224
			Asn226	2.15	
			Gln15	1.77	Cys12
Apigenin	-8.1	4	Asn206	1.51	
			Glu254	2.18	Leu248
			Asn101	2.10	
					Glu11

TABLE 4.12: Active Ligands Showing Hydrogen and Hydrophobic Interactions with EML4

Ligands	**Binding Energy**	**No of H.B**	**Amino Acids**	**Distance**	**Hydrophobic Interaction**
Salfredin B11	-7.2	2	Gln15 Asn228	3.04 3.06	Gln11 Asp179 Leu248 Tyr224 Asn206 Cys12 Gly354
Pyrazole	-4.2	3	Leu248 Asn249 Val250	3.18 3.16 3.27	Ala240 Ser241 Asn356
Pyragallol	-5.7	4	Gly144 Asn102 Ala99 Gly100	3.01 2.30 3.06 3.13	Ile355 Gly143 Asp69 Thr145 Glu71 Glu254 Gly10 Gly144
Salicylic Acid	-5.7	3	Gln11 Gly146 Thr145	3.03 1.96 1.99	Gly143 Glu254 Asn101

TABLE 4.12: Active Ligands Showing Hydrogen and Hydrophobic Interactions with EML4

Ligands	**Binding Energy**	**No of H.B**	**Amino Acids**	**Distance**	**Hydrophobic Interaction**
Syringic Acid	-6	4	Gly143 Gln146 Thr145 Asn101	2.88 3.17 2.88 3.01	Gly144 Ser140 Gln11 Glu254
Gallic Acid	-6.3	3	Asn101 Gly146 Gln11	3.09 1.50 1.95	Ala99 Gly143 Gly10 Thr145 Asp69 Glu71
Camphene	-5.4	0	-	-	Gly144 Glu254 Lys176 Val177 Lys326 Tyr20 Glu207 Asp211 Phe214 Asn329
3,4-dihydroxy benzoic Acid	-6	4	Gly146 Gln11 Thr145 Asn101	2.78 2.91 3.16 3.05	Gly144 Gly143 Gly10

TABLE 4.12: Active Ligands Showing Hydrogen and Hydrophobic Interactions with EML4

Ligands	**Binding Energy**	**No of H.B**	**Amino Acids**	**Distance**	**Hydrophobic Interaction**
4-dihydroxy cinnamic Acid	-6.4	1	Tyr224	3.01	Gln14 Ala12 Ile16 Asn228 Thr179
Caffeic Acid	-6.5	5	Ala99 Glu71 Asn101 Sec140 Cys12	3.04 2.94 2.03 3.02 3.03	Glu154 Gly144 Gly10 Glu11 Asp69 Thr145 Lys326
Myristic Acid	-5.6	1	Sec178	2.51	Tyr210 Lys326 Lys176 Thr349 Phe351 Ile332 Ala333
Stearic Acid	-5.7	3	Gly146 Thu145 Gly144	3.15 2.97 3.13	Gln15 Gly10 Asn206 Thr126 Ile171 Gly143 Glu133

4.7 ADME Properties of Ligands

Lipinski's five drug rule is the initial step in assessing the verbal bioavailability and artificial availability. A second study was performed by calculating the ADMET properties of ligands as a measure of pharmacokinetics using the online tool pkCSM [82]. In pharmacology, there are two broad terms pharmacodynamics and pharmacokinetics which was discussed below.

4.7.1 Pharmacodynamics

Pharmacodynamics is the branch of pharmacology in which we study the effect of drugs on the body.

4.7.2 Pharmacokinetics

Pharmacokinetics is the branch of pharmacology in which we study the effect of body on drugs. We study the absorption of drugs, distribution of drugs, metabolism of drugs and excretion of drugs.

4.7.3 Absorption

In pharmacology especially pharmacokinetics, the transfer of drug from the blood stream into the tissues is called absorption. So, the chemical composition of a drug, as well as the environment in which drug is placed, work together to determine the rate and extend of drug absorption. Absorption is one of the ADME properties that determines the absorption of orally administered drugs and includes Water solubility, Intestinal absorption, Skin permeability, P-glycoprotein substrate and P- glycoprotein I and II inhibitors.

Water solubility (log S) of a compound predicts its solubility in water at 25C. It is predicted as a molar concentration logarithm (log mol/L). Lipid soluble drugs are less soluble in water than water soluble drugs.

The Caco-2 permeability model determines the logarithm of the apparent permeability coefficient (log Papp; log cm/s). A compound has a high Caco-2 absorbency if it has a Papp >8 x 10-6 cm/s (>0.9 in terms of pkCSM predictive value). Intestinal absorption predicts the percentage that will enter a person's small intestine. A compound with less than 30% absorption is less absorbent.

The Skin permeability depicts the absorbency in log Kp value, it has a valuable role in the formation of transdermal drugs. The element with the log Kp >-2.5 shows less skin penetration.

The P-glycoprotein substrates act as a natural barrier and removes toxins from the cell. This model predicts that the given compound is a P-glycoprotein (P-gp) substrate or not. If a compound show P-glycoprotein substrate then it may show low oral absorption. To reduce the absorption, P-glycoprotein can be easily removed from the cell.

P-glycoprotein I/II inhibitor model predicts that a compound may be a P-gp I/II inhibitor or not. P-gp inhibitors reduce the activity of P-gp and have high absorption.

Absorption properties as mentioned in the Table 4.13 and 4.14 shows that all the ligands show less water solubility. Caco2 permeability in the form of log Papp in 10-6 cm/S is within the normal range. The values of intestinal absorption values are good in the range. Skin permeability values in the form of log Kp are low. Apigenin, Salfredin B 11, Pyrazole and Syringic acid are predicted as P-glycoprotein substrate.

TABLE 4.13: a)Absorption properties of ligands

Ligands	**Water Solubility (mol/L)**	**$CaCO_2$ Permeability (cm/S)**	**Intestinal Absorption (%)**	**Skin Permeability (Log Kp)**
Isoquinoline	-1.721	1.549	97.359	-1.824
β-pinene	-4.191	1.385	95.525	-1.653

TABLE 4.13: a)Absorption properties of ligands

Ligands	**Water Solubility (mol/L)**	**$CaCO_2$ Permeability (cm/S)**	**Intestinal Absorption (%)**	**Skin Permeability (Log Kp)**
Apigenin	-3.329	1.007	93.25	-2.735
Salfredin B11	-3.081	1.201	94.508	-3.236
Pyrazole	0.178	1.579	90.415	-3.276
Pyragallol	-1.408	1.122	83.549	-2.751
Salicylic Acid	-1.808	1.151	83.887	-2.723
Syringic Acid	-2.223	0.495	73.076	-2.735
Gallic Acid	-2.56	-0.081	43.374	-2.735
Camphene	-4.34	1.387	94.148	-1.435
3,4-Dihydroxy-benzoic Acid	-2.069	0.49	71.17	-2.727
4-Dihydroxy-cinnamic Acid	-2.378	1.21	93.49	-2.715
Caffeic Acid	-2.33	0.634	69.40	-2.722
Myristic Acid	-4.952	1.56	92.691	-2.705
Stearic Acid	-5.973	1.556	91.31	-2.726

TABLE 4.14: b).Absorption properties of ligands

Ligands	**P-Glycoprotein Substrate**	**P-Glycoprotein I Inhibitor**	**P-Glycoprotein II Inhibitor**
Isoquinoline	No	No	No
β-pinene	No	No	No
Apigenin	Yes	No	No
Salfredin B11	No	No	No
Pyrazole	Yes	No	No
Pyragallol	No	No	No
Salicylic Acid	No	No	No
Syringic Acid	Yes	No	No
Gallic Acid	No	No	No
Camphene	No	No	No
3,4-Dihydroxybenzoic Acid	No	No	No
4-Dihydroxycinnamic Acid	No	No	No
Caffeic Acid	No	No	No
Myristic Acid	No	No	No
Stearic Acid	No	No	No

4.7.4 Distribution

Distribution in pharmacology is the branch of pharmacokinetics that deals with the movement of drugs in all over the body. Distribution as one of the ADME property includes four models namely as Volume of distribution in human (VDss expressed as log L/kg), Function unbound in humans (Fu), Blood brain barrier (BBB) permeability expressed as log PS [83].

TABLE 4.15: Distributive properties of ligands

Ligands	**VDss -Human (L/Kg)**	**Fraction Unbound (Fu)**	**BBB Permeability (log BB)**	**CNS Permeability (Log PS)**
Isoquinoline	0.024	0.338	0.316	-1.91
β-pinene	0.685	0.35	0.818	-1.857
Apigenin	0.822	0.147	-0.734	-2.061
Salfredin B11	0.363	0.465	-0.747	-2.827
Pyrazole	-0.213	0.779	-0.242	-2.947
Pyragallol	0.13	0.712	-0.441	-3.252
Salicylic Acid	-1.57	0.563	-0.334	-3.21
Syringic Acid	-1.443	0.601	-0.191	-2.701
Gallic Acid	-1.855	0.617	-1.102	-3.74
Camphene	0.547	0.354	0.787	-1.71
3,4-Dihydroxy-benzoic Acid	-1.298	0.648	-0.683	-3.305
4-Dihydroxy-cinnamic Acid	-1.151	0.428	-0.225	-2.418

TABLE 4.15: Distributive properties of ligands

Ligands	**VDss -Human (L/Kg)**	**Fraction Unbound (Fu)**	**BBB Permeability (log BB)**	**CNS Permeability (Log PS)**
Caffeic Acid	-1.098	0.529	-0.647	-2.608
Myristic Acid	-0.578	0.171	-0.027	-1.925
Stearic Acid	-0.528	0.051	-0.195	-1.707

Model-I explains the theoretical volume that the total amount of drug will need to be evenly distributed to provide the same concentration in blood plasma. VDss is considered low, if it is less than 0.71 L/kg (log VDss <0.15) and higher if it is above 2.81 L/kg (log VDss >0.45). If VDss is high, it means that more drug dispense to the tissues rather to plasma. If a compound shows more Fu value, its mean it is more effective. BBB protects the brain from exogenous compounds, so BBB permeability is an important parameter 4.15.

4.7.5 Metabolism

CYP1A2, CYP2C19, CYP2C9, CYP2D6 and CYP3A4 models of the various isoforms of Cytochrome P450 that act as an important cleansing enzyme found in the liver. This enzyme reacts to xenobiotic to facilitate their release. Some drugs are triggered by this enzyme while most drugs are neutralized by it.

The ligands listed in table 4.16 do not act as substrate of any isoform except Stearic acid act as CYP2D6 substrate while Pyragallol and Stearic acid act as CYP3A4 substrate. The ligands Isoquinoline and Apigenin act as inhibitor of CYP1A2 isoform. Stearic acid acts as an inhibitor of CYP3A2 isoform.

Table 4.16: Metabolic properties of ligands

Ligands	**CYP2D6**	**CYP3A4**	**CYP1A2**	**CYP2C19**	**CYP2C9**	**CYP2D6**	**CYP3A4**
	Substrate	**Substrate**	**Inhibitor**	**Inhibitor**	**inhibitor**	**Inhibitor**	**Inhibitor**
Isoquinoline	No	No	Yes	No	No	No	No
β-pinene	No	No	No	No	No	No	No
Apigenin	No	No	Yes	No	No	No	No
Salfredin B11	No	No	No	No	No	No	No
Pyrazole	No	No	No	No	No	No	No
Pyragallol	No	Yes	No	No	No	No	No
Salicylic Acid	No	No	No	No	No	No	No
Syringic Acid	No	No	No	No	No	No	No
Gallic Acid	No	No	No	No	No	No	No
Camphene	No	No	No	No	No	No	No

Table 4.16: Metabolic properties of ligands

Ligands	**CYP2D6**	**CYP3A4**	**CYP1A2**	**CYP2C19**	**CYP2C9**	**CYP2D6**	**CYP3A4**
	Substrate	**Substrate**	**Inhibitor**	**Inhibitor**	**inhibitor**	**Inhibitor**	**Inhibitor**
3,4-Dihydroxy-benzoic acid	No	No	No	No	No	No	No
4-Dihydroxy-cinnamic Acid	No	No	No	No	No	No	No
Caffeic Acid	No	No	No	No	No	No	No
Myristic Acid	No	No	No	No	No	No	No
Stearic Acid	Yes	Yes	No	No	No	No	No

4.7.6 Excretion

The organs involved in drug excretion are the kidneys, which play important role in excretion (renal excretion) and the liver (biliary excretion). Other organs may be also be involved in excretion, such as the lungs for volatile or gaseous agents. Drugs can be secreted in sweat, saliva and tears. Models of Excretion property are Total Clearance (CL tot) expressed as log (CL tot) in ml/min/kg and second one is Renal OCT2 substrate which predicts results as Yes/No. OCT2 (organic cation transporter 2) is a renal uptake transporter that plays role in disposition and renal clearance of drugs [85].

All ligands exhibit well total clearance. All ligands showed negative result for model Renal OCT2 substrate except. Excretory properties are listed in Table 4.17 .

TABLE 4.17: Excretory properties of ligands

Ligands	**Total Clearance (ml/kg)**	**Renal OCT2 Substrate**
Isoquinoline	0.286	No
β-pinene	0.03	No
Apigenin	0.566	No
Salfredin B11	0.481	No
Pyrazole	0.62	No
Pyragallol	0.104	No
Salicylic acid	0.607	No
Syringic acid	0.646	No
Gallic acid	0.518	No
Camphene	0.049	No
3,4-Di hydroxy benzoic acid	0.551	No
4-Dihydroxy cinnamic acid	0.662	No
Caffeic acid	0.508	No

TABLE 4.17: Excretory properties of ligands

Ligands	**Total Clearance (ml/kg)**	**Renal OCT2 Substrate**
Myristic acid	1.693	No
Stearic acid	1.832	No

4.8 Lead Compound Identification

The identification of compound as a drug or non-drug is determined by Physiochemical and Pharmacokinetics properties. Physiochemical properties or Lipinski's rule act as first or a primary filter and then pharmacokinetics comes that sorts further potential compounds. Gallic acid do not obey Lipinski's rule of five, so it is knock out in primary screening. Pharmacokinetic studies screen out the compounds Isoquinoline, β-pinene and Camphene (log BB >0.3).

TABLE 4.18: Hit compounds with binding scores with ALK.

Name of Potential Compound	**Binding Score with ALK**
Apigenin	-7.9
Salfredin B11	-7.4
Syringic Acid	-5.5
4-Dihydroxy- benzoic Acid	-5.8
Caffeic Acid	-6

TABLE 4.19: Hit compounds with binding scores with EML4 .

Name of Potential Compound	**Binding Score with ALK**
Apigenin	-8.1
Salfredin B11	-7.2
Syringic Acid	-6
4-Dihydroxy-cinnamic Acid	-6.4
Caffeic Acid	-6.5

Myristic and stearic acid is screen out due to skin sensitivity property. The best compounds are selected on the basis of primary and secondary filters, toxicity predicted values and binding scores. These are Apigenin, Pyrazole, Pyragallol, Salicylic acid, Syringic acid and Caffeic acid.

4.9 Selection of Lead Drugs

Selection of the most efficient drug is based on the physiochemical properties that include molecular formula, molecular weight, water solubility, log P value, absorption, hydrogen bond donors and acceptors, polarization, bioavailability and ADMET probability. The side effects of the selected drugs were also studied using Drug bank database, PubChem and pkCSM tools. Mechanisms of action of selected drugs are listed in Table 4.43. Crizotinib has been selected as a standard drug against ALK receptors which is known very commonly in treating Lungs cancer [86]. Paclitaxel has been selected as standard drug against EML4. It is a standard drug used to treat lung cancers. It acts with the novel mechanism of actions by promoting polymerization of tubulin dimers to form microtubules and stabilizes microtubules by preventing depolymerisation [87].

4.10 Reference Drugs Actions:

4.10.1 Crizotinib Action against ALK

Crizotinib is a tyrosine kinase (TK) inhibitor and target ALK under its activation. ALK inhibits the apoptosis and induces cell proliferation. ALK gene translocation leads to the expression of proteins involved in cancer/oncogenic fusion. In most cases of NSCLC, ALK fusion with EML4 results in kinase activity. Crizotinib inhibits the activity of ALK by inhibiting its phosphorylation, results in inactive protein confirmation. This reduces the growth of cells having this genetic mutation and tumor survivability [88].

4.10.2 Paclitaxel action against EML4

Paclitaxel had reported to induce ROS (Reactive Oxygen Species) generation and it increase hydro peroxide production by increasing the NADPH (Nicotinamide Adenine Dinucleotide Phosphate) oxidase activity that induces oxidative stress and also play a role in anticancer activity. Paclitaxel targets the microtubule proteins. Paclitaxel high concentration causes mitotic arrest at G2 or M phase, while its low concentration induces apoptosis at G0 and G1or S phase. Paclitaxel induce proapoptotic activity by activating multiple signaling pathways [89].

4.11 Physiochemical Properties of Drugs

Physiochemical properties of the selected drugs Crizotinib and Paclitaxel for ALK and EML4 respectively are shown in 4.20

TABLE 4.20: Physiochemical properties of Drugs.

Properties	**Crizotinib**	**Paclitaxel**
Chemical Formula	$C_{21}H_{22}Cl_{12}FN_5O$	$C_{47}H_{51}NO_{14}$

TABLE 4.20: Physiochemical properties of Drugs.

Properties	**Crizotinib**	**Paclitaxel**
Absorption	5 hours	7 hours
Water Solubility mg/ml	0.5 mg/ml	0.0056 mg/ml
log P	5.0377	3.7357
H-bond Donor	02	4
H-bond Acceptor	06	14
Molecular Weight	450.345 g/mol	853.9 g/mol
Rotatable Bonds	5	10
Bioavailability	1	0
Polarizability	45.04 Å3	87.15 Å3
Side Effects	Sensitivity to light, numbness, difficulty falling asleep, dark urine, nausea, vomiting and difficulty in swallowing	Redness of face, neck, arm, occasionally upper neck, bruising, unusual bleeding, tiredness and blurred vision.

4.12 2D Structure of Reference Drugs

2D structures of both the reference drugs (Crizotinib for ALK and Paclitaxel for EML4) were obtained from the online tool PubChem.

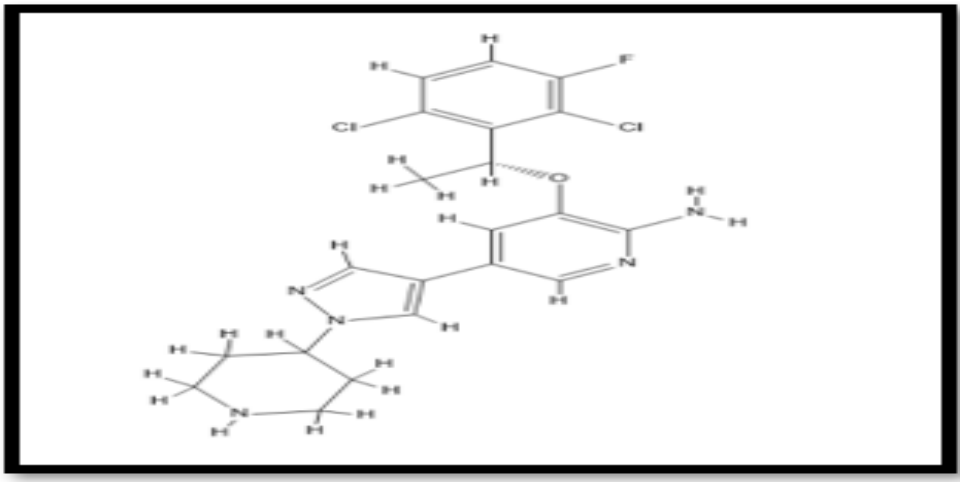

FIGURE 4.13: 2D Structure of Crizotinib Drug- PubChem

Figure 4.13 shows the bonding pattern of Drug Crizotinib for ALK protein. The simplified 2D structure of drug is used to display molecular configuration, profiles and interactions.

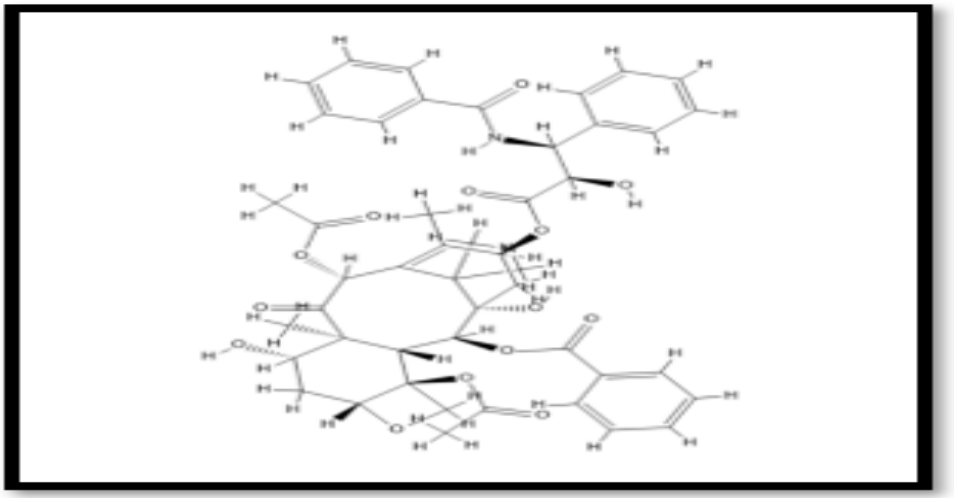

FIGURE 4.14: 2D Structure of Crizotinib Drug- PubChem

Figure 4.14 shows the bonding pattern of Drug Paclitaxel for EML4 protein. The simplified 2D structure of drug is used to display molecular configuration, profiles and interactions.

4.13 Drug ADMET Properties

Online tool pkCSM determines the ADMET properties (Absorption, Distribution, Metabolism, Excretion and Toxicity) of the reference drugs (Crizotinib and Paclitaxel).

4.13.1 Toxicity Prediction of Reference Drug-Crizotinib

The toxicity predictions of reference drug Crizotinib are listed in Table 4.21. The maximum tolerated dose value is shown as -0.095. The drug predicts as hERG II inhibitor which determines that it inhibits potassium channels. LD50 determines the potential of drug and LOAEL predicts the lowest dose that causes adverse effects. Crizotinib is a hepatotoxic that's mean it does cause liver injury.

T.pyriformis toxicity measures toxic end point (pIGC50 that is negative logarithm of the concentration required to stop 50% growth >-0.5 is considered as toxic). Crizotinib predicts pIGC out of this range.

The last model Minnow toxicity predicts LC50 in mM that shows the lethal concentration of a molecule that is enough to kill 50% flathead minnows (flat bait fishes). Crizotinib predicts minnow toxicity value as 0.942 log mM.

4.13.2 Absorption Properties

Absorption properties of Crizotinib are shown in Table 4.21. As evident from the table,

- Crizotinib is less soluble in water and has 92.006% absorption in small intestine of human. Skin permeability is low. Crizotinib is a P-gp substrate and P-gp I/II inhibitor. It means that standard drug has low Oral absorption.

P-gp I/II inhibitor 'Yes' predicts that Crizotinib has reduced pumping activity to pump out the xenobiotic from cell and have high absorption.

4.13.3 Distribution Properties

Distribution properties consist of four models. The first is the volume of distribution in human (VDss) expressed as L/Kg. Crizotinib Shows high VDss =0.801 L/Kg that means the drug is more distributed in tissue rather plasma. Second model is Fraction unbound (Fu) determines the unbound friction in plasma.

It is more than drug may be more effective. Crizotinib has 0.132 Fu predicted value. The third model is BBB permeability (blood brain barrier permeability) is expressed as log BB (value >-1 predicts that drug is not safe for brain). Crizotinib shows BBB permeability -1.164 slightly higher than -1. The last model is CNS permeability (Central Nervous System permeability) is expressed as log PS <-3 considered as safe. Crizotinib shows log PS -1.473 (Table 4.21).

4.13.4 Metabolic Properties

Reference drug Crizotinib metabolic properties are given in 4.21. Cytochrome P450 is found in liver that has a detoxification function and plays a role in excretion of exogenous compounds by oxidizing them.

CYP2D6 and CYP3A4 are the two main isoforms of cytochrome P450. Crizotinib is metabolized by one isoform CYP3A4. This drug is also an inhibitor of CYP1A2, CYP2C9 and CYP3A4. Crizotinib is not an inhibitor of CYP2C19 and CYP2D6 isoform of cytochrome P450.

4.13.5 Excretion Properties

The predicted value of excretion properties of Crizotinib are given in 4.21. Total clearance is expressed as log (CL tot) value is 0.556 ml/kg that predicts the hepatic and renal clearance of Crizotinib. OCT2 is an organic cation transporter 2 that play a role in disposition and renal clearance of drugs. Crizotinib shows Renal OCT2 substrate 'Yes' which means it interfere the function of OCT2 in the cell.

TABLE 4.21: ADMET properties of reference drug- Crizotinib.

ADMET Properties	**Model Name**	**Predicted Values**
Toxicity	AMES Toxicity	No
	Max. Tolerated Dose (human)	-0.095 mg/Kg
	hERG I Inhibitor	No
	hERG II Inhibitor	Yes
	Oral rat acute Toxicity	3.515 mol/Kg
	Oral rat chronic toxicity	1.57 mg/kg
	Hepatotoxicity	Yes
	Skin sensitization	No
	T.pyriformis toxicity	0.296 log ug/L
	Minnow toxicity	0.942 log mM
Absorption	Water solubility	-4.14 mol/L
	Caco2 permeability	0.702 cm/S

TABLE 4.21: ADMET properties of reference drug- Crizotinib.

ADMET Properties	**Model Name**	**Predicted Values**
Distribution	Intestinal absorption (human)	92.006%
	Skin permeability	-2.747 log Kp
	P-glycoprotein substrate	Yes
	P-glycoprotein I inhibitor	Yes
	P-glycoprotein II inhibitor	Yes
	VDss (human)	0.801 L/Kg
	Fraction unbound (human)	0.132 Fu
	BBB permeability	-1.164 log BB
	CNS permeability	-2.222 Log PS
Metabolism	CYP2D6 substrate	No
	CYP3A4 substrate	Yes
	CYP1A2 inhibitor	Yes

TABLE 4.21: ADMET properties of reference drug- Crizotinib.

ADMET Properties	**Model Name**	**Predicted Values**
	CYP2C19 inhibitor	No
	CYP2C9 inhibitor	Yes
	CYP2D6 inhibitor	No
	CYP3A4 inhibitor	Yes
Excretion	Total Clearance (ml/kg)	0.571
	Renal OCT2 substrate	Yes

4.13.6 Toxicity Prediction of Reference Drug- Paclitaxel

The toxicity prediction of reference drug Paclitaxel is listed in 4.22. The maximum tolerated dose value is shown as 0.199. The drug predicts as hERG II inhibitor which determines that it inhibit potassium channels. LD50 determines the potential of drug and LOAEL predicts the lowest dose that causes adverse effects.

Paclitaxel is non-hepatotoxic that's mean it does not cause liver injury. *T.pyriformis* toxicity measures toxic end point (pIGC50 that is negative logarithm of the concentration required to stop 50% growth >-0.5 is considered as toxic).

Paclitaxel predicts pIGC out of this range. The last model Minnow toxicity predicts LC50 in mM that shows the lethal concentration of a molecule that is enough

to cause death of 50% flathead minnows (flat bait fishes). Paclitaxel predicts minnow toxicity value as 2.988 log mM.

4.13.7 Absorption Properties

Paclitaxel shows absorption properties as shown in 4.22. As shown in table, Paclitaxel is less soluble in water and has 100% absorption in small intestine of human. Skin permeability is low. Paclitaxel is a P-gp substrate and P-gp I/II inhibitor. It means that standard drug has low Oral absorption. P-gp I/II inhibitor 'Yes' predicts that Paclitaxel has reduced pumping activity to pump out the xenobiotic from cell and have high absorption.

4.13.8 Distribution Properties

Distribution properties consist of four models. The first is the volume of distribution in human (VDss) expressed as L/Kg. Paclitaxel Shows high VDss =1.458 L/Kg that means the drug is more distributed in tissue rather plasma. Second model is Fraction unbound (Fu) determines the unbound friction in plasma. It is more than drug may be more effective. Paclitaxel has 0.132 Fu predicted value. The third model is BBB permeability (blood brain barrier permeability) is expressed as log BB (value >-1 predicts that drug is not safe for brain). Paclitaxel show BBB permeability as -1.164. The last model is CNS permeability (Central Nervous System permeability) is expressed as log PS <-3 considered as safe. Paclitaxel shows log PS -1.473. The distribution properties are listed in 4.22 .

4.13.9 Metabolic Properties

The Reference drug Paclitaxel metabolic properties are given in 4.22. Cytochrome P450 is found in liver that has a detoxification function and plays a role in excretion of exogenous compounds by oxidizing them. CYP2D6 and CYP3A4 are the two main isoforms of cytochrome P450. Paclitaxel is metabolized by one isoform

CYP3A4. This drug is also an inhibitor of CYP3A4. Paclitaxel is not an inhibitor of CYP2C19 and CYP2D6 isoform of cytochrome P450.

4.13.10 Excretion Properties

The predicted value of excretion properties of Paclitaxel are given in 4.22 . Total clearance is expressed as log (CL tot) value is -0.36 ml/kg that predicts the hepatic and renal clearance of Paclitaxel. OCT2 is an organic cation transporter 2 that play a role in disposition and renal clearance of drugs. Paclitaxel shows Renal OCT2 substrate 'No' which means it is interfering in the function of OCT2 in the cell.

TABLE 4.22: ADMET properties of reference drug-Paclitaxel.

ADMET Properties	**Model Name**	**Paclitaxel**
Toxicity	AMES toxicity	No
	Max. tolerated dose (human)	0.199 mg/Kg
	hERG I inhibitor	No
	hERG II inhibitor	Yes
	Oral rat acute toxicity	2.776 mol/Kg
	Oral rat chronic toxicity	3.393 mg/kg
	Hepatotoxicity	Yes

TABLE 4.22: ADMET properties of reference drug-Paclitaxel.

ADMET Properties	**Model Name**	**Paclitaxel**
	Skin sensitization	No
	T.pyriformis toxicity	0.285 log ug/L
	Minnow toxicity	2.988 log mM
Absorption	Water solubility	-3.158 mol/L
	Caco2 permeability	0.623 cm/S
	Intestinal absorption (human)	100%
	Skin permeability	-2.735 log Kp
	P-glycoprotein substrate	Yes
	P-glycoprotein I inhibitor	Yes
	P-glycoprotein II inhibitor	Yes
Distribution	VDss (human)	1.458 L/Kg
	Fraction unbound (human)	0 Fu

Table 4.22: ADMET properties of reference drug-Paclitaxel.

ADMET Properties	**Model Name**	**Paclitaxel**
	BBB permeability	-1.731 log BB
	CNS permeability	-3.95 Log PS
Metabolism	CYP2D6 substrate	No
	CYP3A4 substrate	Yes
	CYP1A2 inhibitor	Yes
	CYP2C19 inhibitor	No
	CYP2C9 inhibitor	Yes
	CYP2D6 inhibitor	No
	CYP3A4 inhibitor	Yes
Excretion	Total Clearance (ml/kg)	-0.36
	Renal OCT2 substrate	No

4.14 Mechanism of Actions of Standard Drugs

4.14.1 Crizotinib Mechanism of Action

Figure 4.15 shows the mechanism of action of Crizotinib .Crizotinib is a tyrosine kinase (TK) inhibitor and target ALK under its activation. ALK inhibits the apoptosis and induces cell proliferation. ALK gene translocation leads to the expression of proteins involved in cancer/oncogenic fusion. In most cases of NSCLC, ALK fusion with EML4 results in kinase activity. Crizotinib inhibits the activity of ALK by inhibiting its phosphorylation, results in inactive protein confirmation. This reduces the growth of cells having this genetic mutation and tumor survivability [90]. Crizotinib is an orally bioavailable molecule that resist the growth of tumors with ALK activity. Crizotinib induces down regulation of STAT3 phosphorylation along with the significant apoptotic death. Apoptosis induces by the caspase-3 cleavage and down regulation of Bcl-2 family of proteins. Thus Crizotinib has the potential to treat patients with ALK induce Lung cancer [91].

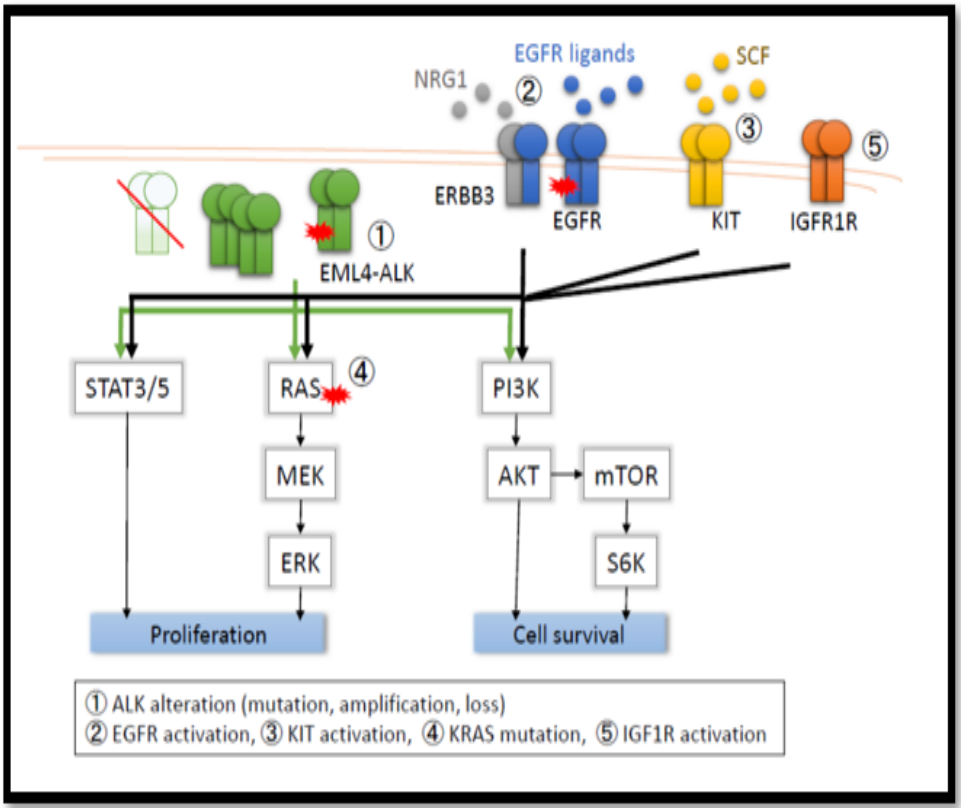

FIGURE 4.15: Mechanism of action of Crozotinib [92].

4.14.2 Paclitaxel Mechanism of Action

Figure 4.16 shows the mechanism of action of Paclitaxel. Paclitaxel had reported to induce ROS (Reactive Oxygen Species) generation and it increase hydro peroxide production by increasing the NADPH (Nicotinamide Adenine Dinucleotide Phosphate) oxidase activity that induces oxidative stress and also play a role in anticancer activity. Paclitaxel targets the microtubule proteins. Paclitaxel high concentration causes mitotic arrest at G2 or M phase, while its low concentration induces apoptosis at G0 and G1or S phase [93]. Paclitaxel induce proapoptotic activity by activating multiple signaling pathways. In vitro, Paclitaxel increases the polymerization of tubulin to stable microtubule. The drug 'Paclitaxel' has a specific binding site on microtubule polymer makes it a different and uniform chemotherapeutic agent. Paclitaxel does not have the ability to polymerize tubulin in the absence of cofactors (like Guanosine triphosphate and microtubule associated protein). Paclitaxel and microtubule proteins are irradiated with UV light and the drug binds with the beta-subunit of tubulin. The microtubule pathway reorganizes in the presence of Paclitaxel [94].

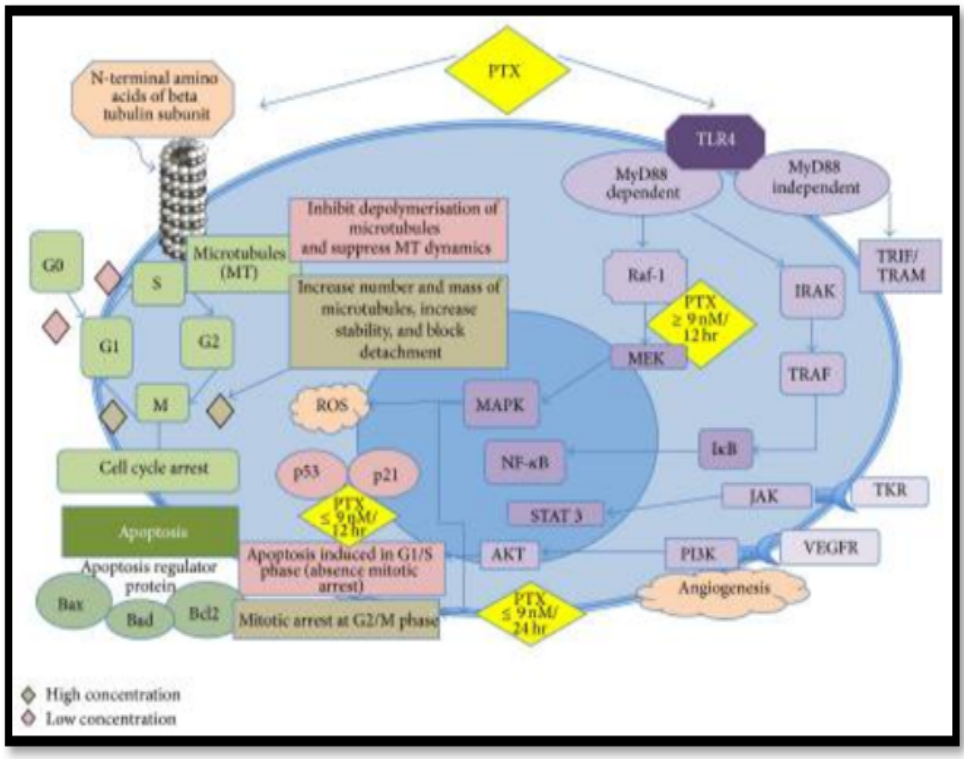

FIGURE 4.16: Mechanism of action of Paclitaxel [95] .

4.15 Effects of Standard Drugs on Body

4.15.1 Crizotinib Effects on Body

Crizotinib is a novel tyrosine kinase inhibitor approved globally for treating patients with advanced or metastatic Non-Small Cell Lung Cancer. Side effects include acne like rashes, dryness, discoloration, perifollicular inflammation, acral erythema, alopecia, visual impairment, peripheral edema etc. Photo allergic dermatitis is less common with Crizotinib [96].

4.15.2 Paclitaxel Effects on Body

Paclitaxel has ben used to treat lung cancer. Side effects of the drugs includes anemia, neutroprenia and alopecia. Patients taking Pclitaxel may report indigestion, viral infection, weakness ,nausea, vomiting and diarrhea [97].

4.16 Docking Results of Standard Drugs

4.16.1 Crizotinib Docking

Docking was performed with Crizotinib and paclitaxel as ligands by online docking tool (CB dock). Drug target was ALK and EML4 receptors respectively. Best docking score was -8.5 with ALK and -8.2 with EML4. Molecular interactions of docked drugs with targets are listed below in 4.23.

TABLE 4.23: Docking Score of reference drugs via CB Dock.

Docking Score	**Crizotinib with ALK**	**Paclitaxel with EML4**
Binding scores	-8.5	-8.2

TABLE 4.23: Docking Score of reference drugs via CB Dock.

Docking Score	**Crizotinib with ALK**	**Paclitaxel with EML4**
Cavity size	1932	11648
HBD	2	14
HBA	6	4
Log P	5.0377	3.7357
Molecular weight (g/mol)	450.345	853.918
Rotatable bonds	5	10
Grid map	23	66
Min energy (kcal/mol)	4.65	17.13
Max energy(kcal/mol)	41.67	168.08

4.17 Standard Drugs and Lead Compounds Comparison

The Standard drug and lead compounds were compared for their physiochemical and pharmacokinetic properties to assess their drug likeness, bioavailability, efficacy and their safety. All these compounds passed the drug likeness criteria. Apigenin has low molecular weight and log P value and is a 3 HBD and 5 HBA whereas Crizotinib shows that it is a 2 HBD and 6 HBA (4.24) .

TABLE 4.24: Apigenin- Crizotinib Lipinski's Rule of Five

Name of Compound	**Log P value**	**Molecular Weight**	**H-Bond Donor**	**H-Bond Acceptor**
Apigenin	2.5768	270.24 g/mol	3	5
Crizotinib	5.0377	450.345 g/mol	2	6

Salfredin B11 has low molecular weight and log P value and is a 1 HBD and 4 HBA whereas Paclitaxel shows that it is a 4 HBD and 14 HBA (4.25).

TABLE 4.25: Salfredin B11- Paclitaxel Lipinski's Rule of Five

Name of Compound	**Log P Value**	**Molecular Weight**	**H-Bond Donor**	**H-Bond Acceptor**
Salfredin B11	2.2468	232.235 g/mol	1	4
Paclitaxel	3.7357	853.918 g/mol	4	14

4.17.1 ADMET Properties Comparison of Crizotinib and Apigenin

Pharmacokinetics properties include Absorption, Distribution, Metabolism, Excretion and Toxicity (ADMET) properties play an important role I screening of compounds as drug candidates. Pharmacokinetic properties of reference drugs and lead compound are listed in Table 4.26 and 4.27 .

Toxicity is the important parameter of pharmacokinetics (ADMET) properties which consist of 10 models. Model 1 of AMES toxicity depicts the standard drug

and lead compound are not mutagenic. Maximum tolerated dose helps to set maximum recommended tolerated dose if value is $\leq$ 0.477 log mg/kg/day then considered low and greater values are considered high. Table 4.23 shows -0.095mg.kg value for Crizotinib and 0.328mg/kg for Apigenin that depicts the bioactive compound Apigenin is safe to use. The model hERG I/II inhibitor depicts that the compounds are inhibitor of potassium channel or not. Crizotinib show itself as hERG II inhibitor. The model Oral rat acute toxicity (LD50) expressed as mol.kg is the amount of drug that cause the death of 50% rats. LD50 value of Crizotinib is higher than Apigenin. Oral rat chronic toxicity (LOEAL) determines the lowest dose of drug which can produce adverse effects of drug over long duration. LOEAL predicted value of Crizotinib is less than Apigenin which shows its potency to be less toxic than bio compound. Hepatotoxicity indicates the injury to liver. Crizotinib shows that it is hepatotoxic while Apigenin is non-hepatotoxic. Both compounds do not cause any allergic reactions.

T.pyriformis toxicity expressed as negative logarithm of the concentration required to inhibit 50% growth (pIGC50) *T.pyriformis* toxicity value >0.5 is considered toxic. Crizotinib and Apigenin both are nontoxic. Minnow toxicity is the lethal concentration values (LC50 expressed in mM) of a compound that is necessary to cause death of 50% minnows. For minnow toxicity values below 0.5 mM is considered toxic. Crizotinib predicted value is 0.942 mM, and 2.432 mM is the predicted value of Apigenin. Altogether, Apigenin is safer compound than Crizotinib (Table 4.26).

Absorption properties comparison as mentioned in the Table 4.26 shows that Water solubility of standard drug is less than the lead compound. Predicted value of water solubility of Crizotinib is less than the Apigenin but both are in safe range. Caco2 permeability predicts about the absorption of orally administered drugs. Both are in normal range. Predicted values of intestinal absorption in human are 92.006% for Crizotinib and 93.25% for Apigenin. Both compounds predict low skin permeability. Crizotinib shows 'Yes' category for P-glycoprotein substrate while Apigenin show 'Yes' category for P-glycoprotein substrate and 'No' category for P-glycoprotein I/II inhibitors model. This means Crizotinib and Apigenin as P-gp

substrate show low oral absorption and p-gp I/II inhibitor reduce the pumping out of xenobiotic and toxins activity of P-gp from cell and may have high absorption.

Distribution properties are based on 4 models. The first model of distribution properties VDss (human) is the uniform distribution of the drug in blood plasma. If value higher than 2.81 L/Kg that means the drug is more distributed in tissue rather plasma. Both compounds have reasonable value of VDss.

Fu is the unbound friction in plasma. Fu value of Apigenin is more than Crizotinib that predicts it is more effective than the standard drug. BB permeability show blood brain barrier permeability, if value higher than 0.3 then drug easily cross the blood brain barrier and if the value is less than the drug may not be evenly distributed in the brain. Both the compounds have BB permeability value in tolerable range that means it provide no harm to the brain. CNS permeability ¡-3 is considered safe. Both compounds have CNS permeability ¡-3 thus considered safe.

Metabolic properties are predicted based on isoforms of cytochrome P450 which includes CYP2D6, CYP3A4, CYP1A2, CYP2C19 and CYP2C9. Crizotinib is predicted as the substrate of CYP3A4 isoform while Apigenin is not the substrate of any isoform. Crizotinib is an inhibitor of CYP1A2 and CYP3A4 isoforms but Apigenin show itself as inhibitor of only CYP1A2 isoform.

Excretion properties consist of two models with predicted values are given in Table 4.26 . Drug clearance is measured by total clearance which occurs as combination of hepatic clearance and renal clearance and the value is expressed as log CL tot in ml/min/kg. Predicted value of drug clearance as total clearance of Crizotinib and Apigenin are considered safe.

Total clearance is related to bioavailability and determines the dosing rate. For Renal OCT2 substrate, Crizotinib show ‘Yes’ which means it interfere in the normal functioning of organic cation transporter 2 who play role in renal clearance of drugs. While Apigenin show ‘No’ towards Renal OCT2 substrate, this means that Apigenin does not interfere in the normal functioning of organic cation transporter.

TABLE 4.26: ADMET properties of drug (Crizotinib) and leading compound (Apigenin)

ADMET Properties	**Model Name**	**Crizotinib**	**Apigenin**
Toxicity	AMES toxicity	No	No
	Max. tolerated dose (human)	-0.095 mg/Kg	0.328 mg/Kg
	hERG I inhibitor	No	No
	hERG II inhibitor	Yes	No
	Oral rat acute toxicity	3.515 mol/Kg	2.45 mol/Kg
	Oral rat chronic toxicity	1.57 mg/kg	2.298 mg/kg
	Hepatotoxicity	Yes	No
	Skin sensitization	No	No
	T.pyriformis toxicity	0.296 log ug/L	0.38 log ug/L
	Minnow toxicity	0.942 log mM	2.432 log mM
Absorption	Water solubility	-4.14 mol/L	-3.329 mol/L
	Caco2 permeability	0.702 cm/S	1.007 cm/S

TABLE 4.26: ADMET properties of drug (Crizotinib) and leading compound (Apigenin)

ADMET Properties	**Model Name**	**Crizotinib**	**Apigenin**
Distribution	Intestinal absorption (human)	92.006 %	93.25 %
	Skin permeability	-2.747 log Kp	-2.735 log Kp
	P-glycoprotein substrate	Yes	Yes
	P-glycoprotein I inhibitor	Yes	No
	P-glycoprotein II inhibitor	Yes	No
	VDss (human)	0.801 L/Kg	0.822 L/Kg
	Fraction unbound (human)	0.132 Fu	0.147 Fu
	BBB permeability	-1.164 log BB	-0.734 log BB
	CNS permeability	-2.222 Log PS	-2.061 log PS
Metabolism	CYP2D6 substrate	No	No
	CYP3A4 substrate	Yes	No
	CYP1A2 inhibitor	Yes	Yes

TABLE 4.26: ADMET properties of drug (Crizotinib) and leading compound (Apigenin)

ADMET Properties	**Model Name**	**Crizotinib**	**Apigenin**
	CYP2C19 inhibitor	No	No
	CYP2C9 inhibitor	Yes	No
	CYP2D6 inhibitor	No	No
	CYP3A4 inhibitor	Yes	No
Excretion	Total Clearance	0.571 ml/kg	0.566 ml/kg
	Renal OCT2 substrate	Yes	No

4.18 ADMET Properties Comparison of Paclitaxel and Salfredin B11

Model 1 of AMES toxicity depicts the standard drug and lead compound are not mutagenic. Maximum tolerated dose helps to set maximum recommended tolerated dose if value is $\leq$ 0.477 log mg/kg/day then considered low and greater values are considered high. Table 4.27 shows 0.199 mg/kg value for Paclitaxel and -0.051mg/kg for Salfredin B11 depicts that the bio compound Salfredin B11 is safe to use. The model hERG I/II inhibitor depicts that the compounds are inhibitor of potassium channel or not. Paclitaxel show itself as hERG II inhibitor. The model Oral rat acute toxicity (LD50) expressed in mol.kg is the amount of drug that cause the death of 50% rats. LD50 value of Paclitaxel is higher than Salfredin

B11. Oral rat chronic toxicity (LOEAL) determines the lowest dose of drug which can produce adverse effects of drug over long duration. LOEAL predicted value of Paclitaxel is higher than Salfredin B11 which shows its potency to be less toxic than bio compound. Hepatotoxicity indicates the injury to liver. Paclitaxel shows that it is hepatotoxic while Salfredin B11is non-hepatotoxic. Both compounds do not cause any allergic reactions. *T.pyriformis* toxicity expressed as negative logarithm of the concentration required to inhibit 50% growth (pIGC50) *T.pyriformis* toxicity value >0.5 is considered toxic. Paclitaxel and Salfredin B11both are non-toxic. Minnow toxicity is the lethal concentration values (LC50 expressed in mM) of a compound that is necessary to cause death of 50% minnows. For minnow toxicity values below 0.5 mM is considered toxic. Paclitaxel predicted value is 2.988 mM, and 1.942 mM is the predicted value of Salfredin B11. Altogether, Salfredin B11 is safer compound than Paclitaxel.

Absorption properties comparison as mentioned in the Table 4.24 shows that Water solubility of standard drug is slightly higher than the lead compound. Predicted value of water solubility of Paclitaxel is slightly higher than the Salfredin B11but both are in safe range. Caco2 permeability predicts about the absorption of orally administered drugs. Both are in normal range. Predicted values of intestinal absorption in human are 100% for Paclitaxel and 94.50% for Salfredin B11. Both compounds predict low skin permeability. Paclitaxel shows 'Yes' category for P-glycoprotein substrate while Salfredin B11show 'No' category for P-glycoprotein substrate and for P-glycoprotein I/II inhibitors model. This means Paclitaxel as P-gp substrate show low oral absorption and p-gp I/II inhibitor reduce the pumping out of xenobiotic and toxins activity of P-gp from cell and may have high absorption.

The first model of Distribution properties VDss (human) is the uniform distribution of the drug in blood plasma. If value higher than 2.81 L/Kg that means the drug is more distributed in tissue rather plasma. Both compounds have reasonable value of VDss. Fu is the unbound friction in plasma. Fu value of Salfredin B11 is more than Paclitaxel that predicts it is more effective than the standard drug. BB permeability show blood brain barrier permeability, if value higher than 0.3

then drug easily cross the blood brain barrier and if the value is less than the drug may not be evenly distributed in the brain. Both the compounds have BB permeability value in tolerable range that means it provide no harm to the brain. CNS permeability ¡-3 is considered safe. Both compounds have CNS permeability in normal range thus considered safe.

Metabolic properties are predicted based on isoforms of cytochrome P450 which includes CYP2D6, CYP3A4, CYP1A2, CYP2C19 and CYP2C9. Paclitaxel is predicted as the substrate of CYP3A4 isoform while Salfredin B11is not the substrate of any isoform. Paclitaxel is an inhibitor of CYP3A4 isoforms but Salfredin B11is not the inhibitor of any isoform.

Excretion properties consist of two models with predicted values are given in Table 4.27 . Predicted values of drug clearance as total clearance of Salfredin B11 are high as compared to Paclitaxel. Total clearance is related to bioavailability and determines the dosing rate. For Renal OCT2 substrate, both compounds Paclitaxel and Salfredin B11 show 'No' this means that Paclitaxel and Salfredin B11 do not interfere in the normal functioning of organic cation transporter 2 who play role in renal clearance of drugs.

TABLE 4.27: ADMET properties of drug (Paclitaxel) and leading compound (Salfredin B11).

ADMET Properties	**Model Name**	**Paclitaxel**	**Salfredin B11**
Toxicity	AMES toxicity	No	No
	Max. tolerated dose (human)	0.199 mg/Kg	-0.051 mg/Kg
	hERG I inhibitor	No	No
	hERG II inhibitor	Yes	No

TABLE 4.27: ADMET properties of drug (Paclitaxel) and leading compound (Salfredin B11).

ADMET Properties	**Model Name**	**Paclitaxel**	**Salfredin B11**
Absorption	Oral rat acute toxicity	2.776 mol/Kg	1.701 mol/Kg
	Oral rat chronic toxicity	3.393 mg/Kg	2.419 mg/Kg
	Hepatotoxicity	Yes	No
	Skin sensitization	No	No
	T.pyriformis toxicity	0.285 log ug/L	0.494 log ug/L
	Minnow toxicity	2.988 log mM	1.492 log mM
	Water solubility	-3.158 mol/L	-3.081 mol/L
	Caco2 permeability	0.623 cm/S	1.201 cm/S
	Intestinal absorption (human)	100%	94. 508%
	Skin permeability	-2.735 log Kp	-3.236 log Kp
	P-glycoprotein substrate	Yes	No
	P-glycoprotein I inhibitor	Yes	No

TABLE 4.27: ADMET properties of drug (Paclitaxel) and leading compound (Salfredin B11).

ADMET Properties	**Model Name**	**Paclitaxel**	**Salfredin B11**
Distribution	P-glycoprotein II inhibitor	Yes	No
	VDss (human)	1.458 L/Kg	0.363 L/Kg
	Fraction unbound (human)	0 Fu	0.465 Fu
	BBB permeability	-1.731 log BB	-0.747 log BB
	CNC permeability	-3.95 Log PS	-2.827 Log PS
Metabolism	CYP2D6 substrate	No	No
	CYP3A4 substrate	Yes	No
	CYP1A2 inhibitor	Yes	No
	CYP2C19 inhibitor	No	No
	CYP2C9 inhibitor	Yes	No
	CYP2D6 inhibitor	No	No
	CYP3A4 inhibitor	Yes	No
Excretion	Total Clearance	-0.36 ml/kg	0.481 ml/kg
	Renal OCT2 substrate	No	No

4.19 Physiochemical Properties Comparison

Physiochemical properties describe the basic and fundamental properties of compounds which also act as primary screeners to sort out compounds with desirable properties. Crizotinib consists of 52 atoms of carbon, hydrogen, chlorine, fluorine, nitrogen and oxygen while Apigenin consist of 30 atoms of carbon, nitrogen and oxygen which show its simplicity as a bio-compound. Molecular weight and log P value of Crizotinib is high than Apigenin. Apigenin donated more hydrogen bonds than Crizotinib. Rotatable bonds more than 10 depict decreased oral bioavailability. Crizotinib has 5 rotatable bonds as compared to Apigenin which has only 1 rotatable bond (Table 4.28).

TABLE 4.28: Physiochemical properties comparison

Drug	**log P value**	**Rotatable Bonds**	**HBD**	**HBA**	**Molecular Formula**	**Molecular Wt. (g/mol)**
Apigenin	2.576	1	3	4	$C_{15}N_{10}O_5$	270.24
Crizotinib	5.037	5	2	6	$C_{21}H_{22}Cl_{12}FN_5O$	450.345

Paclitaxel consists of 113 atoms of carbon, hydrogen, nitrogen and oxygen while Salfredin B11consist of 29 atoms of carbon, hydrogen and oxygen which shows its simplicity as a bio-compound. Molecular weight and log P value of Paclitaxel is high than Salfredin B11. Paclitaxel and Salfredin B11 donated equal hydrogen bonds. Rotatable bond more than 10 depicts decreased oral bioavailability(Table 4.29).

TABLE 4.29: Physiochemical properties comparison.

Drug	**Log P Value**	**Rotatable Bonds**	**HBD**	**HBA**	**Molecular Formula**	**Molecular Weight (g/mol)**
Salfredin B11	2.2468	0	1	4	$C_{13}H_{12}O_4$	232.32

TABLE 4.29: Physiochemical properties comparison.

Drug	**Log P Value**	**Rotatable Bonds**	**HBD**	**HBA**	**Molecular Formula**	**Molecular Weight (g/mol)**
Paclitaxel	3.7357	10	14	4	$C_{47}H_{51}NO_{14}$	853.9

4.20 Docking Score Comparison

Discovering protein-ligand binding site and conformations are important in drug discovery. Therefore standard drug as ligand was docked against the selected receptors by CB-Dock online tool which predicts the cavities of protein and calculates the centers and sizes of the top 5 cavities for all the three proteins. Results of docking of standard drugs and lead compound selected against the two receptors namely ALK and EML4 receptors are shown in tables. The highest binding score shown by Apigenin is -7.9 against ALK which is less than Crizotinib that shows -8.5 against the same protein ALK. The highest binding score shown by Salfredin B11 is -7.2 against ALK which is less than Paclitaxel that shows -8.2 against the same protein EML4. The interaction visualization analysis studies are performed by PyMol molecule visualization tool and Ligplot+ (V.1.4.5).

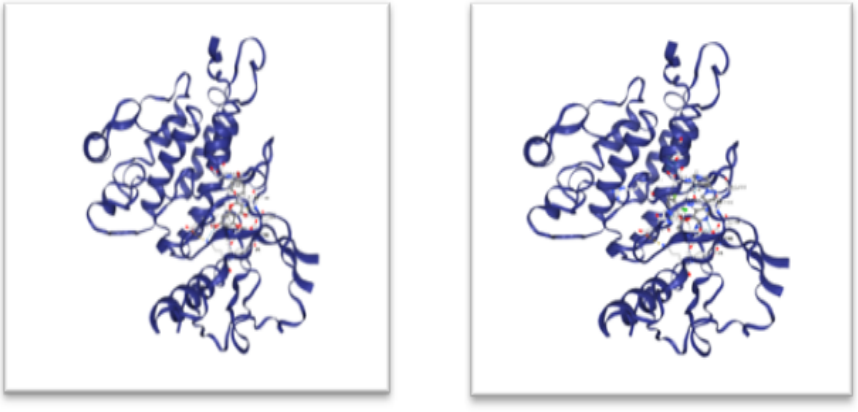

FIGURE 4.17: Best Pose Interaction of Apigenin and Crizotinib as Ligand with ALK.

4.21 Docking Analysis Comparison

4.21.1 Docking Analysis of Drug and Lead Compound with ALK

Best docking score of reference drug and lead compound are analyzed by LIGPLOT+ (V.1.4.5), (Figures 4.19 and 4.20). Docking results are analyzed on the basis of;

1. No. of Hydrogen bonds.
2. No. of steric interactions.
3. No. of interacting amino acids.
4. Interaction with hydrophobic regions.

The detail of hydrogen bonds and hydrophobic interactions are displayed on Table 4.30. Oxygen atoms present in ligand play important role in H-bond formation with target protein. Apigenin makes 2 hydrogen bonds whereas Crizotinib makes 3 hydrogen bonds. Furthermore, hydrophobic interactions are more in number in Crizotinib as compared to Apigenin.

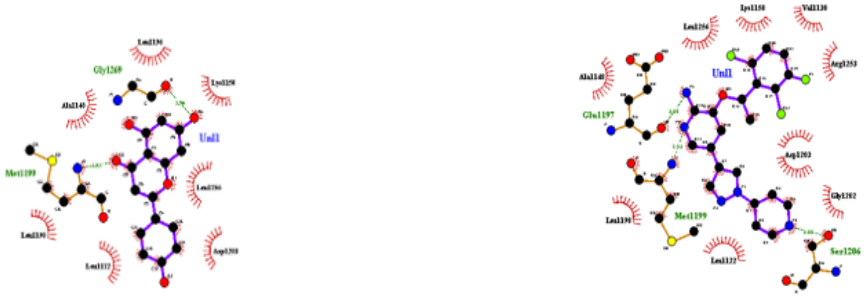

a) Apigenin **b) Crizotinib**

FIGURE 4.18: H- bonds and Interaction of Apigenin and Crizotinib as Ligand with ALK.

TABLE 4.30: Hydrogen Bonds and Interactions comparison of Apigenin and Crizotinib.

Ligands	**Binding Energy**	**No. of H.B**	**Amino Acids**	**Distance**	**Hydrophobic Interaction**
Apigenin	-7.9	2	Met1199 Gly1296	2.96 2.26	Leu1196 Lys1150 Ala1148 Leu1198 Leu1122 Asp1203
Crizotinib	-8.7	3	Met1199 Ser1206 Glu11897	2.93 3.00 3.05	Leu1256 Ala1148 Leu1256 Leu1198 Lys1150 Val1130 Leu1122 Gly1202 Arg1253 Asp1203

4.21.2 Docking Analysis Comparison Docking Analysis of Drug and Lead Compound with EML4

The 2D diagrams generated through Ligplot by the interaction of Paclitaxel and Salfredin B11 with EML4 is shown in Figure. And the properties are mentioned in Table 4.31.

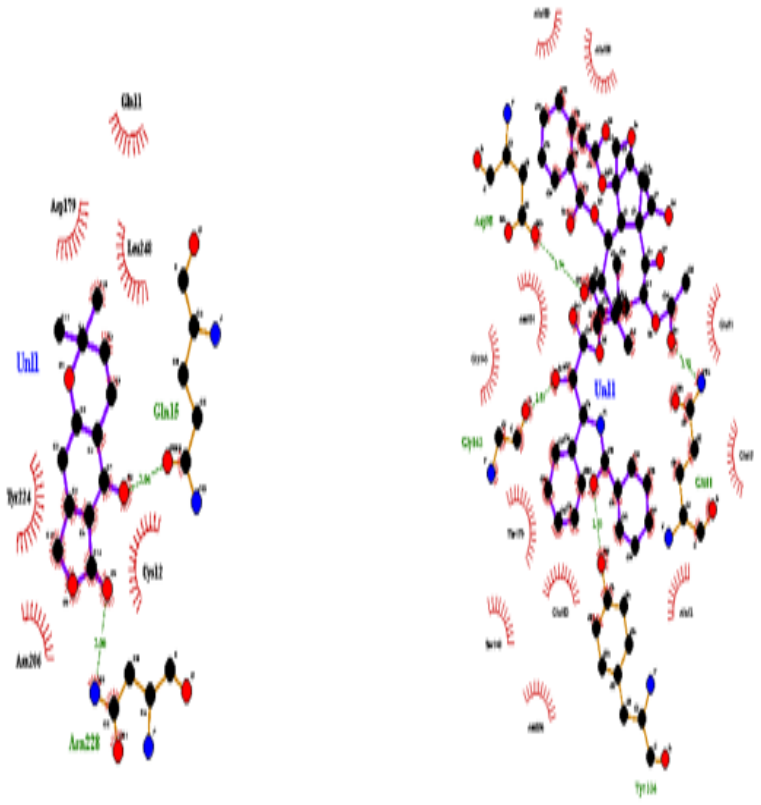

FIGURE 4.19: H- bonds and Interaction of Salfredin B11 and Paclitaxel as Ligand with EML4

The detail of hydrogen bonds and hydrophobic interactions are displayed on Table 4.31. Oxygen atoms present in ligand play important role in H-bond formation with target protein. Salfredin B11 makes 1 hydrogen bond whereas Paclitaxel makes 4 hydrogen bonds. Furthermore, hydrophobic interactions are more in number in Paclitaxel as compared to Salfredin B11.

TABLE 4.31: Hydrogen Bonds and Interactions comparison of Salfredin B11 and Paclitaxel.

Ligands	**Binding Energy**	**No. of H.B**	**Amino Acids**	**Distance**	**Hydrophobic Interaction**
Salfredin B11	-7.4	1	Met1199	2.88	Ala1148 Leu1256 Leu1198 Lys1150 Val1130 Leu1122 Gly1202 Gln15 GluT1 Ala12
Paclitaxel	-7.3	4	Gly143 Asp98 Gln11 Tyr334	3.01 3.90 1.92 3.90	Ser140 Glu71 Asp98 Ala180 Thr179 Asn206 Gly142

Chapter 5

Conclusions and Recommendations

The motive of the present study was to discover the active constituents from the medicinal plants *Nigella sativa* which could act as anticancer agents in Lungs Cancer. For this purpose, 15 ligands were selected after performing studies on literature databases and docked against receptor proteins which are ALK and EML4, involved in lung cancer. The structures of all the 15 ligands were easily available in PubChem and proteins structures were also available in Protein Data Bank. Drug likeliness of compounds was studied and reported by using primary and secondary filter (Lipinski's rule of 5 as primary and pharmacokinetics properties as secondary filter). The docking procedures were performed using CB-Dock online tool. The results were visualized using PyMol and were analyzed through Ligplot version v.1.4.5. After detail analysis of their binding score, physiochemical properties and ADMET properties, Apigenin were selected as lead compound against ALK, Salfredin B11 were selected as lead compound against EML4. Virtual screening results, physiochemical properties and pharmacokinetics properties of these compounds were compared with an FDA approved drugs namely Crizotinib and Paclitaxel. Based on results, it was found that selected lead compounds show better binding affinity to respective protein targets and show less toxicity than standard drugs.

5.1 Recommendations

Lead compounds Apigenin and Salfredin B11 as per this research results should be explored as a drug candidate for the treatment of Lungs cancer.

Bibliography

[1] M. A. Zaimy, N. Saffarzadeh, A. Mohammadi, H. Pourghadamyari, P. Izadi, A. Sarli , L.K. Moghaddam, S.R. Paschepari, H. Azizi , S. Torkamandi and J. Tavakkoly, "New methods in the diagnosis of cancer and gene therapy of cancer based on nanoparticles." *Cancer Gene Ther*, vol. 24, no. 6, pp. 233-243, 2017.

[2] D. A. Hasanpoor and S. Azari, "Quality of life and related factor in cancer patients", *Behbood*, vol. 10, no. 2, pp. 110-19, 2006.

[3] L. A. Torre, F. Bray, R. L. Siegel, J. Ferlay, J. Lortet-Tieulent, and A. Jemal, "Global cancer statistics, 2012," *CA: a cancer journal for clinicians*, vol.65, no. 2, pp. 87-108, 2015.

[4] J. Ferlay, M. Ervik, F. Lam, M. Colombet, L. Mery, M. Piñeros, "Global Cancer Observatory: Cancer Today." *Lyon: International Agency for Research on Cancer*, 2020.

[5] E. H. Pérez, A. Fernández-Medarde, "Advanced targeted therapies in cancer: Drug nanocarriers, the future of chemotherapy." *Eur J Pharm Biopharm*, vol. 93 pp. 52-79, 2015.

[6] M. Soda, Y. L. Choi, M. Enomoto, "Identification of the transforming EML4–ALK fusion gene in non-small-cell lung cancer." *Nature*, vol.448, no. 7153, pp. 561–566, 2007.

[7] F. Napoleone, J. Kenneth, N. H. William, "Bevacizumab (Avastin), a humanized anti-VEGF monoclonal antibody for cancer therapy," *Biochemical and Biophysical Research Communications*, vol 333, no. 2, pp. 328-335, 2005.

[8] W.N. Joel, E.D. Suzanne, A. K. Heather, C. A. Seena, B. Michaela, H. Ying, P. C. David, J. G. Gregory, E. L. Rachel, L. R. Jerome, K.O. Taofeek, J. S. Philip, D. S. Preston, A. K. Ahmed, S. R. Suresh, "Erlotinib, cabozantinib, or erlotinib plus cabozantinib as second-line or third-line treatment of patients with EGFR wild-type advanced non-small-cell lung cancer (ECOG-ACRIN 1512): a randomised, controlled, open-label, multicenter, phase 2 trial," *The Lancet Oncology*, vol. 17, no. 12, pp. 1661-1671, 2016.

[9] M. G. Kris, R. B. Natale, R. S. Herbst, "Efficacy of gefitinib, an inhibitor of the epidermal growth factor receptor tyrosine kinase, in symptomatic patients with non-small cell lung cancer: a randomized trial." *JAMA*, vol. 290, pp. 2149–58, 2003.

[10] M. Fukuoka, S. Yano , G. Giaccone, "Multi-institutional randomized phase II trial of gefitinib for previously treated patients with advanced non-small-cell lung cancer." *J Clin Oncol*, vol. 21, pp. 2237–46, 2003.

[11] M. Muller, S. Strand, H. Hug, E. M. Heinemann, H. Walczak, W. J. Hofmann, "Drug-induced apoptosis in hepatoma cells is mediated by the CD95 (ApO-1/Fas) receptor/ligand system and involves activation of wild-type p53." *J Clin Invest*, vol. 99, pp. 403-13, 1997.

[12] S. Fulda, C. Friesen, K.M. Debatin, "Molecular determinants of apoptosis induced by cytotoxic drugs." *Klinische Padiatrie*, vol. 210, pp. 148-52, 1998.

[13] F. Luppi, A.M. Longo, W.I. de Boer, K.F. Rabe, P.S. Hiemstra, "Interleukin-8 stimulates cell proliferation in non-small cell lung cancer through epidermal growth factor receptor transactivation. Lung Cancer." vol. 56, no. 1, pp. 25-33, 2007.

[14] A. Kazmi, M. A. Khan, and H. Ali, "Biotechnological approaches for production of bioactive secondary metabolites in Nigella sativa: an up-to-date review." *International Journal of Secondary Metabolite*, vol. 6, no. 2, pp. 172-195, 2019.

[15] N. K. Sharma, D. Ahirwar, D. Jhade, and S. Gupta, "Medicinal and Phamacological Potential of Nigella sativa: A Review," *Ethnobotanical Leaflets*, vol. 2009, 2009.

[16] R. Kacem and Z. Meraihi, "Effects of essential oil extracted from Nigella sativa (L.) seeds and its main components on human neutrophil elastase activity." *Yakugaku Zasshi*, vol. 126, no. 4, pp. 301-305, 2006.

[17] Zielińska, Magdalena, D. Katarzyna, P.S. Ewelina, and E.S. Agnieszka. "The Role of Bioactive Compounds of Nigella sativa in Rheumatoid Arthritis Therapy—Current Reports." *Nutrients*, vol. 13, no. 10, pp. 3369, 2021.

[18] X. Liu, M. A. Abd El-Aty, and J. H. Shim, "Various extraction and analytical techniques for isolation and identification of secondary metabolites from Nigella sativa seeds." *Mini Reviews in Medicinal Chemistry*, vol. 11, no. 11, pp. 947-955, 2011.

[19] G. M. Morris, M. L. Wilby, "Molecular Docking. In: Kukol A. (eds) Molecular Modeling of Proteins." *Methods Molecular Biology™*, vol. 443, 2008.

[20] K. Shanmugaraj, S. Anandakumar, and M. Ilanchelian, "Probing the binding interaction of thionine with lysozyme: A spectroscopic and molecular docking investigation." *Dyes and Pigments*, vol. 112, pp. 210-219, 2015.

[21] R. A. Friesner, J. L. Banks, R. B. Murphy, T. A. Halgren, J. J. Klicic, D. T. Mainz and P. S. Shenkin, "Glide: a new approach for rapid, accurate docking and scoring. 1. Method and assessment of docking accuracy." *Journal of medicinal chemistry*, vol. 47, no. 7, pp. 1739-1749, 2004.

[22] D. Rodríguez, Z. G. Gao, S. M. Moss, K. A. Jacobson, and J. Carlsson, "Molecular docking screening using agonist-bound GPCR structures: probing the A2A adenosine receptor." *Journal of chemical information and modeling*, vol. 55, no. 3, pp. 550-563, 2015.

[23] F. Bray, J. Ferlay, I. Soerjomataram, R. L. Siegel, L. A. Torre, and A. Jemal, "Global cancer statistics 2018: GLOBOCAN estimates of incidence

and mortality worldwide for 36 cancers in 185 countries." *CA: a cancer journal for clinicians*, vol. 68, no. 6, pp. 394-424, 2018.

[24] I. I. Wistuba, and A. F. Gazdar, "Lung cancer preneoplasia." *Annu. Rev. Pathol. Mech. Dis.*, vol. 1, pp. 331-348, 2006.

[25] A.M. Romaszko, A. Doboszyńska, "Multiple primary lung cancer: A literature review." *Adv Clin Exp Med.* Vol. 27, no. 5, pp. 725-730, 2018.

[26] E. C. Mary, "Symptoms in Adults with Lung Cancer: A Systematic Research Review," *Journal of Pain and Symptom Management*, vol. 19, no. 2, pp. 137-153, 2000.

[27] O. E. Tulunay, S.S. Hecht, S.S. Carmella, "Urinary metabolites of a tobacco-specific lung carcinogen in nonsmoking hospitality workers." *Cancer Epidemiol Biomarkers Prev*, vol. 14 no. 5, pp. 1283-6, 2005.

[28] K. E. Anderson, J. Kliris, L. Murphy, "Metabolites of a tobacco-specific lung carcinogen in nonsmoking casino patrons." *Cancer Epidemiol Biomarkers Prev*, vol. 12, no. 12, pp. 1544-6, 2003.

[29] Y. Sekido, K. M. Fong, J.D. Minna, "Progress in understanding the molecular pathogenesis of human lung cancer." *Biochim Biophys Acta*, pp. 1378, 1998.

[30] P.T. Reissmann, H. Koga, R. A. Figlin, E.C. Holmes, D.J. Salmon, "Amplification and overexpression of the cyclin D1 and epidermal growth factor receptor genes in non-small-cell lung cancer. Lung cancer study group." *J Cancer Res Clin Oncol*, vol. 125, pp. 61-70, 1999.

[31] K. Naoki, T. H. Chen, W. G. Richards, D. J. Sugarbaker, M. Meyerson, "Missense mutations of the BRAF gene in human lung adenocarcinoma." *Cancer Res*, vol. 62, pp. 7001-3, 2002.

[32] D. S. Ettinger, " Overview and state of the art in the management of lung cancer." *Oncology (Willinston Park)*, vol. 18, pp.3-9, 2004.

[33] E. Brambilla, W. D. Travis, T. V. Colby, B. Corrin, Y. Shimosato. "The new World Health Organization classification of lung tumours." *Eur Respir J*, vol. 18, pp. 1059-68, 2001.

[34] T. Sher, G. K. Dy, and A. A. Adjei, "Small cell lung cancer." *In Mayo Clinic Proceedings*, vol. 83, no. 3, pp. 355-367, 2008.

[35] W. L. Read, N.C. Page, R. M. Tierney, J. F. Piccirillo, R. Govindan. "The epidemiology of bronchioloalveolar carcinoma over the past two decades: analysis of the SEER database." *Lung Cancer*, vol. 45, pp. 137-42, 2004.

[36] W. H. David, I. M. Ali, "Bronchoscopic Therapies for Peripheral Lung Malignancies." *Clinics in Chest Medicine*, vol. 39, no. 1, pp. 245-259, 2018.

[37] S. Qanash, O. A. Hakami, F. Al-Husayni and A. G. Gari, "Flexible Fiberoptic Bronchoscopy: Indications, Diagnostic Yield and Complications." *Cureus*, vol. 12, no. 10, (2020).

[38] E. M. Pickering, O. Kalchiem-Dekel, A. Sachdeva, "Electromagnetic navigation bronchoscopy: a comprehensive review." *AME Med J*, vol. 3, pp. 117, 2018.

[39] D. M. DiBardino, L. B. Yarmus, and R. W. Semaan, "Transthoracic needle biopsy of the lung." *Journal of thoracic disease*, vol. 7, no. 4, 2015.

[40] B. Biswas, S. K. Sharma, R. S. Negi, N. Gupta, V. M. Jaswal and N. Niranjan, "Pleural effusion: Role of pleural fluid cytology, adenosine deaminase level, and pleural biopsy in diagnosis." *Journal of cytology*, vol. 33, no. 3, pp. 159–162, 2016.

[41] L. Lang-Lazdunski, "Surgery for nonsmall cell lung cancer." *European Respiratory Review*, vol. 22, no. 129, pp. 382-404, 2013.

[42] L. Kaskowitz, V. G. Mary, E. Bahman, J. H. Karen, R. Carol, "Radiation therapy alone for stage I non-small cell lung cancer." *International Journal of Radiation Oncology*Biology*Physics*, vol. 27, no. 3, pp. 517-523, 1993.

[43] M. S. Hossain, A. Sharfaraz, A. Dutta, A. Ahsan, M.A. Masud, I. A. Ahmed and L. C. Ming, "A review of ethnobotany, phytochemistry, antimicrobial pharmacology and toxicology of Nigella sativa L." Biomedicine & Pharmacotherapy, vol. 143, pp. 112182, 2021.

[44] B. B. Petrovska, "Historical review of medicinal plants' usage." *Pharmacognosy reviews*, vol. 6, no. 11, pp. 1–5, 2012.

[45] M. Spinella, "The psychopharmacology of herbal medicine: plant drugs that alter mind, brain, and behavior." MIT Press, 2001.

[46] J. D. Phillipson, "Phytochemistry and medicinal plants." *Phytochemistry*, vol. 56, no. 3, pp. 237-243, 2001.

[47] B. Patwardhan, D. Warude, B. Pushpangadan and N. Bhatt, "Ayurveda and traditional Chinese medicine: a comparative overview." *Evidence-based complementary and alternative medicine*, vol. 2, no. 4, pp. 465-473, 2005.

[48] A. Maiuthed, W. Chantarawong and P. Chanvorachote, "*Anticancer Research.*" Vol. 38, no. 7, pp. 3797-3809, 2018.

[49] N. Bhummaphan, P. Chanvorachote, "Gigantol suppresses cancer stem cell-like phenotypes in lung cancer cells." *Evid Based Complement Alternate Med* , pp.1-10, 2015.

[50] J. Zhao, F. Xu, H. Huang, Z. Gu, L. Wang, W. Tan, "Evaluation on anti-inflammatory, analgesic, antitumor, and antioxidant potential of total saponins from Nigella glandulifera seeds." TextitEvid. Based Complement. Alternat Med. 2013, doi:10.1155/2013/827230.

[51] E. Agradi, G. Fico, F. Cillo, C. Francisci, and F. Tome, "Estrogenic activity of phenolic compounds from Nigella damascena evaluated using a recombinant yeast screen." *Planta Med*, vol. 67, pp. 553–555, 2001, doi:10.1055/s-2001-16485.

[52] O. Toncer, and S. Kizil, "Effect of seed rate on agronomic and technologic characters of *Nigella sativa L. Int. J. Agric. Biol*, vol.3, pp. 529–532, 2004, doi:10.1007/978-981-15-4194-0-13.

[53] B. Salehi, C. Quispe, M. Imran, I. Ul-Haq, J. Zivkovic, M. Abu-Reidah Ibrahim, S. Sen, Y. Taheri, K. Acharya, H. Azadi, C. M. del Mar, A. Segura-Carretero, D. Mnayer, G. Sethi, M. Martorell, A. F. Abdull Razis, U. Sunusi, R. M. Kamal, H. A. Rasul Suleria, J. Sharifi-Rad , "Nigella Plants – Traditional Uses, Bioactive Phytoconstituents, Preclinical and Clinical Studies." *Frontiers in Pharmacology*, vol. 12, 2021, doi: 10.3389/fphar.2021.625386.

[54] B. H. Ali, and G. Blunden, "Pharmacological and toxicological properties of Nigella sativa." *Phytother*, vol. 17, pp. 299-305, 2003.

[55] A. A. Akbar, H. Sadiq, K. Lennart, Atta-Ur-Rahman, W. Thomas, "Structural studies on a saponin isolated from Nigella sativa." *Phytochemistry*, vol 27, no. 12, pp. 3977-3979, 1988.

[56] A. A. Akbar, H. Sadiq, K. Lennart, Atta-Ur-Rahman, T. Wehler, "Structural studies on a saponin isolated from Nigella sativa," *Phytochemistry*, vol. 27, no. 12, pp. 3977-3979, 1988.

[57] M. S. Hossain, A. Sharfaraz, A. Dutta, A. Ahsan, M.A. Masud, I. A. Ahmed and L. C. Ming, "A review of ethnobotany, phytochemistry, antimicrobial pharmacology and toxicology of Nigella sativa L." *Biomedicine & Pharmacotherapy*, vol. 143, pp. 112182, 2021.

[58] W. Kooti, W. Hasanzadeh-Noohi, N. Sharafi-Ahvazi, M. Asadi-Samani and D. Ashtary-Larky, "Phytochemistry, pharmacology, and therapeutic uses of black seed (Nigella sativa)." *Chinese journal of natural medicines*, vol. 14, no. 10, pp. 732-745, 2016.

[59] K. David, S. P. Spasenija, I. R. Sacha, "Targeted Therapy in Advanced and Metastatic Non-Small Cell Lung Cancer. An Update on Treatment of the Most Important Actionable Oncogenic Driver Alterations," *Cancers*, vol. 13, no. 4, pp. 804, 2021.

[60] S. H. Jafri, J. Glass, R. Shi, S. Zhang, M. Prince, H. Kleiner-Hancock, "Thymoquinone and cisplatin as a therapeutic combination in lung cancer: In vitro and in vivo." *J Exp Clin Canc Res*, vol. 29, no. 87, 2014.

[61] T. Sasaki, S. J. Rodig, L. R. Chirieac, "The biology and treatment of EML4-ALK non- small cell lung cancer." *Eur J Cancer*, vol. 46, pp. 1773-80, 2010.

[62] P. Dahiya, and S. Purkayastha, "Phytochemical screening and antimicrobial activity of some medicinal plants against multi-drug resistant bacteria from clinical isolates." *Indian journal of pharmaceutical sciences*, vol. 74, no. 5, pp. 443, 2012.

[63] R. Montella, G. Giunta, Laccetti, G., Lapegna, M., Palmieri, C., Ferraro and D. S. Nikolopoulos, "On the virtualization of CUDA based GPU remoting on ARM and X86 machines in the GVirtuS framework." *International Journal of Parallel Programming*, vol. 45, no. 5, pp. 1142-1163, 2017.

[64] N. Earlia, R. Rahmad, M. Amin, C. R. S. Prakoeswa, K. Khairan, and Idroes, R. "The potential effect of fatty acids from Pliek U on epidermal fatty acid binding protein: Chromatography and bioinformatic studies." *Sains Malaysiana*, vol. 48, no. 5, pp. 1019-1024, 2019.

[65] R. Dias, J. de Azevedo and F. Walter, "Molecular docking algorithms." *Current drug targets*, vol. 9, no. 12, pp. 1040-1047, 2008.

[66] W. L. DeLano, "Pymol: An open-source molecular graphics tool." CCP4 *Newsl. Protein Crystallogr*, vol. 40, no. 1, pp. 82-92, 2009.

[67] S. I. Mostafa, "Mixed ligand complexes with 2-piperidine-carboxylic acid as primary ligand and ethylene diamine, 2, 2-bipyridyl, 1, 10-phenanthroline and 2 (2-pyridyl) quinoxaline as secondary ligands: preparation, characterization and biological activity." *Transition Metal Chemistry*, vol. 32, no. 6, pp. 769-775, 2007.

[68] D. E. Pires, T. L. Blundell, and D. B. Ascher, "pkCSM: predicting small-molecule pharmacokinetic and toxicity properties using graph-based signatures." *Journal of medicinal chemistry*, vol. 58, no. 9, pp. 4066-4072, 2015.

[69] S. Malik, H. Cun-Heng, and J. Clardy, "Isolation and structure determination of nigellicine, a novel alkaloid from the seeds of Nigella sativa." *Tetrahedron letters*, vol. 26, no. 23, pp. 2759-2762, 1985.

[70] O. Deeb, and M. Goodarzi, "In silico quantitative structure toxicity relationship of chemical compounds: some case studies." *Current drug safety*, vol. 7, no. 4, pp. 289-297, 2012.

[71] V. K. Morya, S. Yadav, E. K. Kim, and D. Yadav, "In silico characterization of alkaline proteases from different species of Aspergillus." *Applied biochemistry and biotechnology*, vol. 166, no. 1, pp. 243-257, 2012.

[72] J. Yang, and Y. Zhang, "I-TASSER server: new development for protein structure and function predictions." *Nucleic acids research*, vol. 43, 2015.

[73] M. Beato, "Gene regulation by steroid hormones." *Gene expression*, pp. 43-75, 1993.

[74] S. Kim, P. A. Thiessen, E. E. Bolton, J. Chen, Fu, A. Gindulyte, and S. H. Bryant, "PubChem substance and compound databases." *Nucleic acids research*, vol. 44, 2016.

[75] N. Kumar, R. Tomar, A. Pandey, V. Tomar, V. K. Singh, and R. Chandra, "Preclinical evaluation and molecular docking of 1, 3-benzodioxole propargyl ether derivatives as novel inhibitor for combating the histone deacetylase enzyme in cancer." *Artificial cells, nanomedicine, and biotechnology*, vol. 46 no. 6, pp. 1288-1299, 2018.

[76] C. A. Lipinski, "Lead-and drug-like compounds: the rule-of-five revolution." *Drug discovery today: Technologies*, vol. 1, no. 4, pp. 337-341, 2004.

[77] A. Daina, O. Michielin, and V. Zoete, "SwissADME: a free web tool to evaluate pharmacokinetics, drug-likeness and medicinal chemistry friendliness of small molecules." *Scientific reports*, vol. 7, no. 1, pp. 1-13, 2017.

[78] D. E. Pires, T. L. Blundell, and D. B. Ascher, "pkCSM: predicting small-molecule pharmacokinetic and toxicity properties using graph-based signatures." *Journal of medicinal chemistry*, vol. 58, no. 9, pp. 4066-4072, 2015.

[79] G. M. Morris, D. S. Goodsell, R. S. Halliday, R. Huey, W. E. Hart, R. Belew, D. Goodsell, H. Moriuchi, N. Koda, E. Okuda-Ashitaka, H. Daiyasu, K. Ogasawara, H. Toh and K. Watanabe, "Molecular characterization of a novel type of prostamide/prostaglandin F synthase, belonging to the thioredoxin-like superfamily." *Journal of biological chemistry, 283 (2), 792-801. Chemistry*, vol. 19, no. 14, pp. 1639-1662, 2008.

[80] C. Shivanika, D. Kumar, V. Ragunathan, P. Tiwari and A. Sumitha, "Molecular docking, validation, dynamics simulations, and pharmacokinetic prediction of natural compounds against the SARS-CoV-2 main-protease." *Journal of biomolecular structure & dynamics*, vol. 1, 2020.

[81] R. A. Laskowski and M. B. Swindells, "LigPlot+: multiple ligand–protein interaction diagrams for drug discovery", 2011.

[82] A. B. Umar, A. Uzairu, G. A. Shallangwa, and S. Uba, "Docking-based strategy to design novel flavone-based arylamides as potent V600E-BRAF inhibitors with prediction of their drug-likeness and ADMET properties." *Bulletin of the National Research Centre*, vol. 44, no. 1, pp. 1-11, 2020.

[83] Y. Han, J. Zhang, C. Q. Hu, X. Zhang, B. Ma and P. Zhang, "In silico ADME and toxicity prediction of ceftazidime and its impurities." *Frontiers in pharmacology*, vol. 10, pp. 434, 2019.

[84] D. E. Pires, T. L. Blundell and D. B. Ascher, "pkCSM: predicting small-molecule pharmacokinetic and toxicity properties using graph-based signatures." *Journal of medicinal chemistry*, vol. 58, no. 9, pp.4066-4072, 2015.

[85] R. Ujan, A. Saeed, P. A. Channar, E. A. Larik, Q. Abbas, M. F. Alajmi, and S. Y. Seo, "Drug-1, 3, 4-thiadiazole conjugates as novel mixed-type inhibitors of acetylcholinesterase: synthesis, molecular docking, pharmacokinetics, and ADMET evaluation." *Molecules*, vol. 24, no. 5, pp. 860, 2019.

[86] E. L. Kwak, Y. J. Bang, D. R. Camidge, A. T. Shaw, B. Solomon, R. G. Maki, S. H. Ou, B. J. Dezube, P. A. Janne, D. B. Costa, M. Varella-Garcia, W. H. Kim, T. J. Lynch, P. Fidias, H. Stubbs, J. A. Engelman, L. V. Sequist, W. Tan, L. Gandhi, M. Mino-Kenudson, G. C. Wei, S. M. Shreeve, M. J. Ratain, J. Settleman, J. G. Christensen, D. A. Haber, K. Wilner, R. Salgia, G. I. Shapiro, J. W. Clark, A. J. Iafrate, "Anaplastic lymphoma kinase inhibition in non-small-cell lung cancer." *N Engl J Med*, vol. 28, no. 18, pp. 1693-703, 2010, doi: 10.1056/NEJMoa1006448.

[87] D. R. Kohler and B. R. Goldspiel, "Paclitaxel (taxol). Pharmacotherapy," *The Journal of Human Pharmacology and Drug Therapy*, vol. 14, no. 1, pp. 3-34, 1994.

[88] S. Papageorgiou, S. L. Pashley, L. O'Regan, "Alternative Treatment Options to ALK Inhibitor Monotherapy for EML4-ALK-Driven Lung Cancer." *Cancers*, vol. 14, no. 14, pp. 3452, 2022,doi: 10.3390/cancers14143452.

[89] R. Kousar, M. Naeem, M. I. Jamaludin, "Exploring the anticancer activities of novel bioactive compounds derived from endophytic fungi: mechanisms of action, current challenges and future perspectives." *American Journal of Cancer Research*, vol. 12, no. 7, pp. 2897-2919, 2022.

[90] E. L. Kwak, Y. J. Bang, D. R. Camidge, A. T. Shaw, B. Solomon, R. G. Maki, S. H. Ou, B. J. Dezube, P. A. Jänne, D. B. Costa, M. Varella-Garcia, W. H. Kim, T.J. Lynch, P. Fidias, H. Stubbs, J. A. Engelman, L. V. Sequist, W. Tan, L. Gandhi, M. Mino-Kenudson, G. C. Wei, S. M. Shreeve, M. J. Ratain, J. Settleman, J. G. Christensen, D. A. Haber, K. Wilner, R. Salgia, G. I. Shapiro, J. W. Clark, A. J. Iafrate, "Anaplastic lymphoma kinase inhibition in non-small-cell lung cancer." *N Engl J Med*, vol. 363, no. 18, pp. 1693-703, 2010, doi: 10.1056/NEJMoa1006448.

[91] F. S. Hamedani, M. Cinar, Z. Mo, M. A. Cervania, H. M. Amin, S. Alkan, "Crizotinib (PF-2341066) induces apoptosis due to downregulation of pSTAT3 and BCL-2 family proteins in NPM-ALK(+) anaplastic large cell lymphoma." *Leuk Res*, vol. 38, no. 4, pp. 503-8, 2014, doi: 10.1016/j.leukres.2013.12.027.

[92] Isozaki, Hideko and Takigawa, Nagio and Kiura, Katsuyuki, "Mechanisms of Acquired Resistance to ALK Inhibitors and the Rationale for Treating ALK-positive Lung Cancer." *Cancers*, vol. 7, pp.763-783, 2015, doi: 10.3390/cancers7020763.

[93] D. R. Kohler and B. R. Goldspiel, "Paclitaxel (taxol)." *Pharmacotherapy: The Journal of Human Pharmacology and Drug Therapy*, vol. 14, no. 1, pp. 3-34, 1994.

[94] S. B. Horwitz, "Taxol (paclitaxel): mechanisms of action. Annals of Oncology." *Official Journal of the European Society for Medical Oncology*, vol. 5, 1994.

[95] Kampan, Dr. Nirmala and Madondo, Mutsa and McNally, Orla and Quinn, Michael and Plebanski, Magdalena. Paclitaxel and Its Evolving Role in the Management of Ovarian Cancer. BioMed Research International, pp. 1-21, 2015, doi: 10.1155/2015/413076.

[96] P. Dabas, M. S. Janney, S. Arora, R. Subramaniyan, "Crizotinib-induced Photoallergic Dermatitis: A Case Report of an Unconventional Adverse Effect of a Novel Molecule." *Journal of Pharmacology and Pharmacotherapeutics*, vol. 9, no. 4, pp. 195-197, 2018, doi:10.4103/jpp.JPP_106_18.

[97] P. Ma, R. J. Mumper, "Paclitaxel Nano-Delivery Systems: A Comprehensive Review." *J Nanomed Nanotechnol*, vol. 4, no. 2, pp. 1000164, 2013, doi: 10.4172/2157-7439.